



**HAL**  
open science

# Propositions of numerical solution techniques for the tolerance analysis problem in manufacturing: 3D approach

Mojtaba Kamali Nejad

► **To cite this version:**

Mojtaba Kamali Nejad. Propositions of numerical solution techniques for the tolerance analysis problem in manufacturing: 3D approach. Mechanics [physics.med-ph]. Université Joseph-Fourier - Grenoble I, 2009. English. NNT : . tel-00445639

**HAL Id: tel-00445639**

**<https://theses.hal.science/tel-00445639>**

Submitted on 11 Jan 2010

**HAL** is a multi-disciplinary open access archive for the deposit and dissemination of scientific research documents, whether they are published or not. The documents may come from teaching and research institutions in France or abroad, or from public or private research centers.

L'archive ouverte pluridisciplinaire **HAL**, est destinée au dépôt et à la diffusion de documents scientifiques de niveau recherche, publiés ou non, émanant des établissements d'enseignement et de recherche français ou étrangers, des laboratoires publics ou privés.

# UNIVERSITÉ JOSEPH FOURIER

T H E S E

Pour obtenir le grade de

**DOCTEUR**

Spécialité : GÉNIE MÉCANIQUE, CONCEPTION ET PRODUCTION

Préparée au laboratoire **G-SCOP**

Dans le cadre de l'Ecole Doctorale IMEP-2

Présentée et soutenue publiquement par :

**Mojtaba KAMALI NEJAD**

Le 14 octobre 2009

Titre :

**Propositions de résolution numérique des problèmes  
d'analyse de tolérance en fabrication : approche 3D**

---

Directeur de thèse : François VILLENEUVE

Codirecteur de thèse : Frédéric VIGNAT

Jury :

M. Max GIORDANO  
M. Darek CEGLAREK  
M. Luc MATHIEU  
M. Alain DESROCHERS  
M. François VILLENEUVE  
M. Frédéric VIGNAT

Président  
Rapporteur  
Rapporteur  
Examineur  
Directeur de thèse  
Codirecteur de thèse



*UNIVERSITÉ JOSEPH FOURIER*

T H E S E

Pour obtenir le grade de

**DOCTEUR**

Spécialité : GÉNIE MÉCANIQUE, CONCEPTION ET PRODUCTION

Préparée au laboratoire **G-SCOP**

Dans le cadre de l'Ecole Doctorale IMEP-2

Présentée et soutenue publiquement par :

**Mojtaba KAMALI NEJAD**

Le 14 octobre 2009

Title:

**Propositions of numerical solution techniques for the  
tolerance analysis problem in manufacturing: 3D approach**

---

Directeur de thèse : François VILLENEUVE

Codirecteur de thèse : Frédéric VIGNAT

Jury :

M. Max GIORDANO  
M. Darek CEGLAREK  
M. Luc MATHIEU  
M. Alain DESROCHERS  
M. François VILLENEUVE  
M. Frédéric VIGNAT

Président  
Rapporteur  
Rapporteur  
Examineur  
Directeur de thèse  
Codirecteur de thèse



## Résumé

Ce travail contribue à développer des méthodes de résolution associées à la méthode de simulation MMP (Model of Manufactured Part) développée par F.Vignat et F.Villeneuve. Le MMP est un modèle générique 3D des défauts géométriques engendrés sur les pièces fabriquées par un processus de fabrication donné. Ce modèle permet de générer un ensemble de pièces virtuellement fabriquées incluant les incertitudes de fabrication et permet par conséquent de mener l'analyse de tolérances fonctionnelles. Les méthodes de résolution développées autour du MMP permettent aux ingénieurs de fabrication d'évaluer une gamme de fabrication candidate du point de vue géométrique.

Le développement des méthodes de résolution s'est effectué selon 2 axes. Le premier axe consiste à développer des méthodes pour la recherche du pire des cas (WCTA). La première approche de cet axe utilise des méthodes d'optimisation (SQP pour Sequential Quadratic Programming et GA pour les algorithmes génétiques) basées sur la recherche du pire des cas. La recherche du pire des cas consiste en un algorithme d'optimisation multicouche comportant deux boucles principales. La deuxième approche de cet axe consiste à faire une adaptation de la méthode du torseur des petits déplacements avec intervalle (modèle Jacobien Torseur développé au Canada) à la méthode MMP.

Le deuxième axe concerne les méthodes stochastiques permettant une simulation de production d'un ensemble de pièces et l'analyse des résultats d'un point de vue statistique. La méthode stochastique est basée sur une méthode de tirage aléatoire sous contraintes.

Les différentes approches sont finalement comparées entre elles.



## **Abstract**

This research contributes to developing the solution techniques associated with the MMP (Model of manufactured part) simulation method developed by F.Villeneuve and F.Vignat for modeling the different geometrical deviation impacts on the part produced (error stack-up) in a multi-stage machining process. The model cumulates the impacts of various sources of manufacturing errors hence enabling tolerance analysis. The MMP simulation method beside the developed solution techniques allows the manufacturing engineers to evaluate a candidate process plan from a geometrical point of view. The developed solution techniques are classified into two categories: Search for finding the worst case (worst part produced) and stochastic method.

The first approach of the first category uses the optimization algorithms to search for the worst case. A multi-layer optimization algorithm is developed in order to search for the worst case. The performance of two current optimization methods for worst case identification using this algorithm (genetic algorithm and sequential quadratic programming) has been studied.

The second approach of the first category uses a combined solution technique which is built on the Canadian Jacobian torsor model and the French MMP model for tolerance analysis. This method uses the interval arithmetic.

The second category consists in stochastic method which allows simulating a very large sample of production and analyzing the results from a statistical point of view. This method uses Monte Carlo simulation with a constrained random generator. The performance of the developed solution techniques is compared through 3D examples.





# Table of contents

<b>1</b>	<b>INTRODUCTION.....</b>	<b>1</b>
<b>2</b>	<b>STATE OF THE ART .....</b>	<b>7</b>
2.1	TOLERANCING IN PRODUCT LIFE CYCLE.....	7
2.1.1	<i>Tolerancing and concurrent engineering(CE)</i> .....	8
2.1.2	<i>Tolerance related activities</i> .....	9
2.2	TOLERANCE ANALYSIS.....	13
2.3	TOLERANCE ANALYSIS IN ASSEMBLIES .....	16
2.3.1	<i>Dimensional tolerance chain models</i> .....	18
2.3.2	<i>Representation and propagation of 3D Tolerances</i> .....	22
2.3.2.1	Preliminary work.....	23
2.3.2.2	Kinematic formulation of tolerances .....	23
2.3.2.3	Small displacement torsor (SDT) .....	24
2.3.2.4	Matrix representation .....	27
2.3.2.5	Vectorial tolerancing .....	28
2.4	TOLERANCE ANALYSIS IN MULTI-STAGE MACHINING PROCESS (MSMP).....	29
2.4.1	<i>State space approach</i> .....	30
2.4.1.1	Huang et al (2003).....	30
	Part deviation .....	31
	Error stack-up mechanism.....	33
2.4.1.2	Zhou et al (2003).....	33
	Error stack-up mechanism.....	35
	Discussion .....	35
2.4.1.3	Loose et al (2007).....	35
2.4.1.4	Zhong et al (2000).....	37
	Model for representing geometrical errors .....	38
	Error stack-up mechanism.....	38
2.4.2	<i>Tolerance zone approach</i> .....	40
	Error stack-up mechanism.....	40
	Geometrical tolerance analysis.....	41
	Discussion .....	42
2.4.3	<i>Simulation approach</i> .....	42
	Model for representing the geometrical deviations .....	43
	Error stack-up mechanism.....	43
	Discussion .....	45
2.4.4	<i>SDT approach</i> .....	46
2.4.5	<i>Conclusion</i> .....	46

<b>3</b>	<b>MANUFACTURING SIMULATION WHICH LEADS TO A MODEL OF MANUFACTURED PART (MMP)</b> .....	<b>49</b>
3.1	MACHINING PROCESS .....	50
3.1.1	Case of a turning operation .....	51
3.1.2	Case of a milling operation.....	51
3.2	GENERATED DEVIATION IN A MACHINING OPERATION .....	52
3.2.1	Positioning errors .....	53
3.2.2	Machining errors .....	53
3.2.3	Error stack-up.....	54
3.3	THE SIMULATION METHOD LEADS TO MMP .....	55
3.3.1	Small Displacement Torsor (SDT) .....	55
3.3.2	Positioning deviation in a machining setup .....	57
3.3.2.1	Calculating link parameters value .....	60
	Floating link parameters.....	60
	Non-penetration equations for the case of plane-plane elementary connection.....	61
	Non-penetration equations for the case of cylindrical elementary connection .....	61
	Slipping link parameters.....	62
	Example .....	63
3.3.3	Machining (cutting) deviation in a machining setup.....	65
3.3.4	Actual surface deviations relative to the nominal part.....	66
3.3.5	Error stack-up mechanism associated with MMP.....	66
3.3.6	Conclusion .....	68
<b>4</b>	<b>TOLERANCE ANALYSIS WITH THE MMP</b> .....	<b>71</b>
4.1	VIRTUAL GAUGE .....	71
4.2	GAPGP MEASUREMENT .....	73
4.2.1	Case of planar tolerance zone.....	75
4.2.2	Case of cylindrical tolerance zone .....	77
4.3	VIRTUAL GAUGE BEST POSITION .....	78
4.4	WORST CASE SEARCHING .....	79
4.5	CONCLUSION .....	80
<b>5</b>	<b>WORST CASE BASED TOLERANCE ANALYSIS (WCTA) USING OPTIMIZATION ALGORITHMS</b> .....	<b>81</b>
5.1	REFORMULATION .....	81
	Sub I:.....	82
	Sub II:.....	82
5.2	SUB II (VIRTUAL MEASUREMENT OF ONE PART).....	83
5.2.1	Example.....	85
5.2.2	Summary of sub II .....	86

5.3	SUB I (VIRTUAL MANUFACTURING) .....	88
5.3.1	<i>The fixture layouts handled by CHP positioning algorithm</i> .....	89
5.3.2	<i>Quality constraints</i> .....	91
5.3.2.1	Using the Measurement Results (dependent parameters).....	91
5.3.2.2	Using the Measurement Results (independent parameters).....	92
5.3.2.3	Considering a variation Zone with dependent parameters.....	92
5.3.3	<i>Solution strategy</i> .....	94
5.4	OPTIMIZATION TECHNIQUES .....	95
5.4.1	<i>Sequential quadratic programming (SQP)</i> .....	95
5.4.2	<i>Genetic Algorithms</i> .....	96
5.5	CONCLUSION .....	98
<b>6</b>	<b>WORST CASE BASED TOLERANCE ANALYSIS (WCTA) USING INTERVAL METHOD</b>	
	<b>99</b>	
6.1	MATRIX REPRESENTATION OF $GAPGP_{\kappa}$ .....	99
6.2	THE JACOBIAN-TORSOR MODEL .....	101
6.3	INTERVAL METHOD FOR TOLERANCE ANALYSIS.....	103
6.3.1	<i>The functional elements(FE) of the interval method</i> .....	103
6.3.1.1	Surface deviation representation using an SDT with intervals.....	103
6.3.1.2	Link representation using an SDT with intervals.....	104
6.3.1.3	Example.....	105
6.4	TOLERANCE ANALYSIS.....	107
6.5	VIRTUAL GAUGE BEST POSITION .....	110
6.6	CONCLUSION .....	111
<b>7</b>	<b>STOCHASTIC TOLERANCE ANALYSIS AND CASE STUDY.....</b>	<b>113</b>
7.1	STOCHASTIC APPROACH FOR TOLERANCE ANALYSIS USING THE MMP.....	113
7.1.1	<i>Defect generation procedure</i> .....	114
7.1.1.1	Using Measurement Results (independent variables).....	114
7.1.1.2	Using Measurement Results (dependent variables) and Variation zone .....	114
	Case one:.....	114
	Case two:.....	116
7.1.2	<i>Floating link values generation</i> .....	117
7.2	EXAMPLES AND COMPARISON .....	119
7.2.1	<i>“Double inclined plane” example</i> .....	119
7.2.1.1	First section-independent parameters-interval approach .....	120
	Results and discussion.....	121
7.2.1.2	First Section-independent parameters-optimization approach.....	122
7.2.1.3	First section-independent parameters-MC simulation .....	122
	Discussion .....	124
7.2.1.4	Second section with dependent variables (Variation zone) .....	127

---

7.2.1.5	Second section-dependent variables-optimization approach .....	128
7.2.1.6	Second section-dependent variables- MC simulation .....	128
	Discussion .....	130
7.2.2	<i>“Bolt” example</i> .....	132
7.2.2.1	MWP/Fixture assembly .....	132
7.2.2.2	Parameters variation range .....	133
7.2.2.3	Gauge/MMP assembly .....	133
7.2.2.4	Optimization approach .....	134
7.2.2.5	Interval approach .....	134
7.2.2.6	MC simulation .....	138
7.2.2.7	Discussion .....	139
<b>8</b>	<b>CONCLUSION AND PERSPECTIVES .....</b>	<b>141</b>
8.1	PERSPECTIVES .....	143
<b>9</b>	<b>REFERENCES .....</b>	<b>145</b>
<b>10</b>	<b>ANNEX.....</b>	<b>157</b>
10.1	QUADRATIC PROGRAMMING (QP) SUB PROBLEM.....	158
10.1.1	<i>SQP Implementation</i> .....	158
10.1.1.1	Updating the Hessian Matrix .....	158
10.1.1.2	Quadratic Programming Solution.....	159
	Line Search and Merit Function .....	159
	<b>LIST OF FIGURES .....</b>	<b>161</b>
	<b>LIST OF TABLES .....</b>	<b>165</b>

# 1 INTRODUCTION

Today, designers use CAD models when designing a new product in an industrial context. These models specify the ideal geometry for *size*, *location* and *form* [Asme Y14.5m, 1994]. Since it is impossible to manufacture a part to its exact geometry and dimensions, it is accepted that there will be a certain amount of variation in terms of manufacturing geometry and dimensions.

It is the engineering designer's task to specify the allowable variation limits for the geometry of products based on *functional requirements* and practical considerations with respect to production. To this end, designers specify *tolerances*. These establish the allowable variation limits for certain geometric *dimensions* or *forms*. Tolerances (called here *functional tolerances*) are used to control *size*, *location* and *geometry* of features or components to ensure that the part produced meets the functional requirements. In other hand, tolerances specify the ranges of permissible imperfections so a manufactured part will be acceptable for assembly and use. If the product is manufactured within the tolerance range, then it is deemed a good product otherwise, it is a bad product.

Manufacturing engineers are then faced with the problem of selecting the appropriate process plan (machining processes and production equipment) to ensure that design specifications are satisfied. In the discrete part manufacturing industry, engineers develop process plans by selecting appropriate machining processes and production equipment to ensure the quality of the finished components. Developing a suitable process plan for release to production is complicated and time-consuming.

Generally, a number of potential process plans are put forward. These take into account the part's geometry and tolerances, the available production means and their capabilities. The decisions in process planning are usually made based on personal experience and some rules-of-thumb (usually company-specific practices) which as things currently stand heavily relies on engineering requirements, experience, and manual calculation. The candidates should be evaluated from different points of view (i.g. cost, time and quality). Currently, trial runs or very simple simulation models (1D tolerance charts for example [Whybrew K. *et al*, 1990] ) are used to check the quality criterion. The process plan is then modified based on the results

obtained. This approach can be called into question: the trial runs are very costly and time consuming. Researchers have recognized the inefficiency of such a physical trial-and-error process in evaluating a process plan.

Research efforts have been devoted to developing an efficient simulation model for evaluating a process plan without trial-and-error runs such as automated tolerance chart analysis and tolerance synthesis. The purpose of tolerance chart analysis [Wade O. R., 1983] is to verify how functional tolerance requirements can be met when a process plan is given with specified production defects (or manufacturing tolerances). Tolerance synthesis deals with the reverse problem, i.e. determining appropriate production tolerances (manufacturing tolerances) so that design tolerance requirements can be met.

Over the past two decades, researchers have developed various computerized method for tolerance synthesis based on tolerance chart analysis. Some of the works are summarized in [Huang S. H. *et al*, 2004]. Although different simulation models have been developed, the accuracy of these models fails to meet today's requirements. See [Table 1-1](#).

Author(s)	Method/ system	Author(s)	Method/ system
Zhang <i>et al.</i> 2000	Monte Carlo method	Lin <i>et al.</i> 1999	Process data
Ngoi <i>et al.</i> 1998	Noded approach	Konakalla and Gavankar 1997	TOLCHAIN
Britton and Whybrew 1997	CATCH	Ji 1996	Backward derivation
Ji <i>et al.</i> 1995	Tree approach	Ngoi and Fang 1994	Gauss elimination
Abdou and Cheng 1993	TVCAPP	Ji 1993	Linear programming
Ngoi and Ong 1993	Profile representation	Dong and Hu 1991	Nonlinear optimization
Mittal <i>et al.</i> 1990	Path tracing	Li and Zhang 1989	Graphical method
Xiaoqing and Davies 1988	CADP	Ahluwalia and Karolin 1986	CATC

*Table 1-1: Literature relevant to computerized tolerance chart analysis/synthesis [Huang S. H. *et al*, 2004]*

These problems can be overstepped by developing accurate models and methodologies for simulating the manufacturing process and predicting geometrical variations in the parts produced. More accurate models will make it possible to evaluate the process plan, determine the tolerance values in terms of manufacturing capabilities during the design phase, and define the manufacturing tolerances to be checked for each setup.

In the literature available on this subject, the evaluation of a process plan in terms of functional tolerances is called the *tolerance analysis*. The purpose of a tolerance analysis is to verify whether the design tolerance requirements can be met for a given process plan with specified manufacturing deviations. Actually the variation of a machined part arises from the accumulation of different variations all over the production process. In tolerance analysis in a multi-stage machining process, the cumulative effect of individual variations with respect to the specified functional tolerance in all machining stage is studied in order to check a product's functionality compared with its design requirements. This is also referred to as error propagation, error stack-up and tolerance stack-up in a multi-stage machining process.

The tolerance analysis includes:

- The contributors, i.e. the features that caused variation in the analyzed tolerance like, for example, the datum features
- The sensitivities with respect to each contributor
- The percent contribution to variation from each contributor
- The worst case variations, statistical distribution, and acceptance rates

Analysis approaches can be classified from different points of view and critics. According to *dimensionality* three categories can be considered; one-dimensional (1D), two dimensional (2D), and three-dimensional (3D).

According to the analysis *objectives*, two techniques have been used: (1) *worst case tolerance analysis* (WCTA) and (2) *statistical tolerancing analysis* (STA). In worst case tolerancing (i.e., 100% acceptance rate), the aim is to find the worst possible part, in terms of functional tolerance, that a multi-stage machining process might produce. If the worst part in a series of manufactured parts complies with the functional tolerance, it is logical to conclude that all of the parts manufactured will comply. The worst part might be produced when the contributor features are set at their extreme variation value as allowed by their variation scope (according to the manufacturing means capabilities or manufacturing tolerances). Worst case methods give results that are overly pessimistic.

Clearly, there is a need to take into consideration the probabilistic behavior of the manufacturing processes that produce each feature. In statistical tolerance analysis, it is assumed that variation of individual contributor features are independent and are given some



probability distribution. This in turn allows computing some cumulative probability that the product will meet its design tolerance requirements at the end of the manufacturing process. Computations are most often performed using Monte-Carlo simulations.

Additionally, on the one hand, we found that existing methods have not sufficient accuracy to evaluate the tolerance stack-up. On the other hand, most of them do not take into account the 3D tolerance stack-up, manufacturing errors and positioning errors. In this work we have used the Model of Manufactured Part (the MMP) [Villeneuve F. *et al*, 2005a, , 2007] [Vignat F. *et al*, 2007a]; a method for modeling the different geometrical deviation impacts on the part produced (error stack-up or tolerance stack-up) in a multi-stage machining process. This method overcomes the above-mentioned drawbacks by simulating machining and measuring processes along with major manufacturing errors using the Small Displacement Torsor concept (SDT) [Bourdet P. *et al*, 1996]. The model cumulates the impacts of various sources of manufacturing errors hence enabling tolerance analysis. Previously, the same authors presented a generic formulation for tolerance analysis based on searching for the worst case using the MMP. The present work discusses about different solution techniques for identifying the worst case and performing stochastic tolerance analysis.

In this thesis, firstly the existing literature regarding the tolerance analysis in machining will be mentioned. Secondly the simulation method which leads to the MMP will be reminded and with some developments and modifications in mathematical expression and notation will be detailed. This reminder will be followed by the developed solution techniques for the problem of tolerance analysis. The developed solution techniques consist in two main axes:

- 1- Search methods for finding the worst case called Worst Case based Tolerance Analysis (WCTA)
- 2- Stochastic method named Stochastic Tolerance Analysis.

Two approaches are applied for performing WCTA:

- Multi layer optimization
- Interval method

The first approach of this axis uses optimization algorithms and searches the worst part by solving a multi-layer optimization problem. The second approach of this axis is a combined approach called interval method built on two existing models for tolerance analysis

in successive machining operations: the MMP and the Jacobian-Torsor model. It should be pointed out that the notation of the MMP and the Jacobian-Torsor model has been homogenized in this work for better understanding. This technique uses interval arithmetic because it offers the advantage of expressing uncertainties and deviations.

The second axis use MMP for statistical tolerance analysis using Monte Carlo simulation.

Aforementioned solution techniques will be explored and followed by some examples. Their performances will be compared through 3D examples. Finally, a conclusion and some perspectives will be mentioned.



## 2 STATE OF THE ART

In this section, firstly we will establish the tolerancing activities in the product life cycle. A short description of different activities will be explored. Secondly between the different activities we will focus on tolerance analysis (this is also referred to as error propagation, error stack-up, and tolerance stack-up).

### 2.1 TOLERANCING IN PRODUCT LIFE CYCLE

Generally products are designed to fulfill functionality. A product, during its lifecycle, passes through many stages from conceptual design to the end of life. It especially passes through manufacturing and assembly stages where geometrical deviations are generated and accumulated.

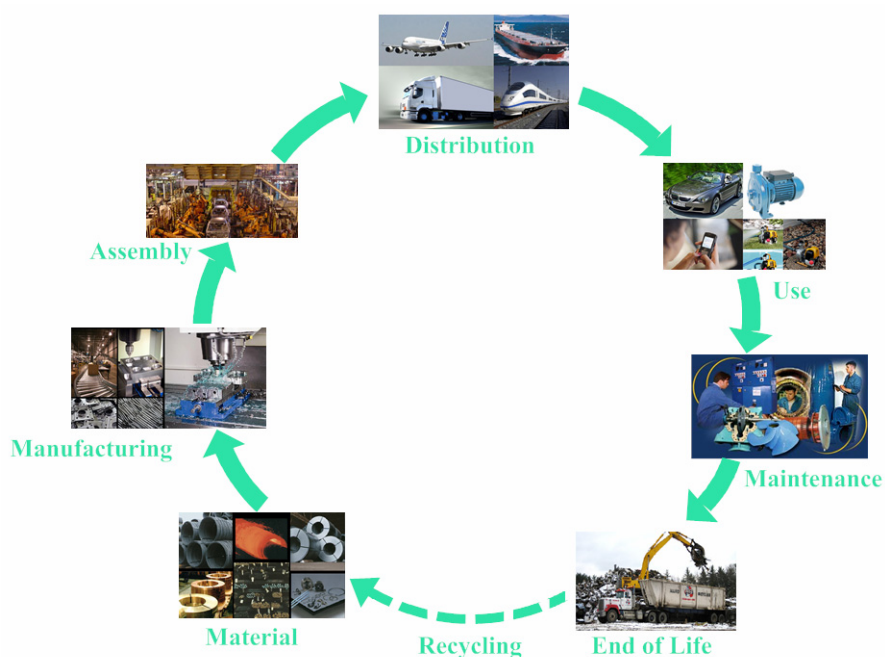


Figure 2–1: Product life cycle

Since it is impossible to manufacture a part to its exact geometry and dimensions, it is accepted that there will be a certain amount of variation in terms of manufacturing geometry and dimensions. The geometrical deviations affect the product functionality therefore they are important for the product life cycle actors. These actors may be the designers, the

manufacturers, the users (clients) ... etc. To satisfy the different actors of product life cycle, it is necessary to manage the geometrical deviations which are produced in **Manufacturing**, **Assembly** and **Use** stages of life cycle. See [Figure 2-1](#) [Nguyen D. S. *et al*, 2009]. To ensure the functionality of a product, designers specify the geometry of products based on functional requirements and practical considerations with respect to production. To this end, designers specify tolerances. These establish the allowable variation limits for certain geometric dimensions or forms [Asme Y14.5m, 1994]. Tolerances are used to control size, location and geometry of features or components to ensure that the part produced meets the functional requirements.

Geometric Dimensioning and Tolerancing (GD&T) is a concept widely used for specifying dimensions and tolerances of the components and sub-assemblies of a product according to their functional requirements. These functional requirements arise from all life cycle issues, such as manufacturing, assembly and inspection [Islam M. N., 2004]. Dimensions and tolerances influence almost all aspects of product development. See [Figure 2-2](#).

### 2.1.1 Tolerancing and concurrent engineering (CE)

Today, most of the products are developed using CAx software in Concurrent Engineering (CE) context. Concurrent Engineering (CE) is an engineering and management philosophy, which also deals with the life cycle issues of a product. CE is based on the idea of carrying out as many stages of product development concurrently as possible, rather than in a sequential order. It calls for the formation of a cross-functional product development team, which includes people from a wide range of departments, such as: product planning, design, manufacture, assembly, quality assurance, marketing, sales and finance.

Dimensions and tolerances influence almost all aspects of product development which are of interest to CE team members who consider all the life cycle issues of a product during its design stage. Therefore, a CE approach will be ideal for the selection of dimensions and tolerances through applications of FD&T methodology. Furthermore, FD&T can serve as a common link between all members of the CE team; hence it can enhance the CE team performance.

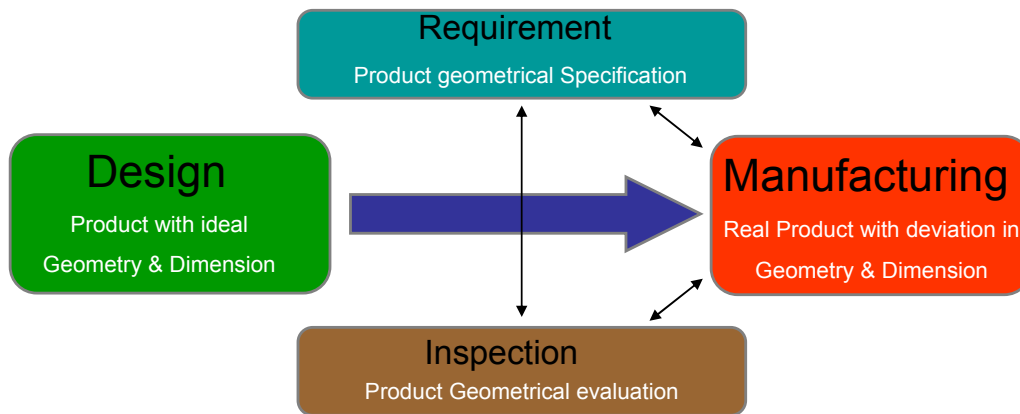


Figure 2–2: Product Development

### 2.1.2 Tolerance related activities

The physical realization of any part always yields imperfect forms with respect to the ideal geometry specified in the engineering design. To describe and preserve functional requirements of design, the allowable variation is specified using modern geometrical tolerances. Ever since the plus/minus limits on dimensions first started to appear on engineering drawings in the early 1900s, tolerances have been one of the most important issues for every engineer involved in the product realization processes.

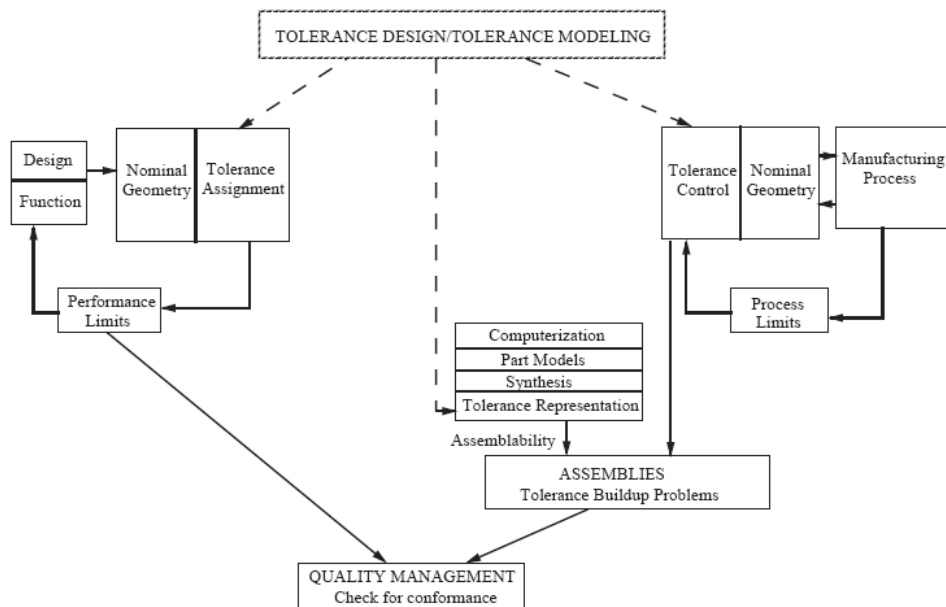


Figure 2–3: The scope of tolerances in engineering [Srinivasan R. S., 1994]

In particular, with the advancement of computers and CAD/CAM techniques in the 1970s, the tolerance-related issues have continuously drawn the attention of many researchers since then. As a result, a tremendous number of research articles have been published over the last 30 years. Tolerance is an essential part of design and manufacturing. Srinivasan mention that *“We may consider the ubiquitous tolerances in various stages of a product life cycle. Since the role of tolerances in a life cycle varies from stage to stage, depending on their own respective objectives, it is not a trivial task to take all these different factors into account when a designer determines a tolerance.”* [Srinivasan R. S. *et al*, 1996].

Figure 2–3 describes the flow of information and physical objects related to tolerances, through a series of different stages. In design, functionality is of concern. Thus, ideally, tolerances should be as close to zero as possible. However, manufacturing places constraints on the ideal [Roy U. *et al*, 1991]. Thus, the tolerancing decision should respect the limited capabilities of the required manufacturing processes as well as the functionality and/or assemblability constraints. The ubiquitousness of tolerances entails the various tolerance-related problems in different stages of life cycle, characterized by their respective objectives and viewpoints. These individual problems are interrelated with each other, which makes the tolerancing research more challenging to be handled efficiently. In [Hong Y. S. *et al*, 2002], the authors have classified the tolerance-related research into seven distinct categories: (See Figure 2–4)

- Tolerance schemes
- Tolerance modeling and representation
- Tolerance specification
- Tolerance analysis
- Tolerance synthesis or allocation
- Tolerance transfer
- Tolerance evaluation

The above categories will be firstly presented but not in detail and then we will investigate on tolerance analysis.

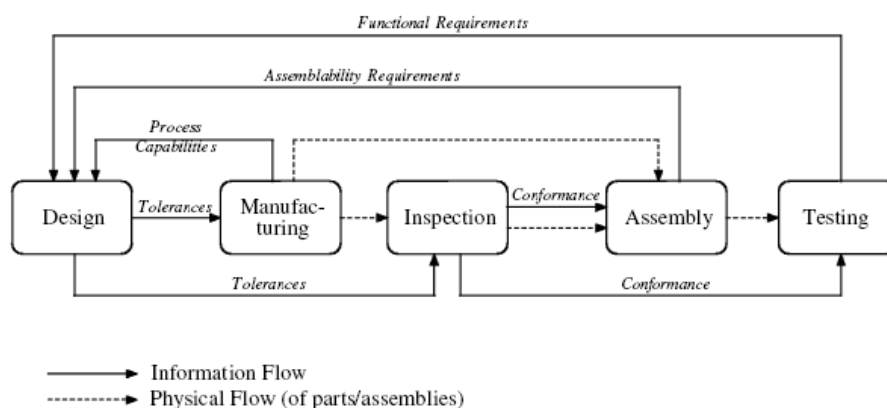


Figure 2–4: Ubiquitous role of tolerances in a product life cycle [Hong Y. S. et al, 2002]

Two types of tolerances, conventional (plus/minus) and geometrical (GD&T) are usually used in current drawing conventions. In more theoretical terms, there are two types of *tolerancing schemes*: parametric and geometrical.

Parametric tolerancing consists in identifying a set of parameters and assigning limits to the parameters that define a range of values [Requicha A. A. G., 1993]. A typical example of parametric tolerancing is the conventional plus/minus tolerancing. A tolerancing scheme called vectorial tolerancing [Wirtz A., 1991] also falls into this category.

Geometrical tolerancing assigns values to certain attributes of a feature, such as forms, orientations, locations, run outs and profiles. Hong has classified the tolerancing schemes into three categories: [Hong Y. S. et al, 2002] (See [Figure 2–5](#)).

#### 1- Parametric tolerancing

- Conventional (plus/minus) tolerancing
- Statistical tolerancing
- Vectorial tolerancing

#### 2- Geometrical tolerancing

#### 3- Next-generation tolerancing

- Assembly tolerancing
- Functional tolerancing



*Tolerance specification* is concerned with how to specify tolerance types and values. This is the area of research that has been least sought out so far. In practice, the tolerances are specified by the designer, mainly based on experience and/or empirical information. Tolerance specification is preferably carried out in conformance with the tolerancing standards (international: ISO 1101, ANSI Y14.5; national: NEN, DIN; or company specific). However, the standards do not prescribe a method of how tolerances must be specified. An investigation on the generative way of specifying tolerances, based on the geometrical and/or technological constraints is continuing. Examples include the research on the concept of TTRS (topologically and technologically related surfaces) [Clément A. *et al*, 1997] and its application toward tolerancing for assembly [Teissandier D. *et al*, 1999a, Teissandier D. *et al*, 1998], tolerancing for function [Weill R., 1997] and tolerancing assistance models [Desrochers A., 2003, Desrochers A. *et al*, 1994, Desrochers A. *et al*, 1995].

Although geometrical tolerancing addresses the weakness and intrinsic ambiguities of parametric tolerancing, it still poses its own weakness, mainly due to its informal way of defining the core concepts. [Hong Y. S. *et al*, 2002]

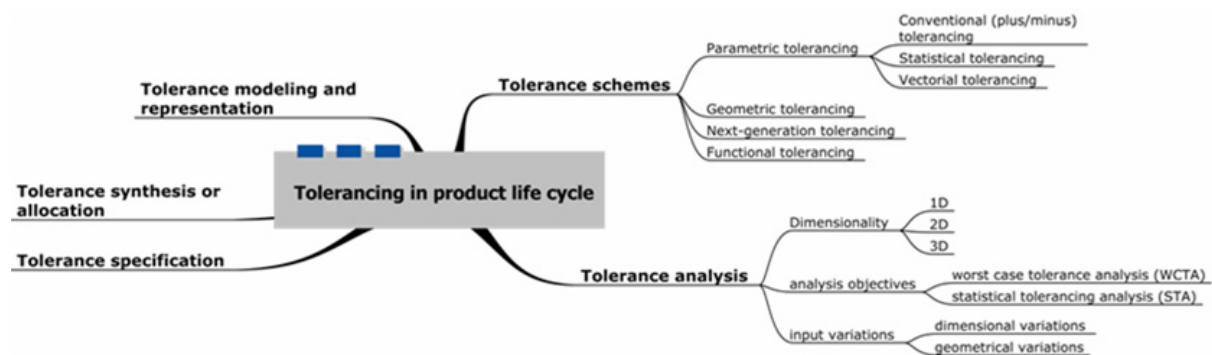


Figure 2–5: Tolerance activities in product life cycle

A branch of research that seeks an efficient way of defining and representing the tolerance information, mathematically or electronically, is called *tolerance modeling and representation*. With the advancement of solid modeling techniques, much effort has been made to incorporate tolerance information into the product model as an intrinsic part of product definition. Several different representation schemes have been proposed over the last two decades but, unfortunately, it is hard to find a *general* standard in this area. Researches from various perspectives are still continuing. For example “GeoSpelling”, the model proposed to ISO for rebuilding standards in the fields of tolerancing and metrology, allows a

unified description of geometrical specification.[Dantan J.-Y. *et al*, 2008, Mathieu L. *et al*, 2005, Mathieu L. *et al*, 2007].

Another important need for other tolerance representation methods comes from the application-specific requirements. Among those, several approaches stand out for their general applicability: the matrix approach , SDT (Small Displacement Torsor) [Bourdet P. *et al*, 1996], TTRS [Clément A. *et al*, 1997], kinematic formulation [Rivest L. *et al*, 1994], etc....

A representation assumes a certain tolerancing scheme, whereas a single tolerancing scheme can be represented in many different ways, i.e. can have multiple representations. Since it is not fundamental to our problem, this section is intentionally kept short. More detailed reviews of previously developed representation methods can be found in [Roy U. *et al*, 1991] [Juster N. P., 1992] [Yu K. M. *et al*, 1994] [Hong Y. S. *et al*, 2002] [Mathieu L. *et al*, 1997].

## 2.2 TOLERANCE ANALYSIS

Salomons defines the main function of tolerance analysis as [Salomons O. W. *et al*, 1996a]:

*Calculate with given tolerance types and tolerance values, the resulting tolerance zones in order to verify the mating functions of the parts constituting the assembly (feasibility of assembly) and calculate the clearances and orientations between the parts constituting the assembly (quality of assembly).*

Shan said:” *The study of the aggregate behavior of given individual variations is referred to tolerance analysis* “ [Shan A. *et al*, 1999].

Shen mention that:” *The objective of tolerance analysis is to check the extent and nature of the variation of an analyzed dimension or geometric feature of interest for a given GD&T scheme. The variation of the analyzed dimension arises from the accumulation of dimensional and/or geometrical variations in the tolerance chain*” [Shen Z. *et al*, 2005].

The design is described by means of sketches, models or drawings, which convey essential geometrical information. Tolerances are assigned to the design, based on experience

or empirical information. The design description is then routed to manufacturing, where suitable machines and processes are selected to achieve the required geometry. It is in this stage that the geometrical deviations are produced and built-up.

Normally, a manufacturing process consists of different setups; the geometrical deviations are produced in each setup and accumulated through the setups. The deviations arising from these manufacturing processes must be maintained within the tolerance range specified by design.

The manufactured parts are then assembled as per the design requirements; tolerance build up, i.e. the combination of tolerances on the individual parts, influences the ease and feasibility of the assembly process. In this stage as well as in manufacturing, the geometrical deviations of different components accumulate and then affect the assembly.

Based on the above short representation of tolerance analysis, it can be found that in a manufacturing process as well as in an assembly, the geometrical deviation buildups. Calculation and investigation on geometrical deviation stack-up in each of the aforementioned sections require its own expertise and attention. For this reason tolerance analysis is divided into to *tolerance analysis in manufacturing* (on which we concentrate in this thesis) and *tolerance analysis in assemblies*.

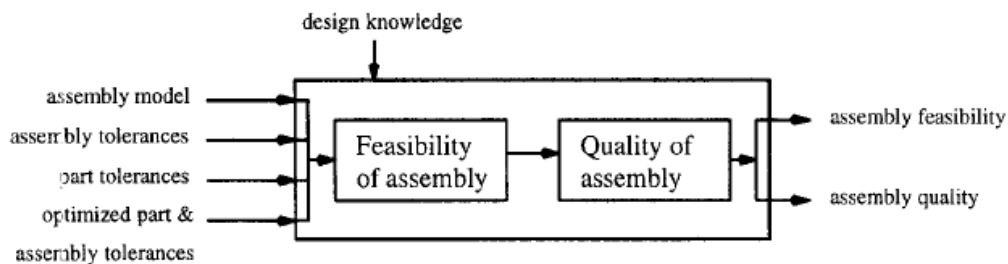


Figure 2–6: Main function of the tolerance analysis tool [Salomons O. W. et al, 1996a]

The purpose of tolerance analysis in manufacturing is to verify whether the part functional tolerances can be met for a given process plan with specified manufacturing deviations. This is also referred to as error propagation, error stack-up, and tolerance stack-up in a multi-stage machining process. [Kamali Nejad M. et al, 2009b]

The purpose of tolerance analysis in assembly is to check the performance of an assembly (or functional requirement) when different parts with deviations are placed together.

See Figure 2–6. In other word, it is a method used to verify the proper functionality of an assembly, taking into account the variability of its individual parts.

The common issue in these two divisions is that in both cases the accumulation of deviations will be calculated in order to check whether the amounts of accumulated deviation are acceptable or not compared with functional tolerances or functional requirements.

Actually there are three main scopes in tolerance analysis:

- 1- The models for representing the geometrical deviations. Such as: matrix representation [Desrochers A., 1999], SDT [Bourdet P. *et al*, 1996], Vectorial representation [Wirtz A., 1991].
- 2- A mathematical relation for calculating the stack. Generally this model represents the effect of the individual deviations into the final stack. The aim of this mathematical relation is to simulate the influences of individual deviations (on the geometrical behavior of the mechanism in the case of an assembly and the quality of the final part in the case of a manufacturing process). Usually, tolerance analysis uses a relationship of the form as the Eq. 2-1 [Nigam S. D. *et al*, 1995]. See Figure 2–7.

$$Y = G(X_1, X_2, \dots, X_n) \quad (2-1)$$

Where  $Y$  is the final stack and  $X = \{X_1, X_2, \dots, X_n\}$  are the individual geometrical deviations.

- 3- The development of the solution techniques or analysis methods. Such as worst-case searching and statistical analysis.

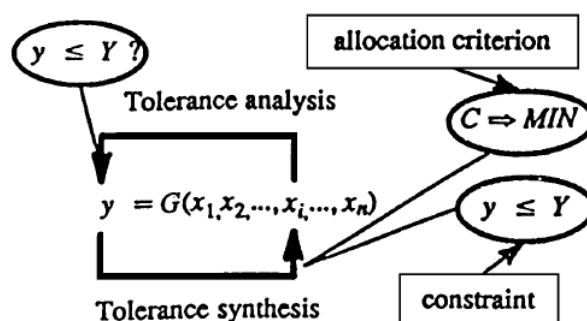


Figure 2–7: Concept of tolerance analysis and synthesis [Shan A. *et al*, 1999]

Tolerance analysis has been the topics of a tremendous number of research publications, especially in the field of mechanical tolerancing. The methods of tolerance analysis can be very different, either deterministic or statistical, the design models to be analyzed can be 1D, 2D or 3D.

According to the analysis *objectives*, two techniques are generally used:

1- *Worst Case Tolerance Analysis (WCTA)*

2- *Statistical Tolerancing Analysis (STA)*.

In the following sections, we will shortly describe the state of the art concerning tolerance analysis in assemblies and then we will investigate on tolerance analysis in manufacturing.

## 2.3 TOLERANCE ANALYSIS IN ASSEMBLIES

Nigam has defined tolerance and tolerance analysis as: *“Tolerances define allowable variations in the geometry and positioning of parts’ in a mechanical assembly, so as to assure its proper functionality. These tolerances need to be analyzed to estimate the tolerance buildup in the assembly. The functionality of an assembly is determined in terms of variations in some critical assembly response functions”* [Nigam S. D. *et al*, 1995].

Another work that describes tolerance analysis in assembly has been done by Salomons [Salomons O. W. *et al*, 1996a]. He has defined tolerance analysis as: *“After tolerance specification [Salomons O. W. *et al*, 1996b], and checking the coherence and completeness of the specified tolerances. Tolerance analysis can be performed. Tolerance analysis is a method to verify the proper functioning of the assembly after tolerances have been specified. Most often, tolerance analysis is performed by verifying two aspects: feasibility and quality of assembly. In feasibility of assembly the fit is verified. In quality of assembly clearances are verified.”*

Another definition of tolerance analysis in assembly has been provided by Shan [Shan A. *et al*, 2003] as: *“Parts are in specification if they are manufactured within their specified tolerances. If those tolerances were determined to ensure assembly and function, the total product will be acceptable. The study of the aggregate behavior of a series of individual*

variations to determine the tolerances is referred to as tolerance analysis. In tolerance analysis, the cumulative effect of individual dimensional variations to the overall assembly is studied, the resultant assembly and function of the product is verified and checked against its design requirements.”

Analysis approaches can be classified from different points of view and critics. According to *dimensionality* three categories can be considered; one-dimensional (1D), two dimensional (2D), and three-dimensional (3D).

According to the analysis *objectives*; two techniques have been used: (1) *worst case tolerance analysis* (WCTA) and (2) *statistical tolerancing analysis* (STA). Forouraghi has mentioned in [Forouraghi B., 2002]:” *In many engineering designs, several components are often placed together in a mechanical assembly. Due to manufacturing variations, there is a tolerance associated with the nominal dimension of each component in the assembly. The goal of worst-case tolerance analysis is to determine the effect of the smallest and largest assembly dimensions on the product performance. Furthermore, to achieve product quality and robustness, designers must ensure that the product performance variation is minimal.*” In other word if designers base the final selection of tolerances for individual features on satisfying the extreme variation limits, implying 100% “*in-spec*”, it is called “worst case”. As a result, the tolerances are usually very small for manufacturing.

In the probabilistic approach, tolerance analysis involves computing the probability of satisfying the functional requirement under given individual tolerances. It can be described as:

$$P(G(X) \geq 0) = \int_{G(X) \geq 0} f(x) dx \quad (2-2)$$

Where

X is a random vector composed of dimensions

$G(X) \geq 0$  represents certain functional requirements

$f(x)$  the multivariate probability density function for X

In the past few decades, research work has been carried out in statistical tolerance design for problems of loop and fit, most of which are linear and 1D problem. When geometrical tolerances are involved, the statistical tolerance design problem becomes a much more complicated 3D and nonlinear one.

Conventionally, the analysis methods are divided into two distinct categories based on the type of input variations analyzed: *dimensional variations* and *geometrical variations* [Hong Y. S. *et al*, 2002]. In the following, various analysis methods are elaborated.

### 2.3.1 Dimensional tolerance chain models

One of the most widely accepted techniques in tolerance analysis is the tolerance chain technique. In this chapter, a more specific term “dimensional tolerance chain” is used to represent the chain in which a conventional (plus/minus) tolerance is assigned on each arc. This is to be differentiated from a set of new techniques for a chain of three-dimensional geometrical tolerances, which are covered later on. To avoid confusion, we will use the term “3D tolerance propagation” for this last case. Methods based on the dimensional tolerance chain are further classified into three approaches:

- Linear/linearized tolerance accumulation models
- Statistical tolerance analysis
- Monte Carlo simulation methods

*Linear/linearized tolerance accumulation models* trace their history back to the very early age of tolerancing. [Fortini E. T., 1967] is one of the first books to summarize this classical approach. Two most common models are used for tolerance accumulation; worst case and statistical (root sum square, or RSS for short):  $T_{ASM} = \sum_{i=1}^n T_i$  and

$$T_{ASM} = \sqrt{\sum_{i=1}^n T_i^2} \text{ respectively.}$$

From the mid-1990s, people from the same research group reported similar analysis results for more complex 2D/3D mechanical assemblies. Chase [Chase K. W. *et al*, 1995, Chase K. W. *et al*, 1996, Chase K. W. *et al*, 1997a, Chase K. W. *et al*, 1997b, Gao J. *et al*, 1998] defined tolerance analysis as a quantitative tool for predicting variation accumulation in assemblies. As shown in [Figure 2–8](#), tolerance analysis brings the production capabilities and performance requirements together in a well-understood engineering model. It provides a common meeting ground where design and manufacturing can interact and quantitatively

evaluate the effects of their requirements. Thus, it promotes concurrent engineering and provides a tool for improving performance and reducing cost.

In order to create an assembly model for tolerance analysis, specific geometrical information and assembly relationships are required. To this aim Chase proposed a Vector loop of assemblies. Kinematic information is added to the model by creating kinematic joints at mating part interfaces, the type of joint being based on the type of mating contact between parts. The joints are then connected by vectors and linked to form kinematic chains or vector loops.

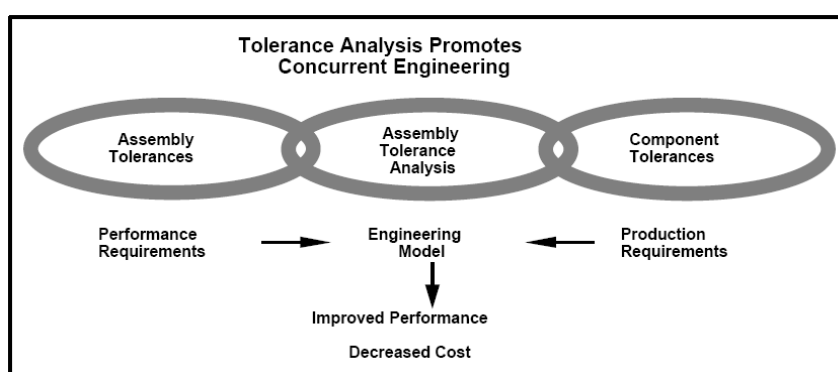


Figure 2–8: Tolerance analysis affects performance and cost [Chase K. W. et al, 1997a]

Robinson and Ward [Robison R. H., 1989][[Larsen G. C., 1991, Ward K., 1992] modeled a set of kinematic joint types (Figure 2–9) to accommodate the possible degrees of freedom in a 3-D assembly. Other constraints, such as geometrical feature tolerances and design specifications, must also be added to the vector loops. This procedure is called the assembly tolerance modeling process. Larsen [Larsen G. C., 1991] further developed Robison's work by automating the procedure of generating the vector loops for assemblies in 2-D space. The algorithms have subsequently been modified for generating vector loop models of assemblies in 3-D space. The vectors are arranged in chains or loops representing those dimensions which "stack" together to determine the resulting assembly dimensions.

The other model elements include kinematic joints, datum reference frames, feature datums, assembly tolerance specifications, component tolerances, and geometrical feature tolerances. Kinematic joints describe motion constraints at the points of contact between mating parts. The assembly tolerance specifications are the engineering design limits on those



assembly feature variations which are critical to performance. Vector models can provide a broad spectrum of the necessary assembly functions for tolerance analysis.

Two advantages of vector assembly models for tolerance analysis are: 1) the geometry is reduced to only those parameters that are required to perform the assembly tolerance analysis, and 2) the derivatives of the assembly function with respect to both the assembly and manufactured dimensions may be obtained more readily from the vector model. This greatly reduces the required computation time. So, assembly variation can be obtained more efficiently, making the system well suited for design iteration and CAD applications

In a similar vein, [Zhang C. *et al*, 1993] reported an analysis result for a cam mechanism. Gao [Gao J. *et al*, 1995] compared the results of the direct linearization with those obtained from the Monte Carlo simulation.

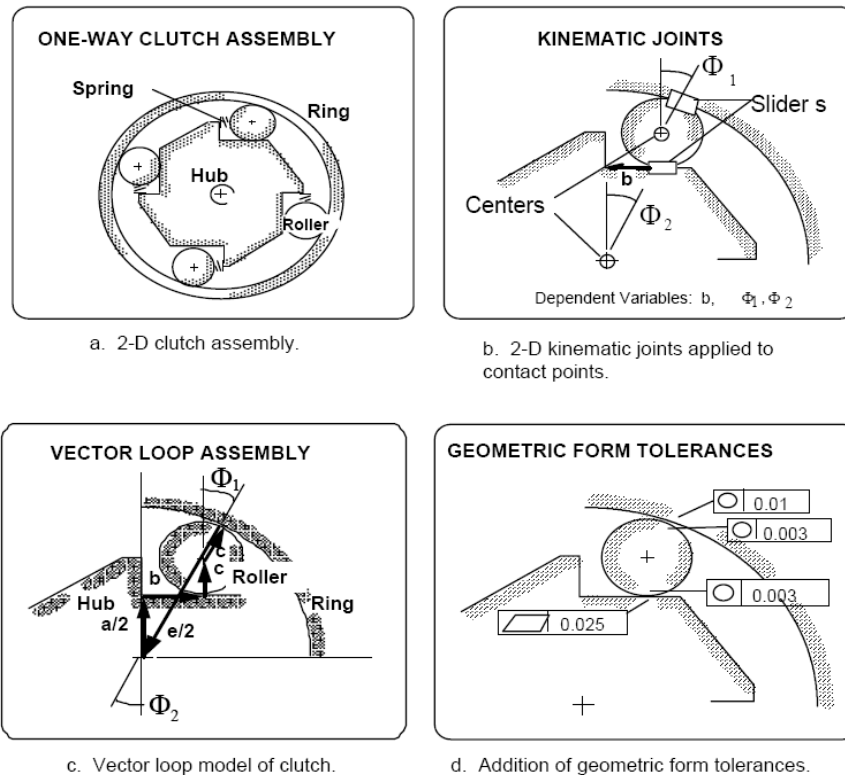


Figure 2-9: Vector loop model of a clutch assembly [Chase K. W. *et al*, 1991]

To provide a theoretical framework for the worst-case tolerance chain analysis, Zhang [Zhang G., 1996] and Zhang and Porchet [Zhang G. *et al*, 1993] proposed a macroscopic framework for tolerance analysis and synthesis, which integrates the tolerancing related activities in both design and manufacturing under the title of “simultaneous tolerancing”.

Another group of tolerance analysis methods, which stems from the dimensional tolerance chain technique, is called the *statistical tolerance analysis*. This method aims to characterize the sum dimension  $Y$  of the design equation  $Y = f(X_1, X_2, \dots, X_n)$ , in statistical terms, starting from an assumption of a certain distribution of  $X_i$ s. It relies mostly on the methods of moments explained in [Evans D. H., 1974], i.e. concentrates on the estimation of moments of  $Y$  such as mean, variance, etc. Bjørke [Bjørke Ø., 1989] is the most representative works in this field. Based on the classification of chain links, he derived various cases of spans and gaps in detail, one by one.

Varghese used a numerical convolution to derive an efficient method to deal with the finite range P.D.F. (Probability Density Function) [Varghese P. *et al*, 1996a]. Lin showed the work that uses the beta distribution, instead of the Gaussian (normal) distribution, in preference of its flexibility [Lin S.-S. *et al*, 1997].

Derivation of the statistical moments of a function of random variables, such as  $Y = f(X_1, X_2, \dots, X_n)$ , in an analytic manner is always a challenge, especially when the functional form is complicated. Thus, for the statistical analysis of real world problems of the, the *Monte Carlo simulation method* is frequently used. By generating the random variants for  $X_i$ s from a certain distribution, the moments for  $Y$  can be estimated statistically, once the design function  $f$  is given. Turner and Wozny [Turner J. U. *et al*, 1987] show the extensive use of Monte Carlo method in the development of the variational geometry system, called GEOTOL, which is based on the feasibility space approach. As stated above, application of this method requires an explicit definition of the design function. However, it is usually difficult to define such a function in 2D/3D mechanical assemblies, so [Gao J. *et al*, 1995] proposed a method for an application of the Monte Carlo method to the implicit assembly constraints. The usage of Monte Carlo simulation is quite limited, due to the lack of explicitly derived equations. In most simulation based analysis, it is of practical concern how to achieve a reasonable confidence level with fewer simulation runs. Thanks to its flexibility, the Monte Carlo method is adopted by most commercial software packages. One of the most popularly used commercial packages is Variation Simulation Analysis, or VSA, whose backbone is also Monte Carlo simulation. The software has been integrated into some of the most popularly used CAD/CAM packages including CATIA, Pro/Engineer and UniGraphics. Further investigations in the tolerance analysis software can be found in [Roy U. *et al*, 1991].

Tolerance analysis based on the dimensional tolerance chain models, which is presented in this section, is a relatively well-established field. More thorough treatment of this topic can be found in [Kirschling G., 1991] and [Liggett J. V., 1992].

### 2.3.2 Representation and propagation of 3D Tolerances

As geometrical tolerances are generally accepted as industry practices, it can be noticed that the dimensional tolerance chain models presented in section 2.3.1 do not meet the ever-tightening requirements of tolerance analysis in various fields. Industry and academia are in need of a suitable analysis scheme that can handle the three-dimensional geometrical tolerances and analyze how those geometrical tolerances are propagated in three-dimensional space, i.e. so-called “3D tolerance propagation” or “3D tolerance stack-up” or “3D tolerance accumulation”. The development of a 3D tolerance propagation scheme requires two essential elements that are closely related each other;

1- *Representation of tolerance zone.* The term “tolerance zone” represents the variation scope for a geometrical element or its feature based on the chosen standard. (e.g. a plane or a cylinder axis). So, we believe that the term variation zone should be used instead as it is used by Shen in [Shen Z. *et al*, 2005]. The main step of the 3D tolerance propagation research usually starts with the investigation on how to model the variation zones. A good model of variation zones should be able to convey the full semantics of geometrical tolerances and, at the same time, it should be equipped with a general structure which can help analyze how the tolerances are propagated in the three-dimensional space. Many models of this kind were proposed in the 1990s, each from a slightly different perspective.

2- *A spatial tolerance propagation mechanism*

In the 1990s, much progress was made in this field, mainly in theoretical aspects, most of which are summarized in this section. The review will be classified and presented in the following order:

- Preliminary work
- Kinematic formulation of tolerances
- Small displacement torsor (SDT)

- Matrix representation
- Vectorial tolerancing

### 2.3.2.1 Preliminary work

*Preliminary work*, which motivated the development of the 3D tolerance propagation techniques, includes the works by Russian scientists, which is introduced in [Portman V. T. *et al*, 1987, Portman V. T. *et al*, 1995] as the spatial dimensional chain technique. Although the geometrical tolerances are not explicitly taken into account, they model the propagation of position errors in terms of an open kinematic chain where the individual error  $\varepsilon_i$  for the  $i^{\text{th}}$  link is represented as an infinitesimal matrix:

$$\varepsilon_i = \begin{pmatrix} 0 & -\gamma_i & \beta_i & \delta_{xi} \\ \gamma_i & 0 & -\alpha_i & \delta_{yi} \\ -\beta_i & \alpha_i & 0 & \delta_{zi} \\ 0 & 0 & 0 & 1 \end{pmatrix} \quad (2-3)$$

Where  $\delta_{xi}$ ,  $\delta_{yi}$ ,  $\delta_{zi}$  are linear position errors and  $\alpha_i$ ,  $\beta_i$ ,  $\gamma_i$  are angular position errors.

Another early work, which formed a fundamental basis for the 3D tolerance propagation methods, is presented in [Fleming A., 1988]. This article shows how a toleranced part can be represented as a network of zones and datums connected by arcs to which equality/inequality constraints are assigned. These constraints are derived by identifying one of the four types of relationships: from datums to zones, between datums, between zones, and from zones to datums. The total effects of the constraints are calculated by finding all paths between two nodes in a network. Contact conditions are also modeled as constraints for the analysis of the assembly of toleranced parts.

### 2.3.2.2 Kinematic formulation of tolerances

One of the foremost works is called a *kinematic formulation of tolerances*, and was introduced by Rivest [Rivest L. *et al*, 1994]. This method exploits the kinematic character of the link imposed by a tolerance between its datum and its toleranced feature. The description of tolerance zones is encapsulated within the kinematic structure. It is reported that this

modeling scheme enables the fundamental tolerance analysis problem to be solved, taking into account the effect of modifiers and datum preference. In a similar vein, Laperrière and Lafond [Laperrière L. *et al*, 1999] proposed a kinematic chain model associating a set of six virtual joints, three for small translations and three for small rotations, to every pair of functional elements in a tolerance chain. They modeled explicitly the propagation of small dispersions along the tolerance chain using Jacobian transforms that provide the desired analysis relationship [Laperrière L. *et al*, 1998] [Lafond P. *et al*, 1999] [Laperrière L. *et al*, 2000] [Laperrière L. *et al*, 2001] . See [Figure 2–10](#).

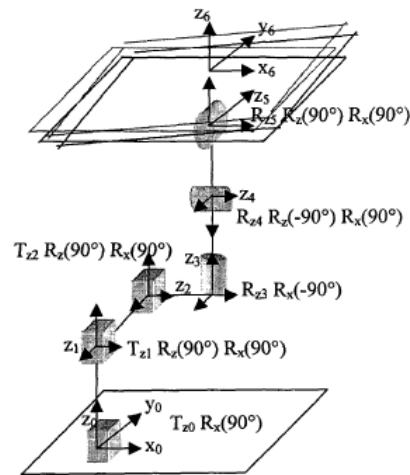


Figure 2–10: Adding virtual joints and coordinate frames to FE pairs (example of two planes of the same part) to model spatial relationships [Lafond P. *et al*, 1999]

### 2.3.2.3 Small displacement torsor (SDT)

A set of 3D tolerance propagation models based on the concept of the *small displacement torsor (SDT)* [Bourdet P. *et al*, 1996] are actively supported by many researchers. SDT is a mathematical object that represents the displacement of a rigid body in which three rotations and three translations are involved. Based on the assumption that the displacements are small, the linearization is used to derive the final torsor  $T$  at point  $O$  in coordinate basis  $\vec{X}, \vec{Y}, \vec{Z}$  : (Eq. 2-4)

$$T = \left\{ \begin{array}{cc} rx & tx \\ ry & ty \\ rz & tz \end{array} \right\}_{(O, \vec{X}, \vec{Y}, \vec{Z})} \quad (2-4)$$

For example, SDT can be used to express the relative position of two planes [Figure 2–11](#). A perfect form plane called “associated surface” is associated to a real one using a minimum distance criterion such as the least square called “associated surface”. The deviation of the associated plane in relation to its nominal position is expressed in the local coordinate basis  $\mathbf{X}, \mathbf{Y}, \mathbf{Z}$  at point  $O$  as indicated in Eq. 2-5. (More details in this regards are presented in the next chapter).

$$T = \left\{ \begin{array}{cc} rx & 0 \\ ry & 0 \\ 0 & tz \end{array} \right\}_{(O, \mathbf{X}, \mathbf{Y}, \mathbf{Z})} \quad (2-5)$$

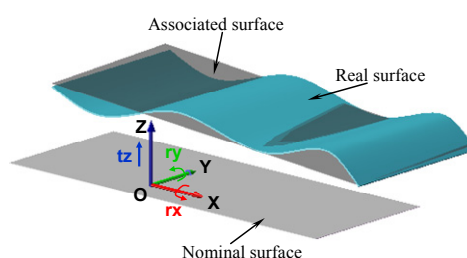


Figure 2–11: Deviation of a plane

Another work trace its origin back to [Giordano M. *et al*, 1992] which introduces a new concept called clearance space. Giordano presented a theoretical representation of the notion of clearance between two parts connected by prismatic surfaces. As an extension of this theoretical work, [Giordano M. *et al*, 1993] another concept called *deviation volume* has been added, and the topological operations on those volumes has been investigated. Two kinds of associations, serial and parallel, are defined in terms of operations in the respective clearance/deviation spaces, which forms a fundamental basis for the development of a 3D tolerance chain. Although Giordano and Duret did not have a specific mathematical object in mind at the time of the theory building, Giordano *et al* then used a torsor to represent deviation volume [Giordano M. *et al*, 1999].

An established theory of the SDT-based 3D tolerance propagation first appeared in [Bourdet P. *et al*, 1995]. It investigates a set of limitations of the traditional tolerance chain models and proposes a model that uses a set of different kinds of torsors: deviation torsor, variation torsor, gap torsor, and small displacement torsor per part.

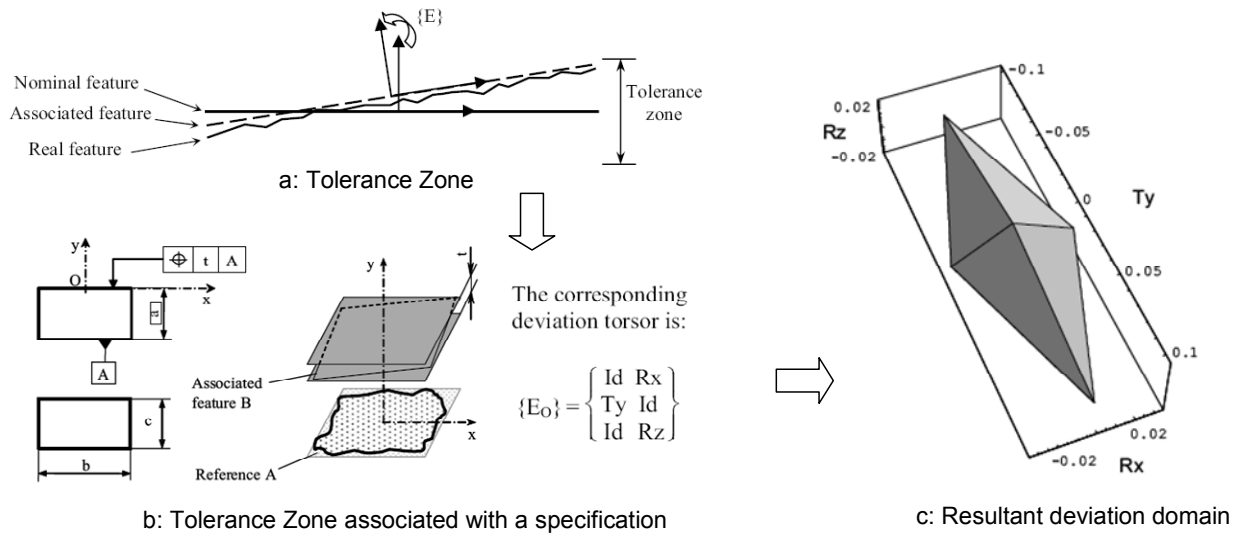


Figure 2-12: Deviation Domain example from [Samper S. et al, 2006]

Two operators, *intersection* and *union*, are also defined, which dictate the rules for 3D tolerance propagation. This tolerance propagation method is refined in [Ballot E. et al, 1998], where the composition and aggregation methods for deviations are formalized. The SDT-based approach has been further advanced in [Teissandier D. et al, 1998] [Teissandier D. et al, 1999a], using the concept of PACV (proportioned assembly clearance volume).

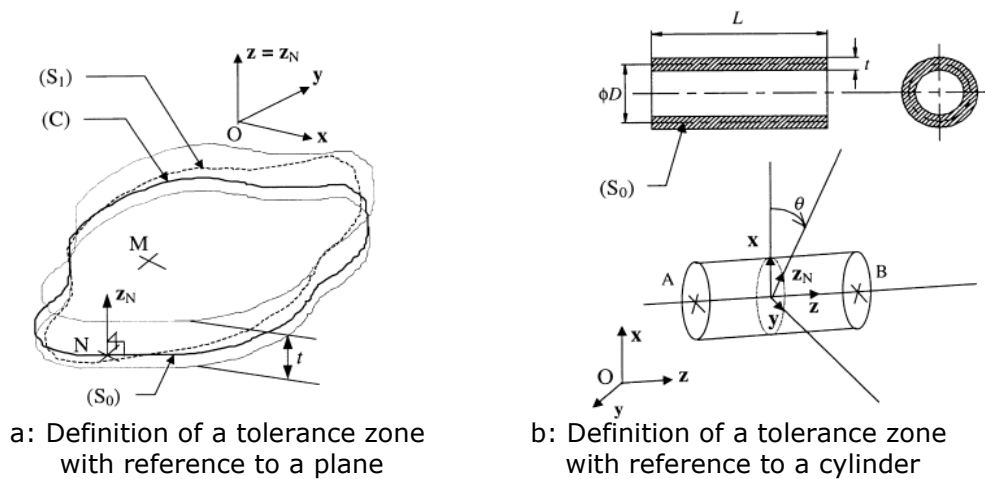


Figure 2-13: The association of a PACV with a complex surface [Teissandier D. et al, 1999a]

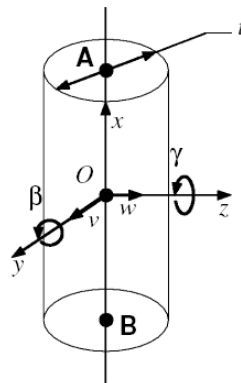
By modeling the tolerated surface, it is reportedly possible to compute the limits of the small displacements of a tolerated surface inside a tolerance zone. The values of these limits define a PACV. They showed how PACVs could be associated in series or in parallel between any two surfaces, which forms a basis for the 3D tolerance chain. Teissandier [Teissandier D.

et al, 1999b] shows that the calculation of PACVs can be done with two operations: the Minkowski sum and the intersection. [Figure 2–13](#).

### 2.3.2.4 Matrix representation

There is another group of researchers who adopt the theory of matrices to model the tolerance zones, e.g. *matrix representation* of tolerances. Among others, [Desrochers A. et al, 1997] is the most representative work of this kind. From a mathematical point of view, the position of a geometrical element with respect to a global reference frame is changed only by the displacement that does not leave it globally invariant, i.e. non-invariant displacement. Keeping this in mind, defining a tolerance (variation) zone can be done by considering only the parameters for non-invariant displacements. For instance, a cylindrical surface is invariant under a rotation and translation along its own axis. So the non-invariant displacement for a cylinder has four degrees of freedom left, as depicted in [Figure 2–14](#), and they can be represented in the form of a homogeneous transformation matrix:

$$D(v, w, \beta, \gamma) = \begin{pmatrix} \cos \gamma \cos \beta & -\sin \gamma & \cos \gamma \sin \beta & 0 \\ \sin \gamma \cos \beta & \cos \gamma & \sin \gamma \sin \beta & v \\ -\sin \beta & 0 & \cos \beta & w \\ 0 & 0 & 0 & 1 \end{pmatrix} \quad (2-6)$$



*Figure 2–14: Cylinder tolerance zone for matrix representation [Desrochers A. et al, 1997]*

This matrix representation is completed by a set of inequalities defining the bounds of the tolerance zone. See Eq. [2-7](#).



$$\sqrt{(Y_{dA}^2 + Z_{dA}^2)} \leq \frac{1}{2}t \quad \text{with} \quad \begin{bmatrix} X_{dA} \\ Y_{dA} \\ X_{dB} \end{bmatrix} = D \times A \quad (2-7)$$

$$\sqrt{(Y_{dA}^2 + Z_{dA}^2)} \leq \frac{1}{2}t \quad \text{with} \quad \begin{bmatrix} X_{dA} \\ Y_{dA} \\ X_{dB} \end{bmatrix} = D \times A$$

$$0 \leq \beta \leq \pi \quad \text{and} \quad 0 \leq \gamma \leq \pi$$

In this method, the propagation of tolerances in a chain is handled by a usual coordinate transformation, which is also represented by a matrix. Salomons shows some applications of this matrix-based method to the tolerance analysis problems [Salomons O. W. *et al*, 1996a]. Other methods using the matrix representation of tolerances can also be found in [Whitney D. E. *et al*, 1994].

### 2.3.2.5 Vectorial tolerancing

Since it is very intuitive to represent a chain of dimensions and tolerances as a link of vectors, some approaches have been reported that use *vectorial tolerancing* [Wirtz A., 1991] [Wirtz A. *et al*, 1993] for the 3D tolerance analysis. See [Figure 2–15](#).

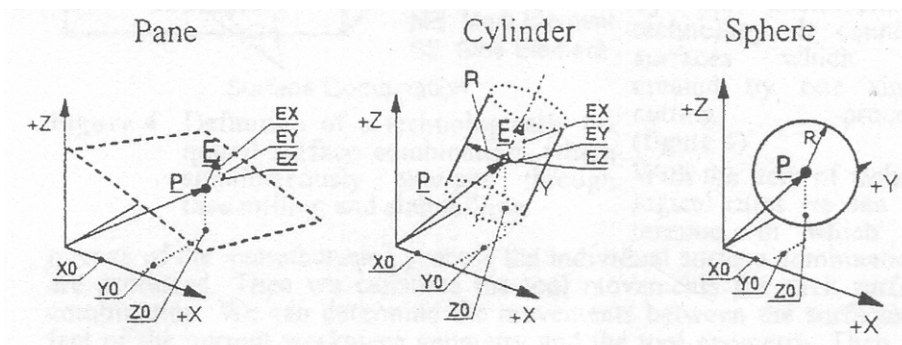


Figure 2–15: Vectorial description [Wirtz A., 1991]

Martinsen has mentioned this approach as a potential application area of vectorial tolerancing [Martinsen K., 1993]. Inspired by this work, Varghese provided a method for geometrical tolerance analysis by means of vectorial tolerancing [Varghese P. *et al*, 1996b]. Because the geometrical and vectorial tolerances are totally different tolerancing schemes, it is not an easy task to convert one to the other. Thus, most of their work is also dedicated to

the conversion work. Radouani [Radouani M. *et al*, 2000] presents a new approach for minimal chains in 3D tolerancing, which is based on homogeneous transformation matrix using vectorial tolerancing. A comparison of GD&T and VD&T tolerance analysis methods is also given.

A detailed review of the literature available on tolerance analysis of assemblies can be found in [Hong Y. S. *et al*, 2002], [Mathieu L. *et al*, 1997], [Nigam S. D. *et al*, 1995] and [Shen Z. *et al*, 2005].

## 2.4 TOLERANCE ANALYSIS IN A MULTI-STAGE MACHINING PROCESS (MSMP)

In the literature available on this subject, the evaluation of a process plan in terms of functional tolerances is called the tolerance analysis in machining. The purpose of a tolerance analysis is to verify whether the functional tolerances of a part can be met for a given process plan with specified manufacturing deviations. In tolerance analysis, the cumulative effect of the individual variations with respect to the specified functional tolerance in all machining operations is studied in order to check a product's functionality compared with its design requirements. This is also referred to as error propagation, *error stack-up and tolerance stack-up in a multi-stage machining process*.

Component (part) and assembly designs are the two major tasks in any design department. Component design provides a single component drawing that include dimensions and dimensional and geometrical tolerances. Some examples of components are: shaft, gear, pulley, etc. However, it is unlikely to have a component functioning alone as there is a need to assemble it with other components. Assembly design studies the suitability of two or more components to meet a functional requirement. When assembling parts together, there should be some manufacturing variation in the part that will cause *assembly tolerance stack-up*. In preceding section we have reviewed in detail some assembly examples.

From a “method” point of view, machining tolerance stack-up analysis simulates manufacturing variations whereas assembly tolerance analysis simulates component variations because of manufacturing variations. The two analyses are close in the sense that we are trying to analyze the effect of deviations accumulation on a *functional requirement* in

the case of assembly tolerance analysis and a *functional tolerance* in the case of machining tolerance analysis. Some research works have been done in assembly tolerance stack-up in the literature. Although this seems quite close to our work on tolerance stack-up for machining, there are exclusive differences between the two problems, their formulations and applications.

A machining process consists in different setups (operations). In machining, the errors are produced in each setup and are propagated through different setups via datum surfaces. The propagation of errors through different setups does not exist in assembly process where all the components are assembled together usually in a same time. As a result, the main difference between error stack-up in machining and assembly from a formulation point of view is this propagation mechanism. Furthermore the positioning phenomenon of a part in a fixture with clamping force is sophisticated enough compared to assembling the components.

This section shall focus on tolerance analysis relating to error propagation in a MSMP. Modeling the error propagation for a set of successive machining operations is surprisingly a less explored topic compared with assemblies. This may be due to the fact that parts and processes are highly complex. Most studies focus on single machine station problems, such as robust fixture design in order to minimize work piece errors [Cai W. *et al*, 1997], definition of the impact of fixture locator tolerance on datum errors [Choudhuri S. A. *et al*, 1999], or the study of machine tool error compensation [Chen J. S. *et al*, 1993]. In the following, the existing approaches for tolerance analysis in machining are explored.

## 2.4.1 State space approach

### 2.4.1.1 Huang *et al* (2003)

Huang proposes a state space model to describe part error propagation in the successive machining operations [Huang Q. *et al*, 2003]. Surface deviation is expressed in terms of deviation from nominal orientation, location and dimensions. The authors assumed that part models need only to describe features relevant deviation therefore they have used a revised version of vectorial surface model that was developed by [Martinsen K., 1993]. In the revised model, a part has  $n$  surfaces related to the error propagation. Those  $n$  surfaces include surfaces to be machined, design datums, machining datums and measurement datums. In a coordinate system, the  $i^{\text{th}}$  surface  $\mathbf{X}_i$  can be described by its surface orientation  $\mathbf{n}_i = [n_{ix}, n_{iy}, n_{iz}]^T$ ,

location  $\mathbf{p}_i = [p_{ix}, p_{iy}, p_{iz}]^T$ , and size  $\mathbf{D}_i = [d_{i1}, d_{i2}, \dots, d_{im}]^T$ . By stacking up  $\mathbf{n}_i$ ,  $\mathbf{p}_i$  and  $\mathbf{D}_i$ ,  $\mathbf{X}_i$  is represented as a vector with dimension  $(6+m)$ , as indicated in Eq. 2-8.

$$\text{Surface } \mathbf{X}_i: \mathbf{X}_i = \begin{bmatrix} \mathbf{n}_i^T \\ \mathbf{p}_i^T \\ \mathbf{D}_i^T \end{bmatrix}_{(6+m) \times 1}^T \quad (2-8)$$

Where  $m$  is the number of size parameters in  $\mathbf{D}_i$ . Size parameter here has broader meaning than that for the dimension of size given by GD&T.

With the representation for an individual part surface, the part is modeled as a vector by stacking up all surface vectors, as indicated in Eq. 2-9.

$$\text{Part model: } \mathbf{X} = [\mathbf{X}_1^T, \mathbf{X}_2^T, \dots, \mathbf{X}_n^T]^T \quad (2-9)$$

### Part deviation

The authors expressed a feature deviation that is the deviation of surface  $\mathbf{X}_i$  from the ideal surface by Eq. 2-10. See Figure 2-16.

$$\text{Surface deviation from nominal: } \Delta \mathbf{X}_i = \begin{bmatrix} \Delta n_i^T \\ \Delta p_i^T \\ \Delta D_i^T \end{bmatrix}^T \quad (2-10)$$

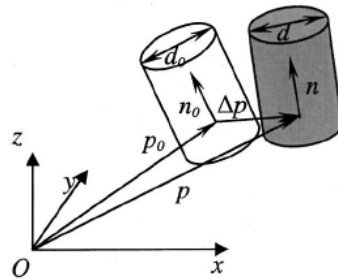


Figure 2-16: Cylinder surface and surface deviation representation

Part deviation is then calculated by using its surface deviation. If  $\mathbf{x}$  denotes part deviation  $\Delta \mathbf{X}$ ,  $\mathbf{x}$  can be expressed by Eq. 2-11.

$$\text{Part deviation from nominal: } \mathbf{x} = [\Delta \mathbf{X}_1^T, \Delta \mathbf{X}_2^T, \dots, \Delta \mathbf{X}_n^T]^T \quad (2-11)$$

In this case  $x(k)$  represents the intermediate part deviation after operation  $k$

The error sources in machining operations are classified as setup errors (fixture errors, datum errors) and machine tool errors. Three coordinate systems have been used as follow:

- M-Coordinate: the machine tool coordinate
- F-Coordinate: the fixture coordinate
- P-Coordinate: the part coordinate

Homogenous transformation is used by the author for modeling the part transformation between different coordinate system. See Eq. 2-12.

$$\begin{bmatrix} \mathbf{X}_F \\ \mathbf{1} \end{bmatrix} = \begin{bmatrix} {}^F R_P & {}^F \mathbf{T}_P \\ \mathbf{0} & \mathbf{1} \end{bmatrix} \begin{bmatrix} \mathbf{X} \\ \mathbf{1} \end{bmatrix} \quad \text{and} \quad \begin{bmatrix} \mathbf{X}_M \\ \mathbf{1} \end{bmatrix} = \begin{bmatrix} {}^M R_F & {}^M \mathbf{T}_F \\ \mathbf{0} & \mathbf{1} \end{bmatrix} \begin{bmatrix} \mathbf{X}_F \\ \mathbf{1} \end{bmatrix} \quad (2-12)$$

Setup errors (position error) are calculated by considering the error of the part in the fixture and the fixture on the machine table as follow:

$$\mathbf{X}_M(k-1) = {}^M R_P(k) \mathbf{X}(k-1) + {}^M \mathbf{T}_P(k) \quad (2-13)$$

Where:

$${}^M R_P(k) = {}^M R_F(k) {}^F R_P(k) \quad \text{and} \quad {}^M \mathbf{T}_P(k) = {}^M R_F(k) {}^F \mathbf{T}_P(k) + {}^M \mathbf{T}_F(k) \quad (2-14)$$

The fixture error is represented by the deviation of its locators. The actual transformation from F-Coordinate to M-Coordinate is represented by the summation of a nominal transformation and the deviation caused by fixture errors as:

$$\begin{aligned} {}^M R_F(k) &= {}^M R_F^o(k) + \Delta {}^M R_F(k) \\ {}^M \mathbf{T}_F(k) &= {}^M \mathbf{T}_F^o(k) + \Delta {}^M \mathbf{T}_F(k) \end{aligned} \quad (2-15)$$

The datum introduces the deviation as well. The actual transformation from P-Coordinate to F-Coordinate is represented by the summation of a nominal transformation and the deviation caused by datum errors:

$$\begin{aligned} {}^F R_P(k) &= {}^F R_P^o(k) + \Delta {}^F R_P(k) \\ {}^F \mathbf{T}_P(k) &= {}^F \mathbf{T}_P^o(k) + \Delta {}^F \mathbf{T}_P(k) \end{aligned} \quad (2-16)$$

For modeling the machine tool errors, the authors assumed that  $k^{\text{th}}$  machining operation generates new part  $\mathbf{X}_M(k)$ , which can be divided into the machined surfaces  $B(k)$   $\mathbf{X}_M(k)$ , and the uncut surfaces  $A(k)$   $\mathbf{X}_M(k-1)$ :

$$\mathbf{X}_M(k) = A(k)\mathbf{X}_M(k-1) + B(k)\mathbf{X}_M^u(k) \quad (2-17)$$

By transforming it back to the part coordinate the part deviation will be:

$$\mathbf{x}(k) = A(k)\mathbf{x}(k-1) + B(k)\mathbf{x}^u(k) + \mathbf{w}(k) \quad (2-18)$$

### Error stack-up mechanism

A part's deviation is expressed in terms of the deviation of its surfaces and is stored in a state vector  $\mathbf{x}(k)$ . This vector is then modified by moving from operation  $k$  to  $k+1$ . See Figure 2–17.

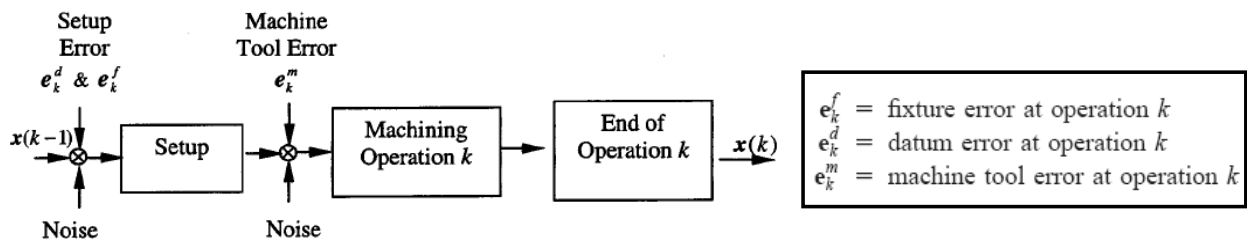


Figure 2–17: Error propagation [Huang Q. et al, 2003]

#### 2.4.1.2 Zhou et al (2003)

Zhou uses the same state model but the surface deviation compared with the nominal state is expressed using a differential motion vector [Zhou S. Y. et al, 2003]. The authors used a location vector and a vector that consists of three rotating Euler angles to present a work piece feature, Figure 2–18. For a part, there is a Reference Coordinate System (RCS) and for each feature there is a local coordinate system (LCS). The deviation of the feature is described by the deviation of the corresponding actual LCS from the corresponding nominal LCS. The

deviation of a LCS is represented by a differential motion vector  $X_n^R \begin{bmatrix} d_n^R \\ \theta_n^R \end{bmatrix}$ . In summary; a

location vector and an orientation angular vector are used by the authors to represent a feature in the RCS. The relative position and orientation of a feature is described as a *homogenous transformation matrix*. The deviation of a feature from its nominal value is represented by a differential motion vector.

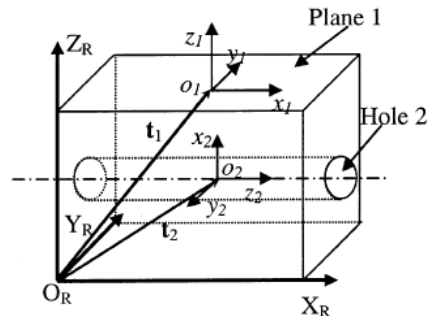


Figure 2–18: Illustration of feature representation [Zhou S. Y. et al, 2003]

They have considered different coordinate systems as follow: (Figure 2–19)

- LCS represents the features of the work piece.
- RCS is the reference for the features of the work piece’s Coordinate: the part coordinate
- Fixture Coordinate System (FCS) is determined by the actual fixture setup
- Nominal Fixture Coordinate System (FCS). In other word “Machine Coordinate System

The authors considered a state vector  $\mathbf{x}(k)$  which is defined as a stack of differential motion vectors corresponding to each feature. There are three major components in  $\mathbf{x}(k)$ :

- 1- Machining error, which is defined as the deviation of the cutting tool from its nominal path
- 2- Fixturing error, which is caused by the imperfection of the locators
- 3- Datum error, which is the deviation of FCS with respect to RCS.

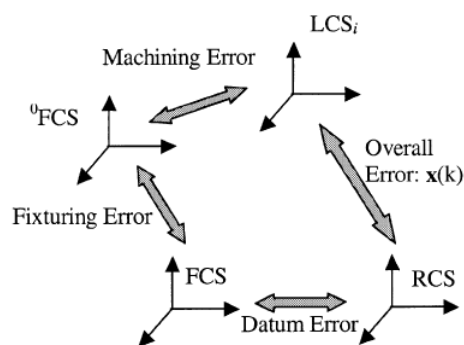


Figure 2–19: Composition of overall feature deviation[Zhou S. Y. et al, 2003]

### Error stack-up mechanism

For calculating the error stack, Zhou *et al*, proposed a linear discrete state space formula:

$$\begin{aligned} \mathbf{x}(k+1) &= A(k)\mathbf{x}(k) + B(k)\mathbf{u}(k) + \mathbf{w}(k) \\ \mathbf{y}(k) &= C(k)\mathbf{x}(k) + \mathbf{v}(k) \end{aligned} \quad (2-19)$$

where  $A(k)\mathbf{x}(k)$  represents the deviations of previously machined features and the deviation of newly machined features that have only contributed by the datum error,  $B(k)\mathbf{u}(k)$  represents the work piece deviation caused by the relative deviation between the work piece and the cutting tool (this deviation is caused by the fixture error and the imperfection of the tool path),  $\mathbf{y}(k)$  is the measurement,  $\mathbf{w}(k)$  is the system noise, and  $\mathbf{v}(k)$  is the measurement noise. Two assumptions are implied in this formulation: 1) machining error on single stage is modeled as a tool path deviation from its nominal path and 2) only position and orientation error are considered. Profile error is not included. See [Figure 2–20](#).

### Discussion

These two models require specific fixture setups (e.g., an orthogonal 3-2-1 fixture layout). Furthermore the authors have not explained how this model can deal with the statistical or worst case tolerance analysis.

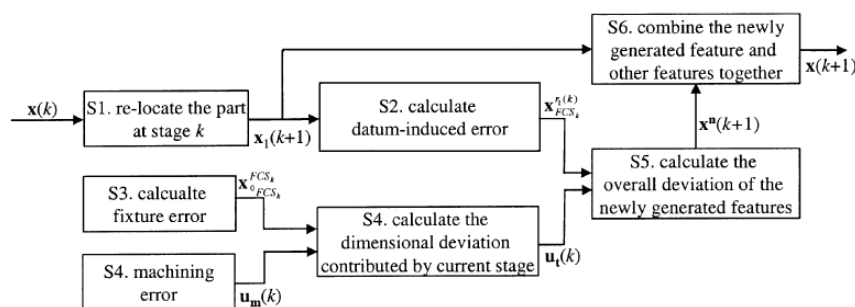


Figure 2–20: Steps of the derivation of the variation propagation model

#### 2.4.1.3 Loose et al (2007)

More recently, Loose used the same state space model just presented before with a differential motion vector but including general fixture layouts [Loose J. P. *et al*, 2007]. The authors used a state vector ( $\mathbf{X}_k$ ) which is a stack of differential motion vectors to represent the



part deviation. The deviation of a feature is expressed by a homogeneous transformation matrix (HMT). See [Figure 2-21](#).

The authors considered a state vector  $\mathbf{X}(k)$  which is defined as a stack of differential motion vectors corresponding to each feature. There are two major components in  $\mathbf{X}(k)$ :

- 1- Machining error, this is defined as the deviation of the cutting tool from its nominal path ( $q_i$ )
- 2- Setup errors which is caused by the imperfection of the locators and the datum errors. ( $q_p$ )

The setup errors (positioning error) can be expressed as Eq. [2-20](#):

$$q_p = J^{-1} \cdot (F_1 \cdot U + F_2 \cdot q') \quad (2-20)$$

Where  $U$  is the fixture error because of its  $m$  locators and  $q'$  is the datum error.  $F_1$  and  $F_2$  are the contributions of the fixture errors and datums errors respectively and  $J^{-1}$  is the Jacobian.

The overall deviation of a realized surface in operation  $k$ , is the summation of the two above defined errors:

$$q' = F_3 \cdot q_p + F_4 \cdot q_i \quad (2-21)$$

Combining Eq. [2-20](#) and Eq. [2-21](#), the deviation of the  $i^{\text{th}}$  newly generated feature can be obtained as:

$$q'_i = F_3 \cdot J^{-1} \cdot F_2 \cdot q' + F_3 \cdot J^{-1} \cdot F_1 \cdot U + F_4 \cdot q_i \quad (2-22)$$

Where  $q_p$  is the setup error (because of fixture and datum) and  $q_i$  is machining errors.  $F_3$  and  $F_4$  are the contributions. The error stack-up mechanism used by the authors is the same as those proposed by Zhou [Zhou S. Y. *et al*, 2003], with the same assumptions.

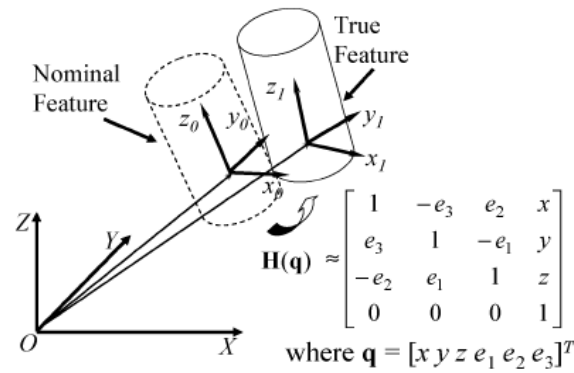


Figure 2–21: Concept of state vector [Loose J. P. et al, 2007]

Although a general fixture layout is considered, the error calculation of a fixture is based on its locator deviations (a locator is a punctual connection). Hence, positioning cases with Plane/Plane contact or Cylinder/Cylinder floating contact are not envisaged.

More recently Zhong used the state space modeling for performing some sensitivity and diagnosability analysis in multi-station machining process. [Zhang M. et al, 2007]. [Figure 2–22](#).

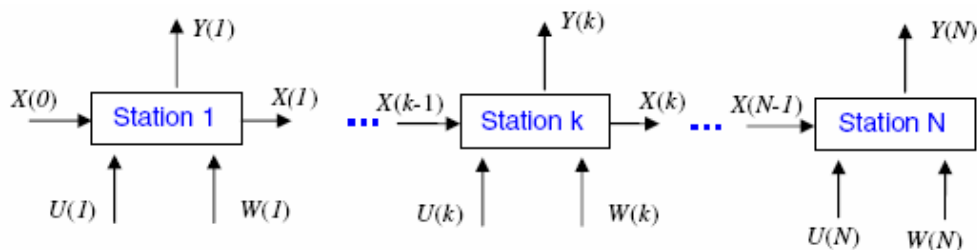


Figure 2–22: Dimensional errors flow in a multi-station manufacturing process [Zhang M. et al, 2007]

#### 2.4.1.4 Zhong et al (2000)

Zhong proposed a general evaluation method for machining systems. One of the considered criteria is quality. To reveal the relationship between quality performance and system configurations, a general variation propagation model is developed by the authors to predict quality performance for different machining system configurations. [Zhong W. et al, 2000]. See [Figure 2–23](#).

The proposed method by Zhong has been used for modeling variation propagation in machining systems [Zhong W. *et al*, 2002] and diagnosis of multiple fixture faults in machining processes [Camelio J. *et al*, 2004].

### Model for representing geometrical errors

A work piece is represented by the dimensional and geometrical information of its features, with respect to the local coordinate system (LCS\_P) of the part. For example, a plane can be defined with six parameters including coordinates of a normal and a point on it. Other features can be represented in a similar way.

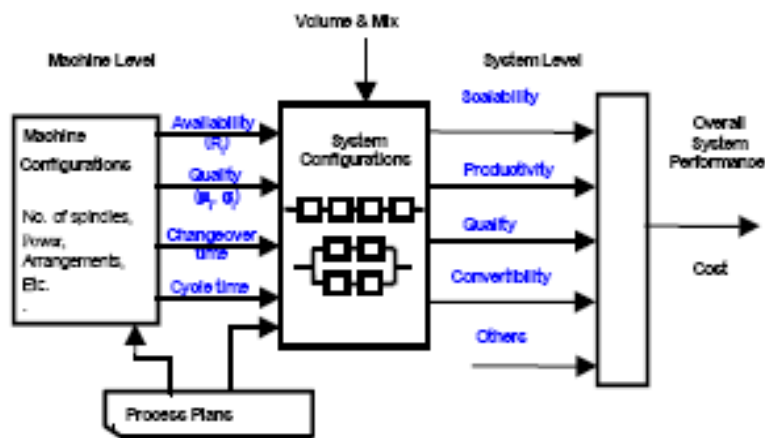


Figure 2–23: System Performance Analysis Approach [Zhong W. *et al*, 2000]

A workpiece is represented by a set of points including the measurement, locating and clamping points. As shown in Figure 2–24, these points are extracted from the meshed 3-D model generated from the CAD software. It is called the point-based model for workpiece. Each point in the point-based model has the ideal coordinates (x,y,z) in its local coordinate system (LCS\_P). To generate the deviations, a certain amount of variation is applied to the ideal coordinate value of each point with the assumption that the points are normally distributed within the tolerance range. All surfaces of a work piece can be represented by the vector  $\mathbf{X}$ . Authors used the Homogeneous Transformation Matrix (HTM) to represent the deviation of a rigid body with respect to its ideal position.

### Error stack-up mechanism

A machining station (one machining setup) is modeled as a system with an input and an output. See Figure 2–25. The stack-up mechanism can be summarized in three steps:

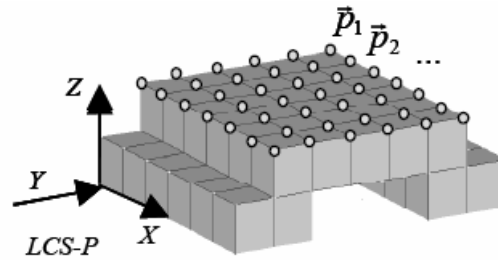


Figure 2–24: Point-based workpiece model [Zhong W. et al, 2002]

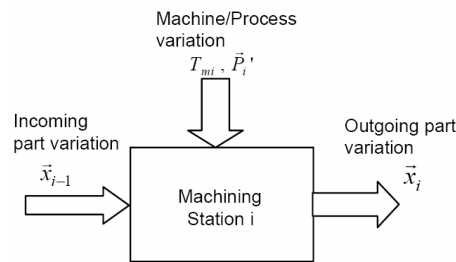


Figure 2–25: Model of machining station

- 1- Pre-machining stage: where the workpiece geometrical dimension is represented by  $\mathbf{X}_{i-1}$  from the previously machined workpiece or raw material.
- 2- Machining stage: where the ideal interaction between the tool path and workpiece surface  $\vec{p}'_i$  is mapped onto the workpiece to create a new surface  $\vec{p}_i$ . This operation is affected by variations from machine tools, fixtures, cutting tools, external cutting and clamping forces, pre-machining stage variation and datum errors.
- 3- Post-machining stage: where the geometrical features of the workpiece are updated to  $\mathbf{X}_i$ , which is input to the next operation. After the last operation,  $\mathbf{X}_i$  represents the end-of-line product. See [Figure 2–26](#).

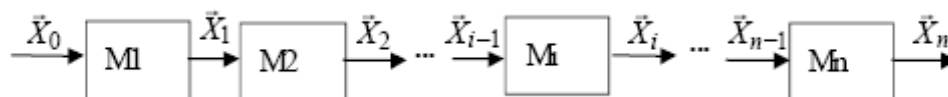


Figure 2–26: Serial machining system [Zhong W. et al, 2000]

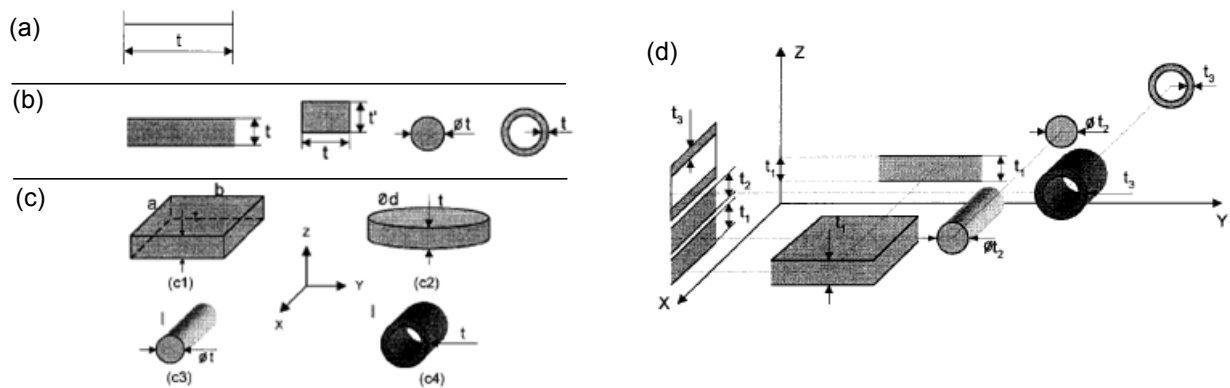
## 2.4.2 Tolerance zone approach

Lin proposed a tolerance stack-up analysis based on tolerance zone analysis [Lin E. E. *et al*, 2001]. As it is underlined before, we believe that the term “variation zone” should be used. Manufacturing errors are classified according to two types of error directly related to the accuracy of a finished part: locating errors and machining errors. Surface deviation is expressed as a tolerance zone. For the aim of deviation modeling, the authors defined three types of tolerance zones: 1D, 2D and 3D. See [Figure 2–27](#).

Authors categorized the manufacturing errors as:

- 1- *Locating error*. The variation between the position of an actual datum feature and the position of an ideal datum.
- 2- *Machining error*. The variation between the position of an actual machining feature and the position of an ideal machining feature.

The authors divided the stack-up mechanism into two sections, the error stack-up mechanism and geometrical tolerance analysis.



*Figure 2–27: Typical tolerance zones (a) 1D, (b) 2D and (c) 3D tolerance zones. (d) The projecting relation of tolerance zones [Lin E. E. *et al*, 2001]*

### Error stack-up mechanism

For error stack-up mechanism, the authors proposed to use the dimension chain (tolerance chart). For 3D parts it is necessary to use the projected chains. From these chains it is possible to perform the worst case or statistical analysis. They assumed that the formulation

of dimensional tolerance stack-up is relatively straightforward. Suppose that in a space, the relation of a resultant dimension  $d$  with its component dimensions is as Eq. 2-23.

$$d = f(x_1, x_2, \dots, x_i, y_1, y_2, \dots, y_m, z_1, z_2, \dots, z_n) \quad (2-23)$$

Where:

$d$ : resultant dimension

$x_i, (i = 1, 2, 3, \dots, l)$  component dimensions in the **X**-coordinate

$y_j, (j = 1, 2, 3, \dots, m)$ : component dimensions in the **Y**-coordinate

$z_k (k = 1, 2, 3, \dots, n)$ : component dimensions in the **Z**-coordinate

Theoretically, the worst case is found by using Eq. 2-24.

$$\Delta d = \sum_{i=1}^l \left| \frac{\partial f}{\partial x_i} \Delta x_i \right| + \sum_{j=1}^m \left| \frac{\partial f}{\partial y_j} \Delta y_j \right| + \sum_{k=1}^n \left| \frac{\partial f}{\partial z_k} \Delta z_k \right| \quad (2-24)$$

Where:

$\Delta d$ : variation of resultant dimension

$\Delta x_i, \Delta y_j, \Delta z_k$ : variations of component dimensions

The statistical analysis use Eq. 2-25.

$$\Delta d = \left[ \sum_{i=1}^l \left( \frac{\partial f}{\partial x_i} \Delta x_i \right)^2 + \sum_{j=1}^m \left( \frac{\partial f}{\partial y_j} \Delta y_j \right)^2 + \sum_{k=1}^n \left( \frac{\partial f}{\partial z_k} \Delta z_k \right)^2 \right]^{\frac{1}{2}} \quad (2-25)$$

### Geometrical tolerance analysis

Generally the authors assume that the variation of a machined surface is caused by the deviation of machining datum and the error of machining. To represent these two types of errors they have used tolerance zones. The relation of these errors on the realized surface is determined by their position in the space. Because of the complexity of 3D parts, the authors proposed to use the homogenous translation and rotation matrices and decomposing 3D tolerance stack-up into series of 2D tolerance stack-up analysis.

For example in Figure 2–28, in 2D, suppose surface  $B$  is used as machining datum for machining surface  $C$  and  $D$  and the variation zone (tolerance zone) of face  $B$  is equal to the tolerance zone of face  $B$ . See Figure 2–28 (a). The variation zone indicates two possible maximum movements of the part: horizontal translation of  $\Delta B$  and rotation of  $\theta$ . Figure 2–28 (b) and (c). The error of face  $D$  used to be considered as equal to the translation of face  $B$ . The translation of face  $B$  has no effect on the error of face  $C$ . The effect of the error of face  $B$  on face  $C$  is through the rotation of  $\theta$ . See Eq. 2-26.

$$\begin{aligned} \Delta_D &= \Delta_B \\ \tan \theta &\cong \frac{\Delta_B}{L_3} \cong \frac{\Delta_C}{L_1} \\ \Delta_C &\cong \frac{L_1}{L_3} \Delta_B \end{aligned} \tag{2-26}$$

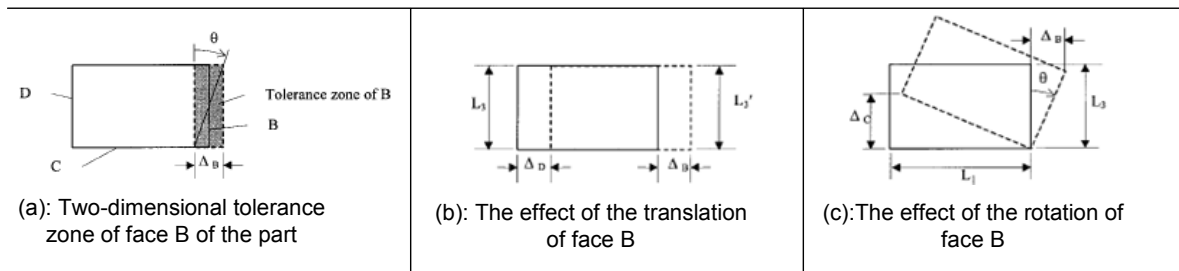


Figure 2–28: 2D tolerance stack-up analysis [Lin E. E. et al, 2001]

### Discussion

In Lin’s work, the datum errors are considered but the fixture error and the contact condition between part and fixture has been neglected.

This model can not be used for modeling a successive machining operation, because there is not a memory and coordinate system for keeping the variation of realized surface. In Lin’s work, only a primary datum face is considered for tolerance stack-up analysis. In practical locating and clamping, a secondary datum face and a tertiary datum face should also be considered. This situation is considered as an open issue in their work.

They have not mentioned how it is possible to handle the tolerance stack-up analysis, when the machining datum and measuring datum are different. Furthermore they have not mentioned how it is possible to find a relation between datum errors and machined surface deviation in the case of a complex 3D part.

### 2.4.3 Simulation approach

Huang proposed a method to verify a process plan in term of machining tolerance prediction [Huang S. H. et al, 2004, Musa R. A. et al, 2004]. Tolerance stack analysis in this study is based on actual machining error synthesis and error propagation tracking through

multiple processes. It has been conducted by Monte Carlo simulation on sample point transition in process.

### Model for representing the geometrical deviations

Each surface has been modeled by uniformly distributed sample points (point cloud) which is a basic technique used in CMM based inspection. Each point has an ideal coordinate  $p_m = (x_m, y_m, z_m)$  in the work piece coordinate system (WCS). This ideal coordinate will be changed according to the different deviation sources. See Figure 2–29.

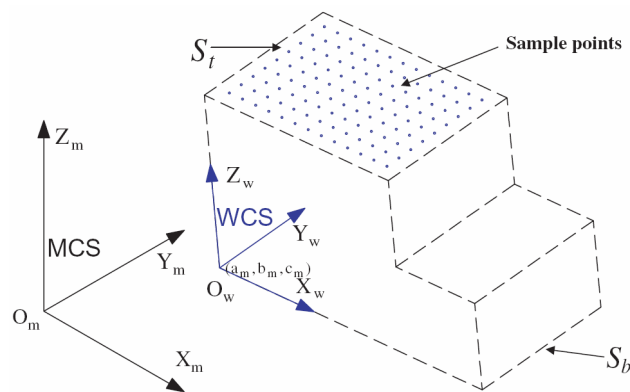


Figure 2–29: A simple work piece represented by point cloud [Huang S. H. et al, 2004]

### Error stack-up mechanism

Key issues involved in Huang's methodology are:

- Sample point generation
- Manufacturing error source
- Error synthesis and tracking
- Virtual inspection.

Simulation method involved in the above mentioned work consists of the following steps:

- 1- *Establish WCS* (work piece coordinate system) for the work piece. Reference point is taken as a vertex of a prismatic part or the centre of a circle, as the origin  $O_w$  and establishes the WCS for the work piece.



- 2- *Represent the raw work piece.* Based on the WCS established in Step 1, generation of sample points to represent each surface of the raw work piece according to its quality as specified (e.g. using surface flatness). The number of points depends on the geometry of the surface.
- 3- *Locate the work piece.* Generation of the points to represent each datum using the given flatness value, then transforming these points using error components based on the given fixture accuracy. The fixture accuracy is obtained by experimental tests of a specific fixture with a nearly perfect part. Fit a least square surface to the obtained points. Find the point of intersection between these surfaces. Consider the intersection point as the translational errors parameter. The rotational components can be obtained by finding the angle of each surface normal with the Cartesian axis. This permits to find the work holding error and calculate the transformation matrix that maps WCS to MCS (Machine Coordinate System).
- 4- *Simulate machining operation.* Map all work piece sample points to the MCS. At each sample point, machine tool error and cutting tool error are sampled from their respective models and synthesized to compute the simulated cutting tool position. If  $\mathbf{p}_m = (x_m, y_m, z_m)$  is a nominal point, due to manufacturing error, after machining it will be  $\mathbf{p}'_m = (x'_m, y'_m, z'_m)$  instead. The resultant coordinates (in MCS)  $P'_m(u)$  (after machining  $u$ ) replace those of the sample point (machined previously in  $v$ )  $P'_m(u - v)$ . See [Figure 2–30](#).
- 5- *Store and propagate work piece accuracy information.* The new sample point coordinates obtained in Step 4 are mapped back to the WCS ( $P'_m(u) \rightarrow P'_w(u)$ ), see Eq. [2-27](#). At this point, the accuracy of the work piece surfaces that have been machined has changed. These surfaces might be used as locating datum in the subsequent machining operations.

$$\mathbf{p}'_w = \mathbf{p}'_m \cdot \mathbf{T}_t^{-1}(a_m, b_m, c_m) \cdot \mathbf{T}_r^{-1}(\theta_x) \cdot \mathbf{T}_r^{-1}(\theta_y) \cdot \mathbf{T}_r^{-1}(\theta_z) \quad (2-27)$$

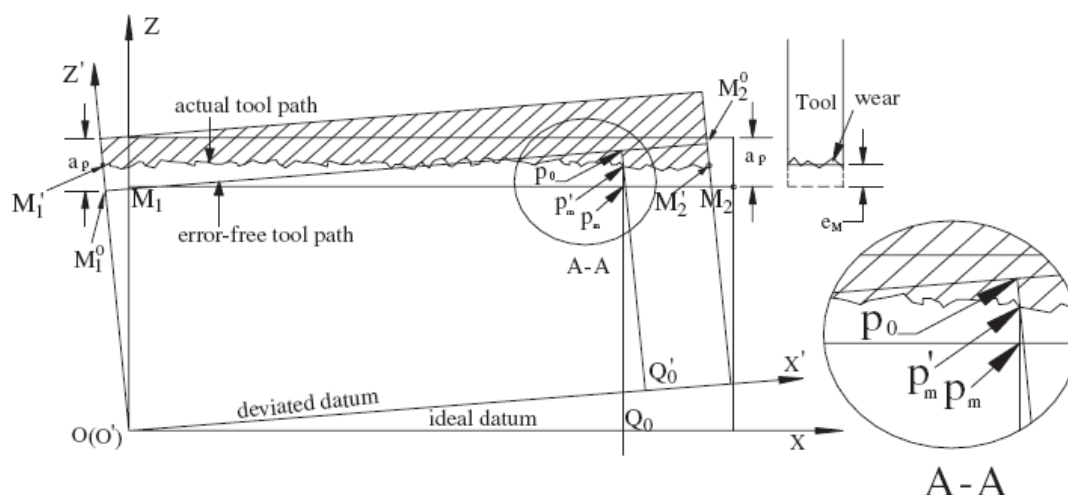


Figure 2–30: Illustration of errors synthesis [Huang S. H. et al, 2004]

- 6- Inspect the finished component based on design tolerance requirements, the dimensional and geometrical accuracy of the machined component are evaluated using CMM inspection algorithms.
- 7- Perform statistical analysis. Determine the desired number of simulation runs  $n$ , and then we will have  $n$  values to interpret for a particular functional tolerance.

### Discussion

This method is a good tool for the simulation of the machining using Monte Carlo simulation. The result of the Monte Carlo simulation is close to reality. Using the sample point instead of an associated surface for representing the machined surfaces is closer to reality.

The main disadvantage of this work is the positioning procedure of the part. Concerning work holding errors, the authors have not considered part-fixture interaction and the hierarchy procedure of positioning. As the authors proposition, the fixture errors are established by test of fixture with a perfect part (gauge block). After finding the fixture errors, the errors related to part datum will be added to this value.

Authors explained only the plane-plane contact, and it is not clear how this system can deal with a floating cylinder-cylinder contact. This simulation method, because of Monte Carlo and sampling point generation, needs much running time.

#### 2.4.4 SDT approach

The first approach using SDT for the aim of error stack-up analysis in machining goes back to [Villeneuve F. *et al*, 2001] in which Villeneuve adapted the SDT concept for analyzing error-stack-up in machining. This approach was followed up firstly by Vignat for the case of turning operation [Vignat F. *et al*, 2003] and then more globally for machining process by devolving the Model of Manufacture Part (MMP) [Vignat F., 2005, Vignat F. *et al*, 2005, , 2007b, Vignat F. *et al*, 2008]. The details of these works are provided in chapter 3.

Secondly Legoff and Tichadou followed the work of Villeneuve by proposing a graphic representation of the manufacturing process [Legoff O. *et al*, 2004, Tichadou S. *et al*, 2005]. The graph models the successive machining setups along with the positioning surface, hierarchical order and machined surfaces for each setup. This graph makes it possible to highlight the most influential paths in terms of functional tolerance. More specifically, the authors propose two analysis methods. The first uses a small displacement torsor model. The second is based on the use of a CAD/CAM system to virtually manufacture the part while integrating the manufacturing errors. The authors then virtually measure the parts made and check their compliance with design requirements.

Another work in this area is done by Louati [Louati J. *et al*, 2006] for 3D modeling of geometrical errors propagation in machining to optimize a manufactured part setting. This work is followed by Ayadi [Ayadi B. *et al*, 2008]. The main inconvenient of these two last works is the way that the positioning errors of part have been calculated. The positioning errors are calculated by analyzing a set of hierarchical punctual contact elements. This needs longtime and difficult computation.

#### 2.4.5 Conclusion

The study of the available literature about error stack-up in machining shows that, the problem of process plan evaluation in term of functional tolerances still needs much more investigation. Although researchers have recognized the important role of manufacturing defects in the quality of machined parts and machining error stack-up, little research has been done on the stack-up of manufacturing defects and their effects on final part quality.

Current methods are believed to have major drawbacks that reduce the accuracy of tolerance stack-up evaluation. These drawbacks are:

- 1- Worst-case is exaggeratedly pessimistic in calculating tolerance stack-up.
- 2- Statistical analysis assumes independency between dimensions. Additionally, statistical analysis assumes that the contributing links are normally distributed.
- 3- Tolerance stack between features is performed in one dimension; which does not represent the actual three-dimensional features of interest. 3-D simulation must be the driving force behind the entire dimensional management process [Craig M., 1996]
- 4- Manufacturing errors are not taken into account.
- 5- Geometric tolerance stack-up cannot be estimated. The stack-up of geometric tolerance is usually ignored [Lin E. E. *et al*, 2001].

Firstly there is not a general and accurate 3D model for the error propagation in machining. Moreover, for the few existing 3D models (See [Figure 2–31](#)), solution techniques to the problem of tolerance analysis based on searching for the worst case or stochastic method have not been explored and presented clearly. This is what we called “solution technique”. The lack of solution techniques owes to the fact that machining errors are not well modeled yet in term of variation range and there are many factors that produce the deviations (machine tool, tool wear, temperature, etc).

In this thesis, we will investigate the development of the solution techniques to the problem of tolerance analysis by using the Model of Manufacture Part. Solution technique developing will be divided in two separate sections:

- 1- Searching for the worst case
- 2- Stochastic analysis

Another part of this study will explain clearly how it is possible to simulate the variation range of the machining error (surface quality) for performing the simulation.

As we have discussed before, from our point of view, using the term “tolerance zone” for representing the manufacturing errors is not a good choice. We propose using “variation zone” to this aim.

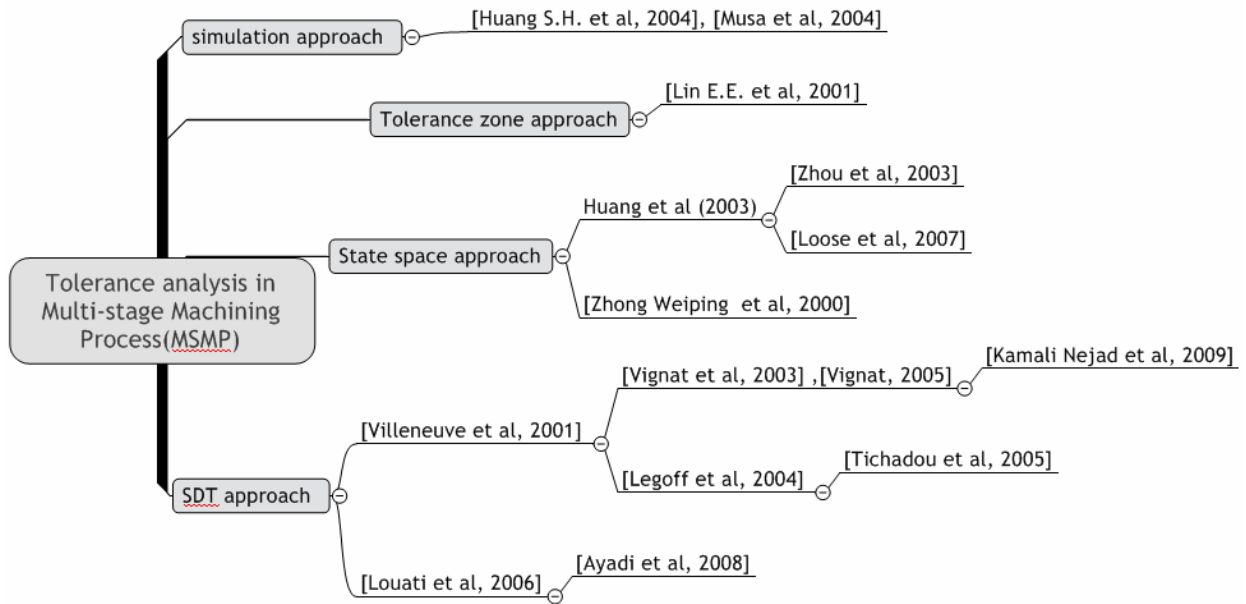


Figure 2–31: Existing literature about Tolerance analysis in machining

### 3 MANUFACTURING SIMULATION WHICH LEADS TO A MODEL OF MANUFACTURED PART (MMP)

In the design phase of the manufacturing process, products are specified with nominal dimensions and tolerances using Computer Aided Design (CAD) tools. Tolerances mean the allowable variability for certain geometrical dimensions or forms. For example, a dimension can be specified with  $(X_0 \pm \Delta X_0 / 2)$ , where  $X_0$  is the nominal dimension, and  $\pm \Delta X_0 / 2$  is the tolerance. If the product is manufactured and measured within the tolerance range, then it is deemed a good product. Otherwise, it is a bad product. Therefore, it is very important to understand the relationship between the design and manufacturing in terms of tolerance specification. Currently, the specifications heavily rely on engineering requirements, experience, and manual calculation. As a result, the tolerance specifications have to be revised from time to time in the manufacturing phase following the design phase. This type of changes may lead to negative impact on industrial operations. Therefore, it is very meaningful to research and develop scientific methodologies for determining the tolerance specifications during the design phase of the manufacturing process.

The development and application of manufacturing simulation which leads to a Model of Manufactured Part (MMP) is chosen as the research topic by F.Villeneuve and F.Vignat. Though the developed simulation method is applied to different manufacturing processes [Vignat F. *et al*, 2009], in this thesis the *machining process* (a typical type of manufacturing process) is chosen and related simulation method will be explored.

In this chapter, this simulation method, which leads to MMP for the case of machining process, will be reminded. We performed some modifications in terms of notation and we improved the mathematical expressions of this method.

To better explain the simulation method which leads to MMP, the following sections present: first, the literature survey of the machining process and different deviation produced in a machining process and second, the simulation method which leads to MMP (a geometrical 3D stack-up model) for error propagation in a multi-stage machining process.

### 3.1 MACHINING PROCESS

Machining (or cutting) refers to a material removal process from a workpiece to form a new surface using various cutting tools shape and path. Generally, in a machining operation, the part is fixed by a positioning tool called “*fixture*” and a cutting tool with relative movement to the fixed part removes the material in different passes. During the machining operation, the workpiece is located and fixed on a fixture. The fixture is located on the machine, which has a relative movement (together with the workpiece) relative to the cutting tool. The movement of the table and those of the cutting tool are performed by electrical motors on the machine. The speed, the depth and the direction of the movement and rotation can be controlled through manual operations or automation (e.g., computer numerical control or CNC).

The movement of the cutting tool relative to the fixed part varies from one operation to other (e.g. in turning or milling). Most frequent machining operation types consist of milling and turning (lathe). In this thesis we concentrate on these two types of machining operation.

A fixture is a device used in machining, inspecting, assembly and other manufacturing operations to locate and hold a workpiece firmly in position so that the required manufacturing processes can be carried out according to design specifications [Gao J. *et al*, 1998].

Machining fixture is a precision device meant for locating and constraining the workpiece during machining. Fixture mainly consists of **locators**, **clamps**, and **support pads** [Prabhakaran G. *et al*, 2007]. The functions of these elements are to position the workpiece correctly with respect to the machine tool, hold the workpiece rigidly in position, and support the workpiece during the machining operation. An important consideration in the fixture design process is to design the fixture layout. The fixture layout is the process of positioning the fixturing elements and the design of fixture layout is to decide on the type, number, material, and position of the fixturing elements. Fixture design plays an important role at the planning phase before shop floor production. Proper fixture design is crucial to product quality in terms of precision, accuracy and surface finish of the machined parts.

### 3.1.1 Case of a turning operation

The lathe is used for producing revolution cylindrical work. The workpiece is rotated while the cutting tool movement is controlled (in 2D) by the machine. The lathe may be used for: boring, drilling, tapping, turning, facing, threading, polishing, grooving, knurling and trepanning. Turning is a lathe operation in which the cutting tool removes metal from the outside diameter of a workpiece. This operation can produce revolution cylinders, planes, cones and etc... See [Figure 3–1](#). The most frequent fixtures in turning operation are: chuck jaws, chuck jaws and center, between two centers etc. See [Figure 3–2](#).

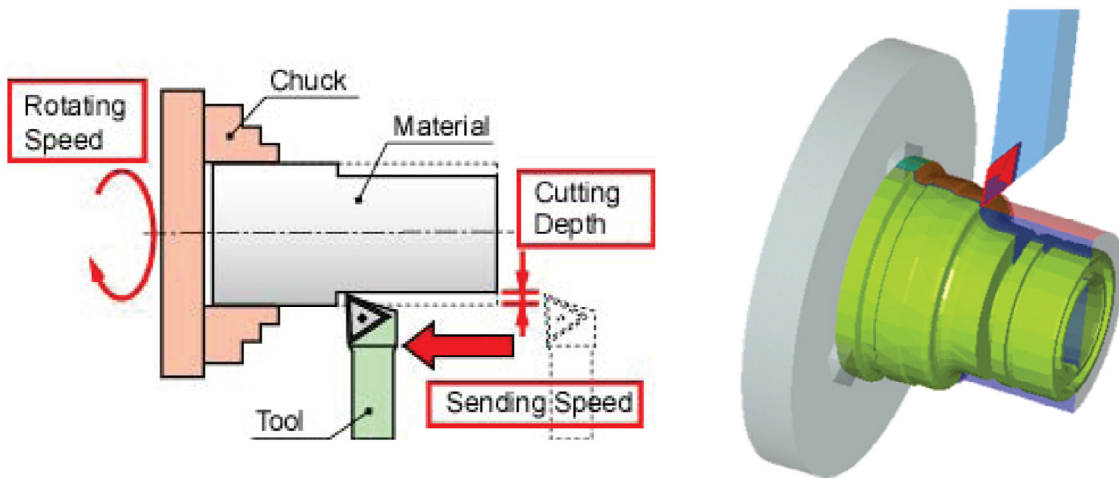


Figure 3–1: Different possible operation on a lathe

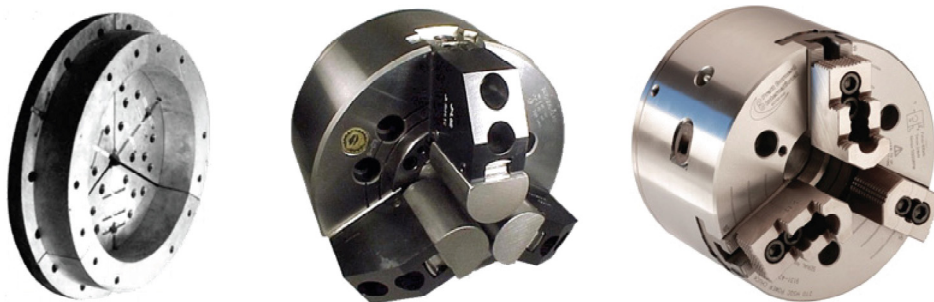


Figure 3–2: Most frequent fixtures in turning operation

### 3.1.2 Case of a milling operation

Milling generates flat, angular, or curved surfaces by cutting away material through the relative movement (called feeding) between a workpiece and a rotating multiple-tooth cutting tool. Milling is generally conducted on a milling machine which holds the workpiece, rotates



the cutter, and feeds the cutter relative to the workpiece. Figure 3–3 shows a milling machine and some milling operations. Figure 3–4 shows traditional and modular fixtures used in milling operation.

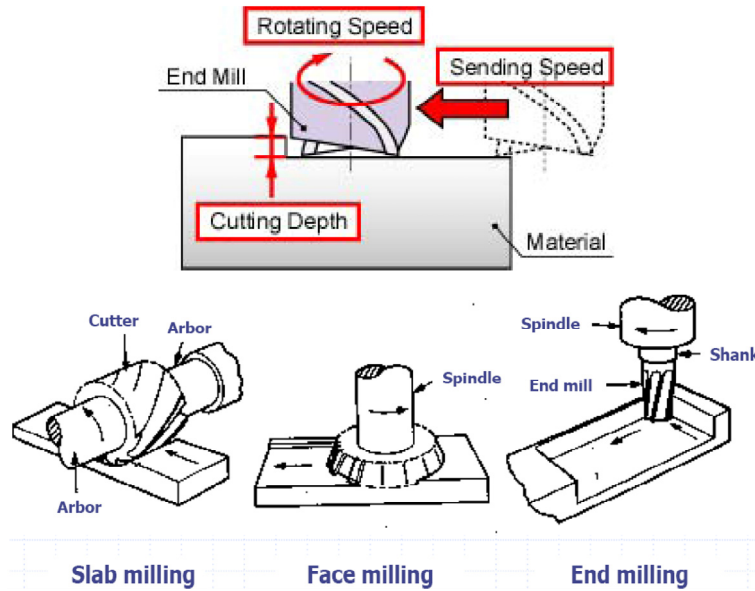


Figure 3–3: Milling operations

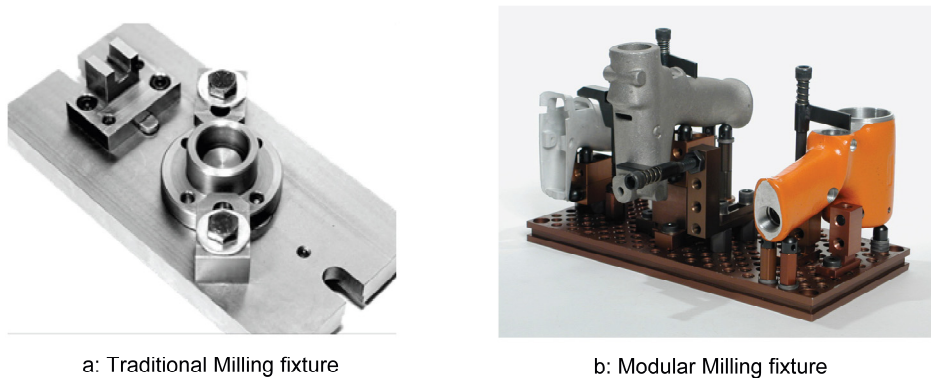


Figure 3–4: Traditional and modular fixture used in milling operation

### 3.2 GENERATED DEVIATION IN A MACHINING OPERATION

Due to the manufacturing imperfection, any of the aforementioned components, such as the workpiece, the fixture, the machine and the cutting tool, can have geometrical errors (also control units error). These geometrical errors affect the relative position between the cutting tool and the workpiece and therefore affect the geometrical dimensions of the newly generated surface.

The MMP consider two types of errors in a machining operation:

- Positioning errors
- Machining errors

The positioning errors accumulate the errors caused by the workpiece called “datum errors” and the errors caused by the fixture (Figure 3–5). The machining errors cumulate the errors caused by machine tool e.g. tool deformation, tool wear, machine tool precision, etc.

### 3.2.1 Positioning errors

The impact of workpiece errors (datum error) and fixture locating component’s errors on the final manufactured part can be illustrated by a simple machining process as shown in Figure 3–5. Workpiece is represented as a metal cube (the front view is shown in Figure 3–5). Perpendicularity between the drilled hole and surface represents the workpiece quality and is defined by a geometric tolerance as shown in Figure 3–5. In Case 1, the deviation is caused by a datum error, which is produced at the previous phase when the metal cube is prepared.

In case 2, the workpiece is located on the fixture locators. Ideally the hole is designed to be perpendicular to the top surface. Due to the fixture locator error, the workpiece deviates from its ideal position. As a result, the hole generated will not be perpendicular to the top surface. This means that errors from the fixture are transferred into the newly generated hole.

The contact condition between workpiece and fixture plays an important role concerning the deviation of the newly generated surface. We will explain this role in section 3.3.2.

### 3.2.2 Machining errors

The machine tool, itself (See Figure 3–5, case 3) can be subject to deviations resulting from many key factors like cutting tools and machining condition, tool wear, temperature (thermal expansions), cutting-force, control etc. A comprehensive review of the literature available on this subject is given in [Ramesh R. *et al*, 2000a, , 2000b].

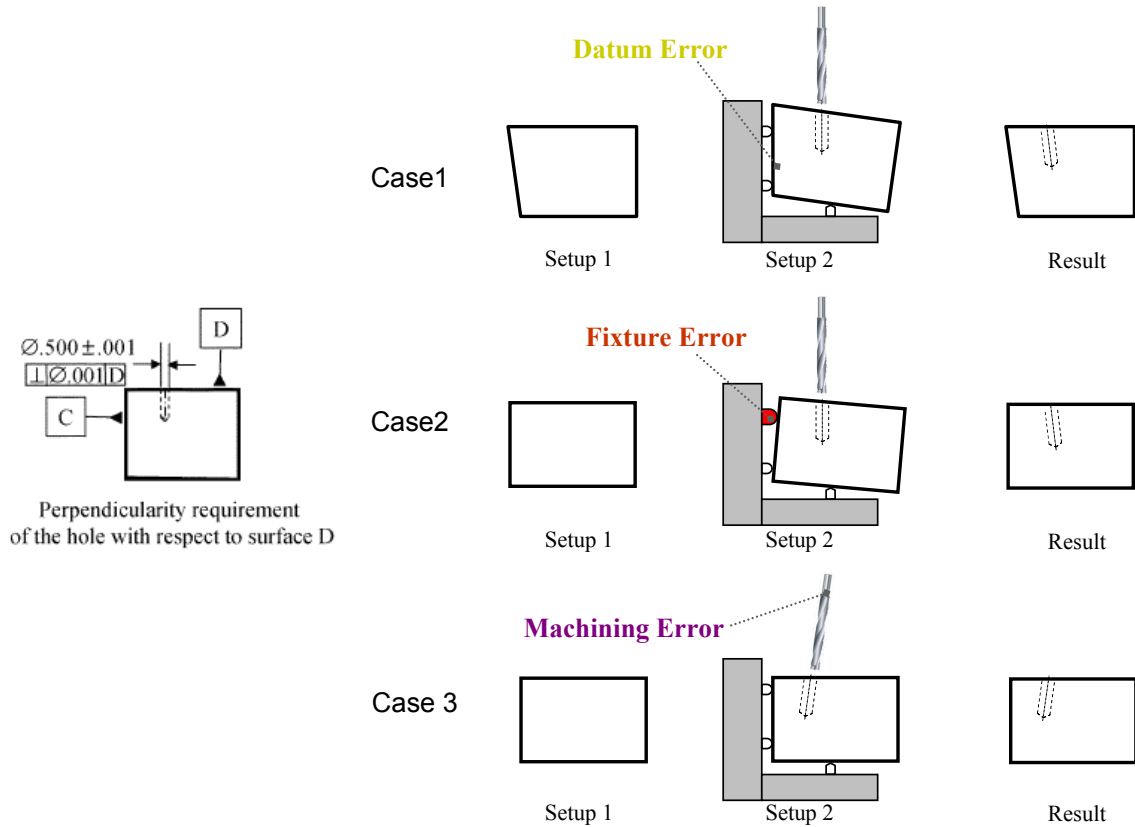


Figure 3–5: Errors in a machining operation [Loose J. P. et al, 2007]

### 3.2.3 Error stack-up

Manufacturing of a part consists of one or several successive machining operations called setup. Each setup consists of two operations: *positioning* and *machining*. The deviation produced in each setup depends on the positioning and machining deviations. We consider that the produced deviation in each setup is the summation of positioning deviation and machining deviation. See Eq. 3-1.

$$\text{Deviation produced in a set up} = \text{Positioning deviation} + \text{Machining deviation} \quad (3-1)$$

The produced deviations (in each setup) are accumulated over the successive setups. The total deviation of a manufactured part will be the summation of the deviation produced in each setup. See Eq. 3-2.

This summation is not just a simple operation. As reviewed in chapter 2, the researchers have invested in this area for decades. In 1D, this accumulation could be considered as the

linear summation of defects but in 2D and especially in 3D, geometrical models are needed to calculate the defects in each setup and their accumulation over the successive setups.

$$\sum_{i=1}^{\text{Number of setups}} \text{Deviation produced in setup}_i \quad (3-2)$$

Villeneuve and Vignat [Vignat F. *et al*, 2003, Vignat F. *et al*, 2005, , 2007b, Villeneuve F. *et al*, 2001, Villeneuve F. *et al*, 2005a, , 2007] propose a method for modeling multi-stage machining processes that takes into account the geometrical and dimensional deviations produced in each machining setup and the influence of these deviations on further setups. The aim of the model called Model of Manufactured Part (MMP) is to support the simulation of the manufacturing process and to accumulate generated deviations for tolerance analysis and synthesis. In the MMP, the errors generated by a manufacturing process are considered to be the result of two independent phenomena: *positioning* and *machining*.

### 3.3 THE SIMULATION METHOD LEADS TO MMP

In this section, the simulation method and related geometrical model used to describe the deviations will be explored.

#### 3.3.1 Small Displacement Torsor (SDT)

The geometrical model used to describe the deviations of the surfaces of the MMP is based on the Small Displacement Torsor (SDT) concept proposed by Bourdet et al [Bourdet P. *et al*, 1996] for assembly simulation. This concept is equivalent to screw theory for application in kinematics and statics of mechanisms.

A SDT consists of two vectors representing the values of three small rotations  $r_x, r_y, r_z$  denoted by  $\mathbf{R}$  and three small translations  $t_x, t_y, t_z$  denoted by  $\mathbf{L}$  concerning a surface. The SDT concept has been extended to manufacturing process simulation by Villeneuve et al [Villeneuve F. *et al*, 2001]. It is based on an ideal part made up of ideal (perfect form) surfaces. This ideal part can be associated with a real part, surface by surface, using a minimum distance criterion such as the least square. The surfaces of the ideal part are

deviated and these deviations are measured in relation to their nominal position. For each surface, the deviations are expressed by a SDT whose structure depends on the surface type. In Figure 3–6 , SDT that expresses the position of the associated plane relative to the nominal one in a local coordinate system LCS (with origin O) is presented in Eq. 3-3. The variation of an intrinsic element of a surface should be added to SDT (e.g. radius variation of a circle or cylinder).

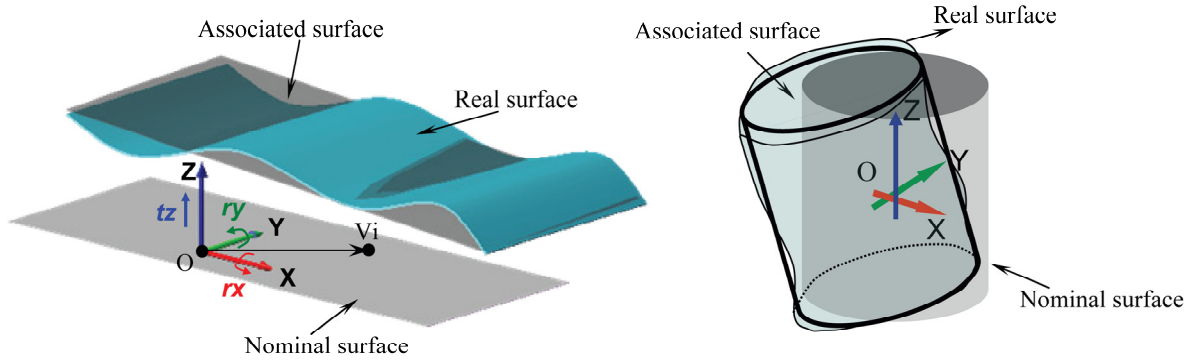


Figure 3–6: Deviation of a plane and cylinder

$$T_{Plane} = \{ \mathbf{R} \quad \mathbf{L}_O \}_{(O, \mathbf{X}, \mathbf{Y}, \mathbf{Z})} = \begin{Bmatrix} rx & 0 \\ ry & 0 \\ 0 & tz \end{Bmatrix}_{(O, \mathbf{X}, \mathbf{Y}, \mathbf{Z})} \quad (3-3)$$

This SDT can be expressed at any point  $V_i$  of the plane by Eq. 3-4.

$$T_{Plane} = \{ \mathbf{R} \quad \mathbf{L}_{V_i} \}_{(V_i, \mathbf{X}, \mathbf{Y}, \mathbf{Z})} = \{ \mathbf{R} \quad \mathbf{L}_O + \mathbf{R} \times \overline{OV_i} \}_{(V_i, \mathbf{X}, \mathbf{Y}, \mathbf{Z})} \quad (3-4)$$

SDT which expresses the relative position of the associated cylinder and the nominal one (See Figure 3–6) in a local coordinate system (with origin O and z along the cylinder axis) is presented in Eq. 3-5:

$$T_{Cylinder} = \{ \mathbf{R} \quad \mathbf{L}_O \}_{(O, \mathbf{X}, \mathbf{Y}, \mathbf{Z})} = \begin{Bmatrix} rx & tx \\ ry & ty \\ 0 & 0 \end{Bmatrix}_{(O, \mathbf{X}, \mathbf{Y}, \mathbf{Z})} \quad (3-5)$$

### 3.3.2 Positioning deviation in a machining setup

As mentioned before, due to the manufacturing imperfection, the workpiece or the fixture can have geometrical errors. These geometrical errors affect the relative position between the cutting tool and the workpiece therefore affecting the geometrical position of the newly generated surface.

During the machining operation, the workpiece is located and fixed on a fixture while cutting tool makes the new surfaces by removing the material. The surfaces of the fixture which take part in positioning process are called “positioning surface”. The positioning surface of the fixture in setup  $j$  will be denoted as  $kS_j$  for surface  $k$  of fixture. The SDT which represents the deviation of this surface  $k$  related to its nominal position will be denoted by  $T_{S_j, Hk}$ . See Table 3-1. Parameters of these torsors (DH) are saved in the MMP and are limited by constraints (CH) representing the fixture quality. These constraints limit either one or a set of parameters.

In the simulation method which leads to MMP the intermediate part in setup  $j$  is called “MWP( $j$ )” (Model of Work Piece at the end of setup  $j$ ) [Vignat F. *et al*, 2007b]. In each setup a MWP will be positioned in a fixture and some new surfaces will be generated in it by the cutting tool. The surfaces of MWP which take part in a positioning process are called “datum” surfaces. This datum surface could be a rough surface made by casting or rolling operation or could be a surface generated by the previous machining setup. The deviation of this surface will be expressed by a SDT  $T_{P, Pi}$  for surface  $i$  of the MWP. See Table 3-1.

The geometrical errors of positioning surfaces of fixture and datum surfaces of parts influence the relative position of the part relative to the machine tool. For setup  $j$  the positioning deviation is expressed by a small displacement torsor  $T_{S_j, P}$ . This deviation is a function of the MWP datum, the fixture surface deviations and the MWP/Fixture assembly condition. The two first error sources have already been presented, hence we will now discuss the assembly condition.

The MWP/Fixture assembly is determined by elementary connections treated on a hierarchical basis (primary, secondary, etc.). Each elementary connection (planar, centering, punctual, etc.) links a surface of the MWP and a surface of the fixture. The links between

these surfaces are of two types: *floating* or *slipping* [Dantan J.-Y., 2000, Villeneuve F. *et al*, 2007].

Deviations	SDT	Torsor parameters	Constraints
Machined surface deviation relative to the machine-tool $T_{Sj, Pi}$	$\begin{Bmatrix} rx_i & tx_i \\ ry_i & ty_i \\ rz_i & tz_i \end{Bmatrix}$	DM= $\{rx_i, ry_i, \dots\}$	CM
Fixture surface deviation $T_{SjHk}$	$\begin{Bmatrix} rx_{kSj} & tx_{kSj} \\ ry_{kSj} & ty_{kSj} \\ rz_{kSj} & tz_{kSj} \end{Bmatrix}$	DH= $\{rx_{kSj}, ry_{kSj}, \dots\}$	CH
Links (MWP/Fixture) $T_{HkSj, Pi}$	$\begin{Bmatrix} lrx_{kSj} & ltx_{kSj} \\ lry_{kSj} & lty_{kSj} \\ lrz_{kSj} & ltz_{kSj} \end{Bmatrix}$	LHP= $\{lrx_{kSj}, lry_{kSj}, \dots\}$	CHP
Surface deviation relative to the nominal part $T_{P, Pi}$	$\begin{Bmatrix} rx_{P, Pi} & tx_{P, Pi} \\ ry_{P, Pi} & ty_{P, Pi} \\ rz_{P, Pi} & tz_{P, Pi} \end{Bmatrix}$	Function of DM, DH and LHP	
i= Surface number (machined one) k= Surface number (positioning one) j= Setup number		P= Nominal surface H= Fixture surface	

Table 3-1: MMP parameters notation

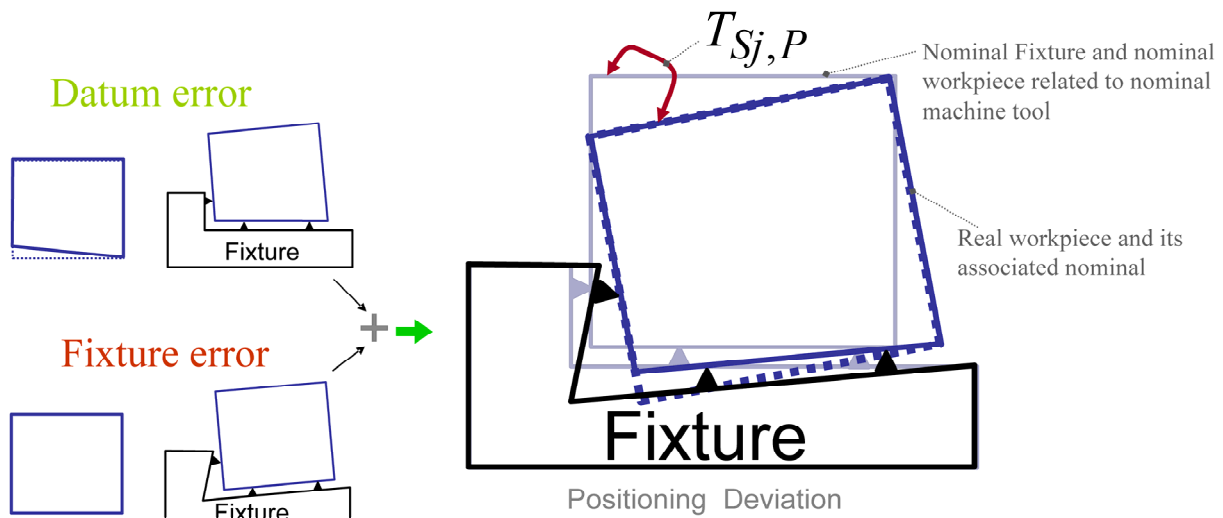


Figure 3-7: Positioning deviation

An elementary connection is defined by the type of link and is expressed by a link torsor  $T_{HkSj, Pi}$  for surface k of the fixture and surface i of the MWP in setup j. The components of these link torsors are called link parameters. The undetermined components are denoted by “U”. The undetermined link parameters are related to the degrees of freedom (DOF) of the

elementary connection. The most frequent elementary connections are Punctual, Plane/Plane and Cylinder/Cylinder links. These links and their associated link torsor are illustrated in Table 3-2. It should be mentioned that each elementary connection has its own local coordinate system (LLCS). Combination of these elementary connections covers more than 95% of positioning cases in manufacturing operations.

The positioning deviation for setup j will be the summation of the MWP datum SDT, the fixture surface SDT and the link SDT for the MWP/Fixture assembly as indicated in Eq. 3-6.

$$\begin{array}{ccc}
 \text{Positioning deviation} & & \text{Fixture error} \\
 \downarrow & & \downarrow \\
 T_{S_j,P} = -T_{P,P_i} + T_{S_j,H_k} + T_{H_k S_j,P_i} & & \\
 \uparrow \text{MWP datum error} & & \uparrow \text{Links}
 \end{array} \tag{3-6}$$

The set of elementary connections are combined to describe the complete MWP/Fixture assembly. This procedure gives the position of the MWP in the fixture as a function of the driving link parameters (those acting upon the global positioning of the MWP) established according to the connection hierarchy.

This consists in a “unification” of the elementary connections treated on a hierarchical basis (primary, secondary...). The resolution of the problem (“unification” following the rules of assembly) describes the components of the workpiece position in the assembly space. These components are dependent on the connected surfaces deviation and the contact condition between these surfaces.

The goal of the unification procedure is to determine  $T_{S_j,P}$  that is the torsor modeling the positioning deviation of the workpiece relative to the nominal machine tool in setup  $S_j$  (Figure 3-7). Each positioning surface  $H_k S_j$  of the fixture (surface  $k$  of fixture in setup  $S_j$ ) connected to a surface  $P_i$  of the MWP contributes to this position. All elementary connections contribute to make a position of the MWP. Therefore  $T_{S_j,P}$  calculated by the way of elementary connection  $n$  is the same as the  $T_{S_j,P}$  calculated by the way of elementary connection  $m$ . Calculating  $T_{S_j,P}$  by the way of each elementary connections gives a system of equation. Solving this system of equations with Gauss's method (Gauss's elimination) gives the unique



position of MWP in fixture. An automatic algorithm has been developed for this purpose. For further discussion of this algorithm, readers should refer to [Villeneuve F. *et al*, 2007].

### 3.3.2.1 Calculating link parameters value

According to the type of connection (floating or slipping), the link parameter values (LHP) are determined by a specific algorithm (CHP) including constraints and, in certain cases, a positioning function.

#### *Floating link parameters*

The floating links parameters ( $LHP_f$ ) need only to comply with the Non-Penetration Condition (NPC) between the MWP and the fixture. In other word MWP should not penetrate to the fixture material. The non-penetration conditions (NPC) are checked at all potential contact points at the boundary of the contact zone, See [Figure 3–8](#).

We consider 3 different cases:

- 1- If the contact zone boundary is circular, we check all around the boundary line using a non-linear inequality equation.
- 2- If the contact zone boundary is a polygon, we check the vertices
- 3- If the contact zone boundary is a freeform, we have to discretize the boundary and check in the distretized contour vertices

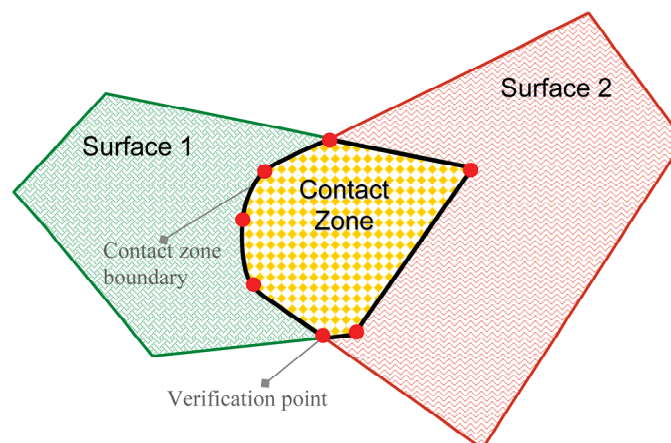


Figure 3–8: Contact zone boundary and verification points

**Non-penetration equations for the case of plane-plane elementary connection**

For the case of plane-plane elementary connection (See Figure 3–9), for obtaining the non-penetration equations at verification point Vnp, related link torsor  $T_{HkSj, Pi}$  should be expressed at point Vnp in its own local coordinate system (LLCS which is in the barycentre of the contact zone) and then projected along the verification directions  $\hat{n}^+$  as indicated in Eq. 3-7.

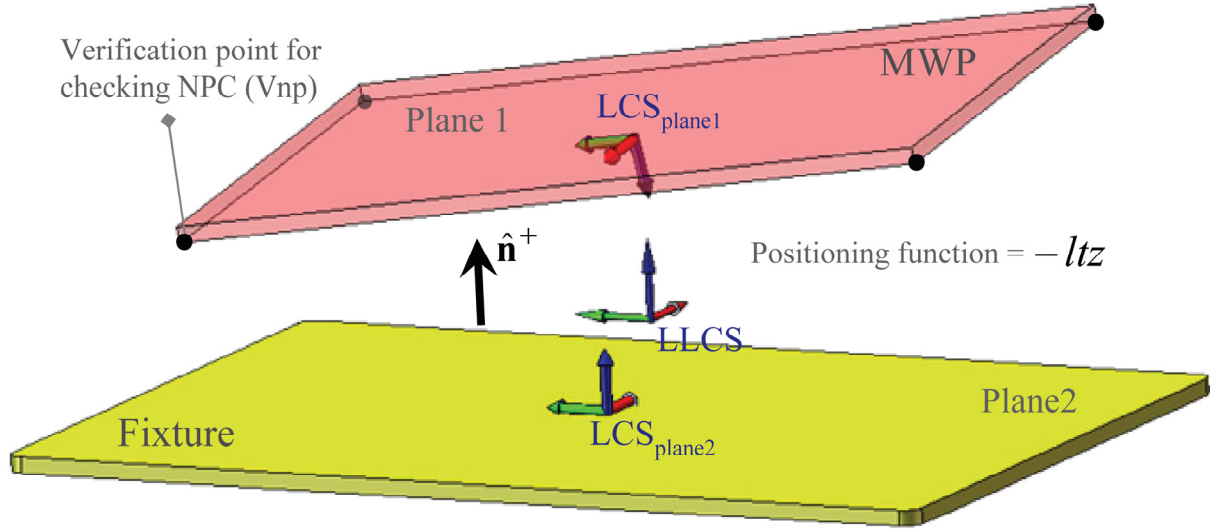


Figure 3–9: Plane-Plane elementary connection

$$\begin{aligned}
 T_{HkSj, Pi} &= \left\{ \mathbf{R} \quad \mathbf{L}_{Vnp} \right\}_{Vnp, LLCS} \\
 NPC_{np} &: \left\{ \hat{\mathbf{n}}^+ \cdot \mathbf{L}_{Vnp} \geq 0 \right\} \quad (\text{for all Vnp points})
 \end{aligned}
 \tag{3-7}$$

**Non-penetration equations for the case of a cylindrical elementary connection**

For the case of a cylindrical link, the distances between the end points of the two concerned cylinders’ axis are calculated by means of non linear equations (See Figure 3–10). In this case, the distance MWP cylinder’s axis and fixture’s axis is measured in two points, the first point in the upper circle and the other one in the lower circle. To this aim, the related link torsor  $T_{HkSj, Pi}$  should be expressed at point Vnp in its own local coordinate system (LLCS is at the middle point of the cylinder axis ). The **distance** vector on a plane perpendicular to  $\hat{\mathbf{n}}$  is found with a double cross product. ( $\hat{\mathbf{n}}$  is a normal vector representing the cylinder axis). See Eq. 3-8.

$$\begin{aligned}
 T_{HkSj, Pi} &= \{ \mathbf{R} \quad \mathbf{L}_{V_{np}} \} \{ V_{np}, LLCS \} \\
 \mathbf{distance} &= \hat{\mathbf{n}} \times \mathbf{L}_{V_{np}} \times \hat{\mathbf{n}} \\
 Clearance &= r_1 - r_2 \\
 NPC_{nc} &: \{ Clearance - \|\mathbf{distance}\| \geq 0 \}
 \end{aligned}
 \tag{3-8}$$

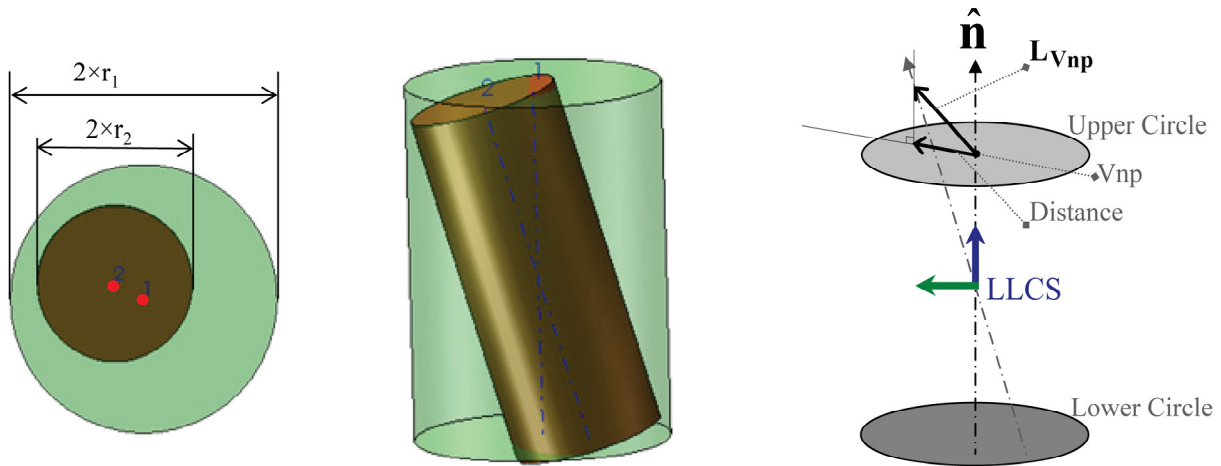


Figure 3–10: Cylinder-Cylinder elementary connection

### Slipping link parameters

Concerning the positioning algorithm (CHP) for the slipping links parameters (LHP<sub>s</sub>), a positioning function in line with non penetration conditions has to be applied. This function expresses the displacement of two surfaces that have to be in slipping contact (the function value increases when the surfaces move closer together). In the case of a Plane/Plane connection, this positioning function expresses the displacement of an MWP point along a direction that is normal to the plane and in a direction that brings the two planes closer together. This function will be applied in the barycenter of the contact zone (See Figure 3–9). In the case of two cylinders, the positioning function is the radius of the smaller cylinder and its maximization leads to its expansion. (See Table 5-3)

This displacement function has to be maximized, in line with the non-penetration conditions (NPC) between the MWP and the fixture. These non-penetration conditions (NPC) apply to all potential contact points at the boundary of the contact zone (See Figure 3–8). In some cases, this implies discretizing the edges of the contact zone.


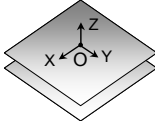
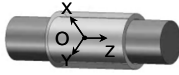
Elementary connection	Coordinate system	Link Torsor	Positioning function (in case of slipping connection)
Punctual		$\begin{Bmatrix} U_{lrx} & U_{ltx} \\ U_{lry} & U_{lty} \\ U_{lrz} & l_{tz} \end{Bmatrix}$	$-l_{tz}$
Plane-Plane		$\begin{Bmatrix} l_{rx} & U_{ltx} \\ l_{ry} & U_{lty} \\ U_{lrz} & l_{tz} \end{Bmatrix}$	$-l_{tz}$
Cylinder-Cylinder		$\begin{Bmatrix} l_{rx} & l_{tx} \\ l_{ry} & l_{ty} \\ U_{lrz} & U_{ltz} \end{Bmatrix}$	$r n_a$ (Diameter of interior cylinder)

Table 3-2: Elementary connections and related link torsor with their LLCs

### Example

For the example in Figure 3-11, the process plan consists in two machining setups. The part is supposed thin enough to be considered as a 2D part. In the first setup (S1) the square block is cut by a sawing operation. In setup 2, the prepared block is put in a fixture for machining surface 3. The MWP/Fixture assembly procedure involves two elementary connections: a primary and a secondary link. In the primary link, surface 1 (datum P1) of the MWP and surface 1S2 of the fixture are connected (Figure 3-12).

The secondary link is formed of the connection between surface 2 (datum P2) and surface 2S2. Given that 2 degrees of freedom have already been blocked by the primary link, there will be one driving link parameter for this secondary link and the problem is over constrained. As previously underlined, an automatic algorithm has been developed to find the driving link parameters. This link is a slipping link, meaning that the positioning algorithm consists in maximizing the positioning function under non-penetration conditions. The non-penetration conditions are checked at two boundary points. See Table 3-3.

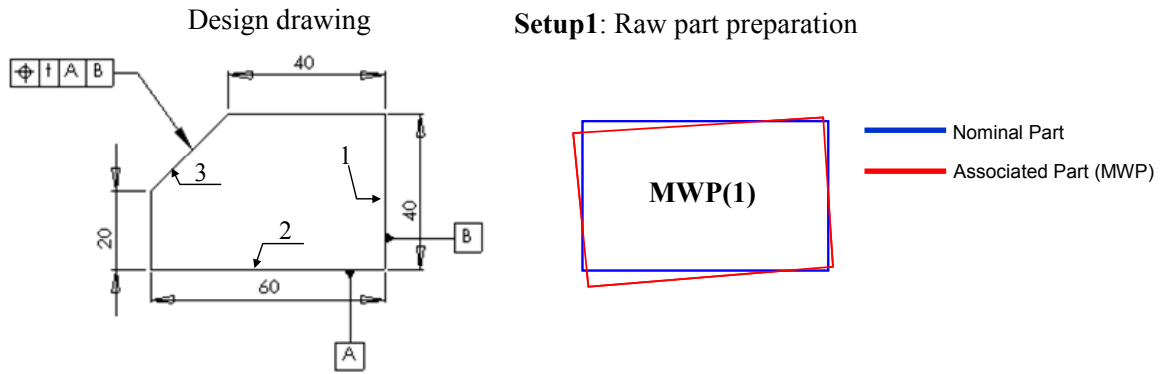


Figure 3-11: 2D example, functional tolerance

The SDT parameters which express the deviation of the two datum surfaces (P1 and P2) and those for the two positioning surfaces of fixture are mentioned in the upper side of Table 3-3. The torsors parameters are all expressed in the corresponding surface LCS. For each set of values allocated to the surface defects parameters mentioned in the upper side of Table 3-3 the links parameters are calculated.

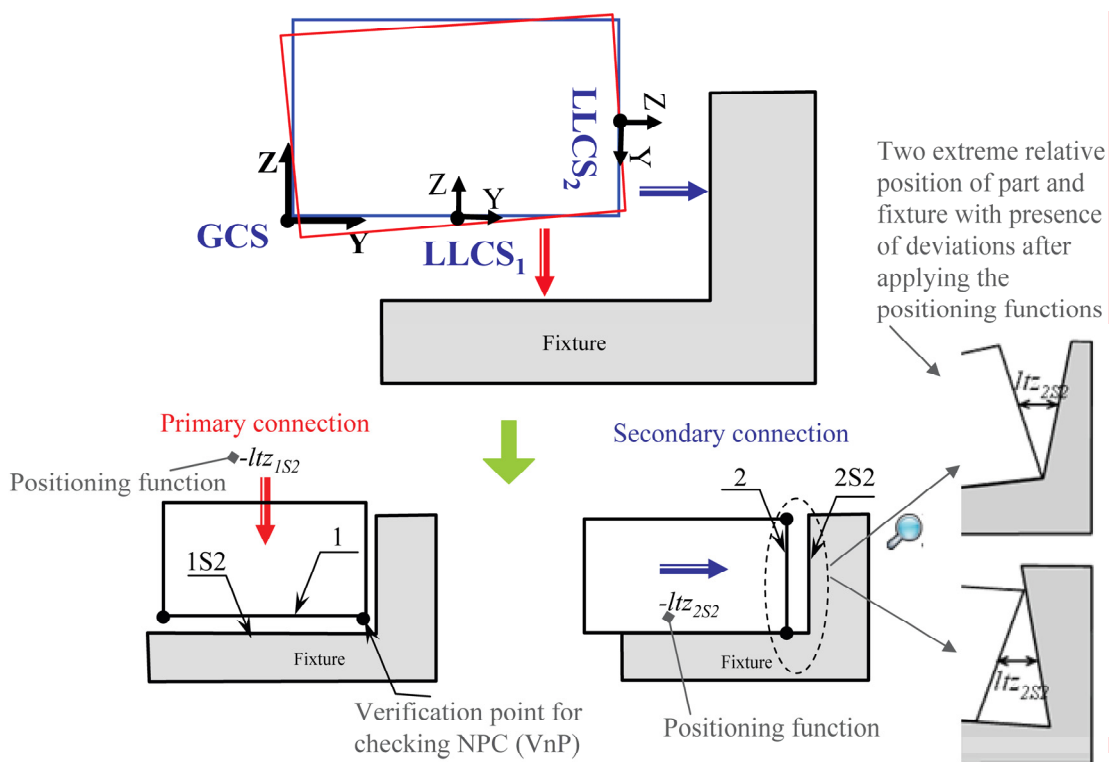


Figure 3-12: 2D example MWP/Fixture assembly illustration

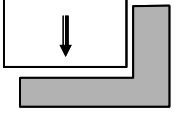
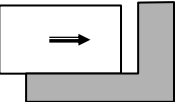
Setup 2					
Fixture			MWP		
Surface	Surface defects (DH)	Constraints (CH)	Surface	Surface defects (DM)	Constraints (CM)
Plane 1S2	$rx_{1S2}, tz_{1S2}$	cf. <sup>1</sup>	Plane 1	$rx_1, tz_1$	cf.
Plane 2S2	$rx_{2S2}, tz_{2S2}$	cf.	Plane 2	$rx_2, tz_2$	cf.
Assembly					
Hierarchy	Driving link parameters LHP	Type of link	Positioning algorithm (CHP)		
			Positioning function to be maximized	Non-penetration conditions	
Primary	$lr_{x_{1S2}}, ltz_{1S2}$	Slipping	$-ltz_{1S2}$	$-30 lr_{x_{1S2}} + ltz_{1S2} \geq 0$ $30 lr_{x_{1S2}} + ltz_{1S2} \geq 0$	
Secondary	$ltz_{2S2}$	Slipping	$-ltz_{2S2}$	$20 lr_{x_{1S2}} + ltz_{2S2} - 20 (rx_1 - rx_{1S2} - rx_2 + rx_{2S2}) \geq 0$ $-20 lr_{x_{1S2}} + ltz_{2S2} + 20 (rx_1 - rx_{1S2} - rx_2 + rx_{2S2}) \geq 0$	

Table 3-3: MWP/Fixture Assembly (NPC and positioning functions) based on the example in Figure 3-11

### 3.3.3 Machining (cutting) deviation in a machining setup

The machine tool itself can be subject to some deviations (see Figure 3-13) because of many key factors like cutting tools and machining condition, tool wear, temperature (thermal expansions), cutting-force (machine deformation), control, etc...

The machined surface deviation is expressed in relation to the nominal machine tool as  $T_{Sj, Pi}$  for surface  $i$  machined in setup  $j$ . This SDT includes the deviation of the surface swept by the cutting tool compared with its nominal position in the machine tool and local deformations due to the cutting process. Thus it represents the deviation of the realized surface relative to the nominal machine. This does not involve the produced deviation because of the fixture errors. The parameters of this torsor are called machining deviation parameters (DM). They are limited by constraints (CM) representing machine and tool capabilities.

<sup>1</sup>cf. refers to the chosen quality constraints over the surface defects parameters. See 5.3.2

Research has been done on modeling and analyzing individual error effects with emphasis on improving machine tool accuracy. A comprehensive review of the literature available on this subject is given in [Ramesh R. *et al*, 2000a, , 2000b]. Since machining error sources are not the main topics of this manuscript, there shall be no further discussion of these here.

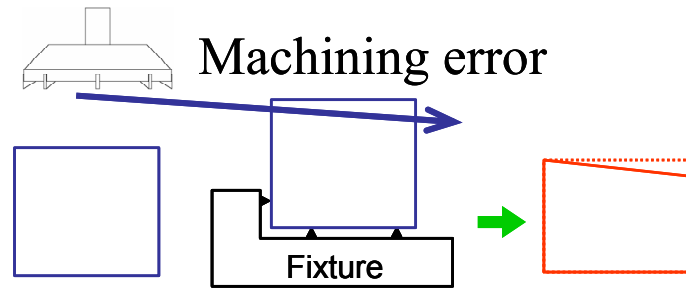


Figure 3–13: Machining errors

### 3.3.4 Actual surface deviations relative to the nominal part

For each MWP(j) surface made in setup j, the positioning and machining deviations are added. The deviation relative to the nominal part is determined and expressed as  $T_{P,Pi}$  for surface i of the MWP See Eq. 3-9. This Torsor will be kept in the MWP data for possible further use in another setup for an assembly procedure or for the purposes of tolerance analysis.

$$T_{P,Pi} = -\underset{\substack{\uparrow \\ \text{Positioning deviation}}}{T_{Sj,P}} + \overset{\substack{\downarrow \\ \text{Machining deviation}}}{T_{Sj,Pi}} \quad (3-9)$$

### 3.3.5 Error stack-up mechanism associated with MMP

As underlined before in the simulation method lead to MMP, the errors generated by a manufacturing process are considered to be the result of two independent phenomena: *positioning* and *machining*. These deviations are accumulated over the successive setups (See Figure 3–14). The result is expressed in terms of deviation of the actual surfaces compared with those of the nominal part. This nominal part that goes from one setup to another is the key of the error stack-up calculation. This nominal part is assigned to the workpiece at the

beginning of the calculation. The position of the nominal part is an arbitrary choice but it must not be changed for the successive setups. In order to capture the error stacks, an intermediate virtual part (MWP) and the nominal part are put through the different setups. See Figure 3–15.

At the end of the modeling process, a virtual manufactured part (MMP) is created. This MMP stores data about the deviations generated (combination of parameters and range of variation) during the full machining process. See Figure 3–16.

The geometrical description of the MMP is based on the nominal part model that could be produced by CAD. This nominal model is composed of:

- A nominal global coordinate system (GCS)
- A set of nominal surfaces with, for each surface:
  - The type of surface
  - A local coordinate system (LCS)
  - The boundaries (edges and vertices)

The MMP does not only represent a model of one manufactured part containing a description of the process in terms of geometrical deviations and accumulated defects. In fact, because it indicates the variation range of the generated defects (by the way of constraints), it represents the series of parts produced. The MMP describes the defects, classifies them and indicates their variation range.

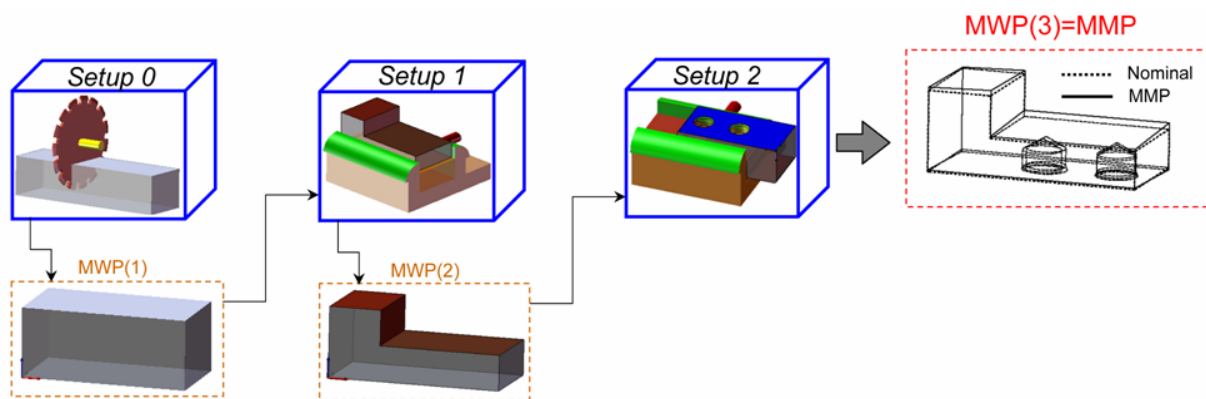


Figure 3–14: Tolerance (error) stack-up model



The SDT describes the MMP surface deviations, i.e. the MMP parameters, which can be classified according to four categories:

- Machining deviations ( $rx_i, ry_i, tz_i \dots$ )
- Fixture surface deviations ( $rx_{iSj}, ry_{iSj}, tx_{iSj}, \dots$ )
- Link parameters ( $lr_{iSj}, lt_{iGj} \dots$ )
- Actual surface deviations relative to the nominal part ( $rx_{P,Pi}, ry_{P,Pi}, \dots$ )

The surface made in a previous setup (e.g. setup j-1) might be used in setup j for positioning procedure. The diagram in Figure 3–15 shows the successive movement of MWP(i) through the different setups.

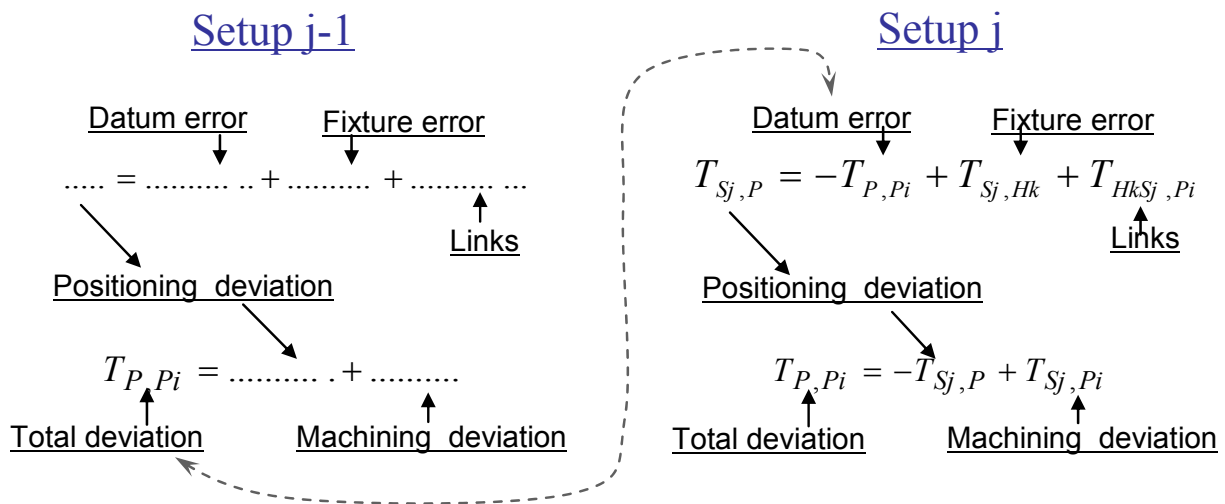


Figure 3–15: Stack-up of formulation

### 3.3.6 Conclusion

The deviation relative to the nominal part is determined and expressed by  $T_{P,Pi}$  for surface i of the MMP. See Eq. 3-9. This Torsor will be kept in the MMP data for possible further use in an assembly procedure or for the purpose of tolerance analysis. For the example of Figure 3–14, the surface deviations relative to the nominal part regarding surface 3 are expressed in Figure 3–16. As it can be found from this figure, each machined surface of the part has its local coordinate system and a  $T_{P,Pi}$  which represents its deviation related to the nominal part.

In the following chapter, we show how the MMP obtained can be used for performing tolerance analysis and then we develop some different solution techniques for the problem of tolerance analysis.

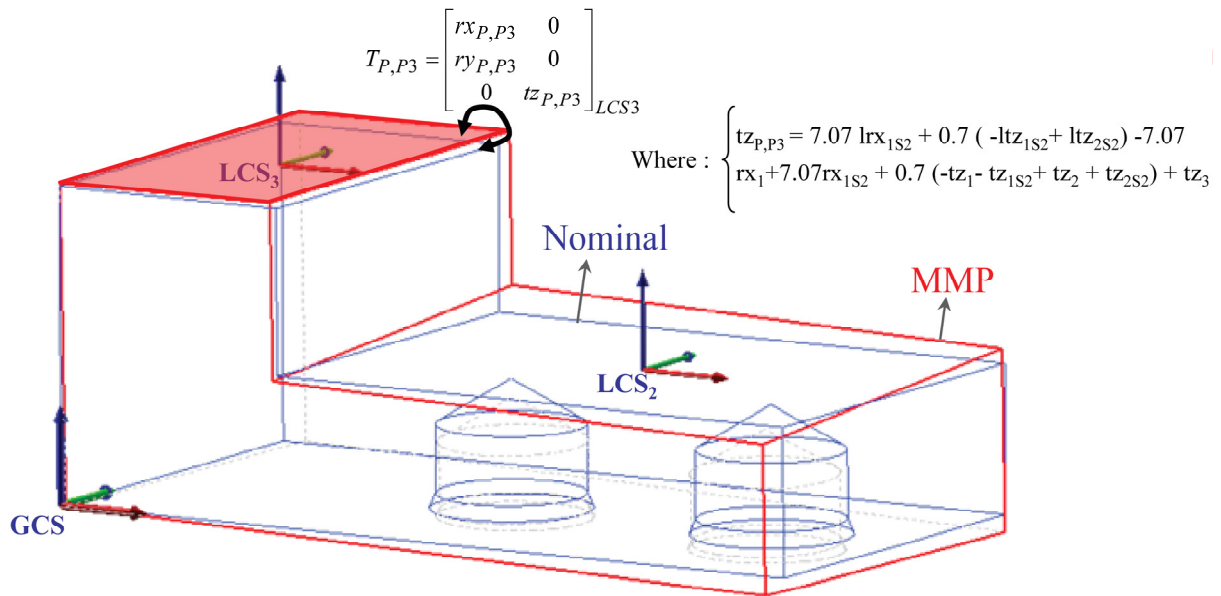


Figure 3–16: The MMP



## 4 TOLERANCE ANALYSIS WITH THE MMP

The evaluation of a process plan in terms of functional tolerances is called *tolerance analysis*. The purpose of tolerance analysis is to verify whether the design tolerance requirements can be met for a given process plan with specified manufacturing deviations. Actually the variation of a machined part arises from the accumulation of different variations all over the production process. In tolerance analysis in a multi-stage machining process, the cumulative effect of individual variations with respect to the specified functional tolerance in all machining stage is studied in order to check a product's conformity compared with its functional tolerance.

As outlined before, one of the MMP applications is tolerance analysis. In the present work, functional tolerance compliance is checked by using a virtual gauge. Each tolerance is modeled by a virtual gauge according to the standard concerned. A virtual gauge is a nominal part made up of positioning surfaces and tolerance zones [Pairel E., 2007, Pairel E. *et al*, 2007]. This gauge is assembled with the MMP according to the chosen standard rules (usually ISO or ASME).

### 4.1 VIRTUAL GAUGE

Design requirements for a part are usually expressed as functional tolerances that have to be interpreted according to a standard such as ISO or ASME. See [Figure 4-1](#).

A virtual gauge  $G$  (See [Figure 4-2](#)) is a nominal part made up of positioning surfaces denoted as  $G_i$  (in red) and tolerance zones denoted as  $TZ_j$  (in green). This gauge is assembled with the MMP according to the chosen standard rules (usually ISO or ASME).

The definition of the virtual gauge is done following the indications on the technical drawing provided by the designers and based on the chosen standard (usually ISO or ASME) which describe how to verify the compliance condition of a part against the functional tolerance. In the verification method by virtual gauge, the part is compliant if the real or associated toleranced element can be found within the tolerance zone (TZ). This tolerance zone is free, partially or completely related to a reference system. The design specifications,

allow identifying the datum system and the tolerated surfaces. The datum system or the tolerated surface could be associated with maximum or minimum material condition. From these conditions and the standard interpretations we build for each functional tolerance a virtual gauge [Pairel E., 2007, Pairel E. *et al*, 2007].

In Figure 4-1, case 1, TZ is completely free with three degrees of freedom (two rotations and one translation). TZ can freely move in order to check the tolerated surface. In this study we do not analyze this type of tolerance because our model considers associated surfaces without form defects (e.g. planarity).

In case 2, TZ is partially related to a datum surface. This imposes blocking two degrees of freedom of the TZ. In this case TZ can have only one translation. The virtual gauge has then an internal mobility. This means that TZ can move (one translation is allowed) related to the datum system.

In case 3, TZ is completely fixed related to a datum surface and it can not have any degree of freedom. This rule is imposed by the chosen standard.

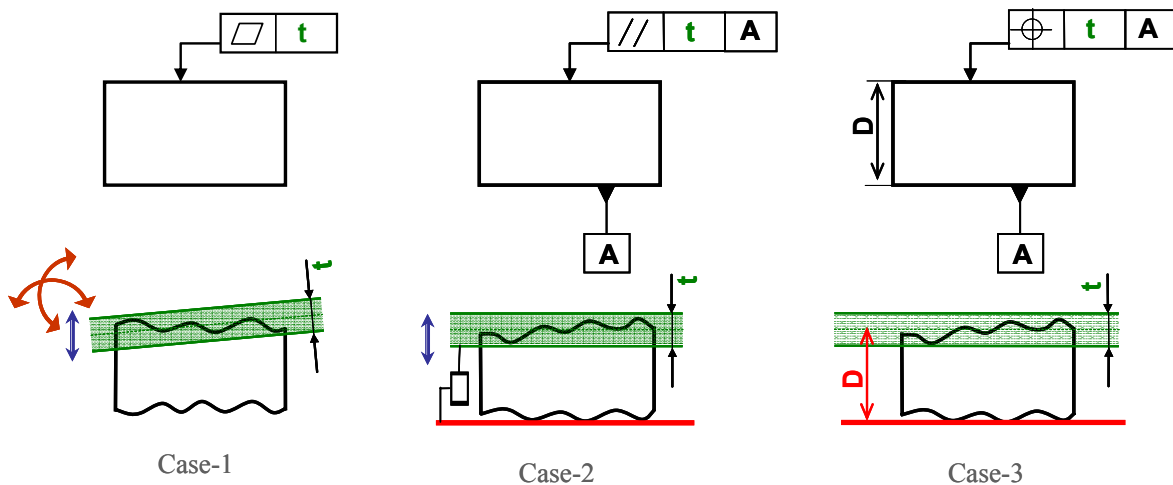


Figure 4-1: Virtual gauge, case-2 with internal mobility

The two main elements of a virtual gauge are positioning surfaces and tolerance zone. The positioning surfaces of a virtual gauge depend on the datum system of the part for a considered functional tolerance. The most frequent tolerance zones are planar, cylindrical and conic.

- The datum surface can be a plane, a cylinder or two cylinders.

- Tolerance zone can be planar, cylindrical (for the case of an axis), cylindrical (for the case of a toleranced cylinder with maximum material condition)

The virtual gauge assembly is not always complete and some limited relative displacements remain possible due to the material condition modifiers, incomplete datum frames or the type of tolerance (e.g. orientation tolerance). This gives to the virtual gauge some degrees of freedom and internal mobility [Dantan J.-Y. *et al*, 2002]. For example, in [Figure 4-2](#):

- 1- Case 1: virtual gauge assembly consists in one slipping plane-plane and one slipping cylinder/cylinder connection. This gives one degree of freedom to the virtual gauge. The gauge can freely rotate around the cylinder G4 (or cylinder 4) axis.
- 2- Case 2: virtual gauge assembly consists in one slipping plane-plane and one floating cylinder-cylinder connection. This gives to the gauge one degree of freedom in rotation (the same as case 1) and two translations (perpendicular to cylinder G4 axis) because of the existing clearance in floating cylinder-cylinder connection.

In this thesis, we treat the position and orientation tolerances. Based on the fact that we not consider the form defects, the form tolerances are not treated in this study.

## 4.2 *GapGP* MEASUREMENT

This gauge is assembled with the MMP according to the chosen standard rules (usually ISO or ASME). The Gauge and MMP assembly process is based on a set of hierarchically organized elementary connections. The Gauge/MMP assembly link parameter values (LGP) are determined by a specific algorithm (CGP) similar to the CHP algorithm used to calculate the MWP/Fixture assembly link parameters. This algorithm is composed of constraints and, in some cases, positioning functions to be maximized. The algorithm and the elementary connections presented in section 3.3.2 are applicable to the Gauge/MMP assembly.

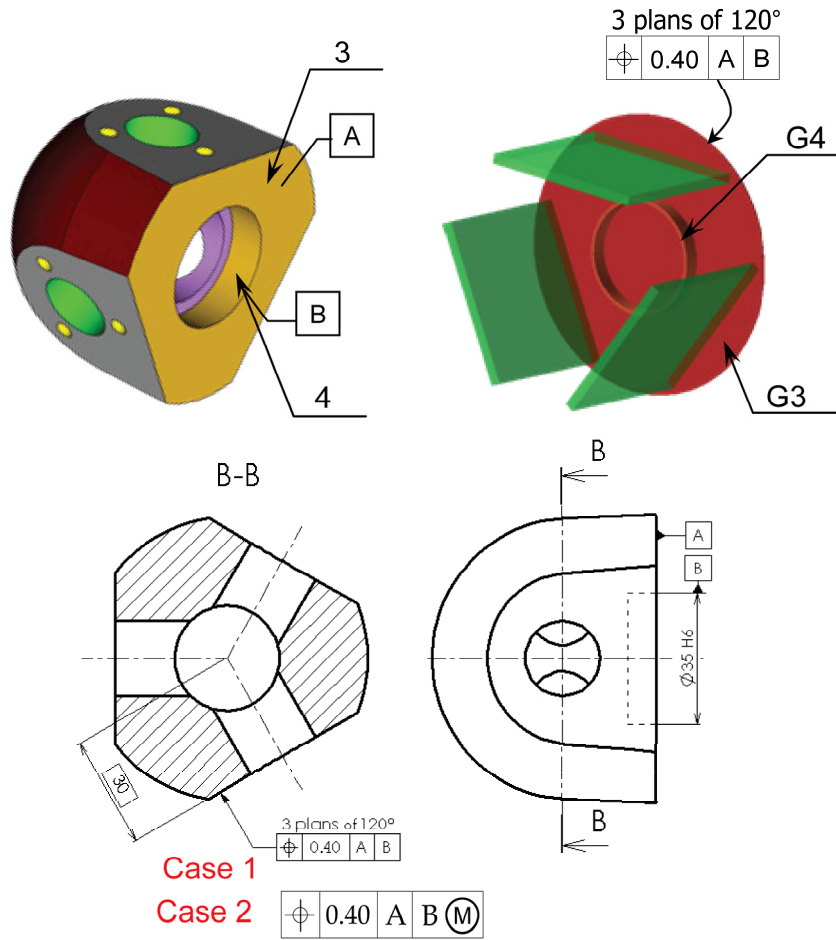


Figure 4–2: Virtual gauge with DOF

Once the gauge and MMP assembly is finished, functional tolerance compliance is verified by a  $GapGP_k$  signed distance measured between the Tolerance Zone (TZ) of the virtual gauge and the concerned surfaces of the MMP.

In order to calculate the  $GapGP_k$  signed distances, first it is necessary to calculate the positioning deviation of the virtual gauge related to MMP. The positioning deviation torsor  $T_{P,G}$  (which expresses the deviation and the DOF) for the case of a Gauge/MMP assembly is calculated using Eq. 4-1 which is similar to Eq. 3-6 used in the case of the MWP/fixture assembly.

The  $GapGP_k$  distance is measured at the necessary points  $V_v$  ( $v$  is the Vertex index) along the boundary of the tolerated surface (Figure 4–4). These points are the vertices of the convex contour of the surface. In case of continuous contour, an appropriate discretization has to be performed.

Each  $GapGP_k$  is expressed as a function of the MMP parameters (DM, DH, LHP), and Gauge/MMP link parameters (LGP). For calculating the  $GapGP_k$  distance, first the deviation between the tolerance zone TZ<sub>i</sub> (i is the zone number) and the MMP tolerated surface i has to be calculated. This deviation is expressed with  $T_{TZ_i, P_i}$ . Two different cases could be considered: case of planar tolerance zone and case of a cylindrical tolerance zone.

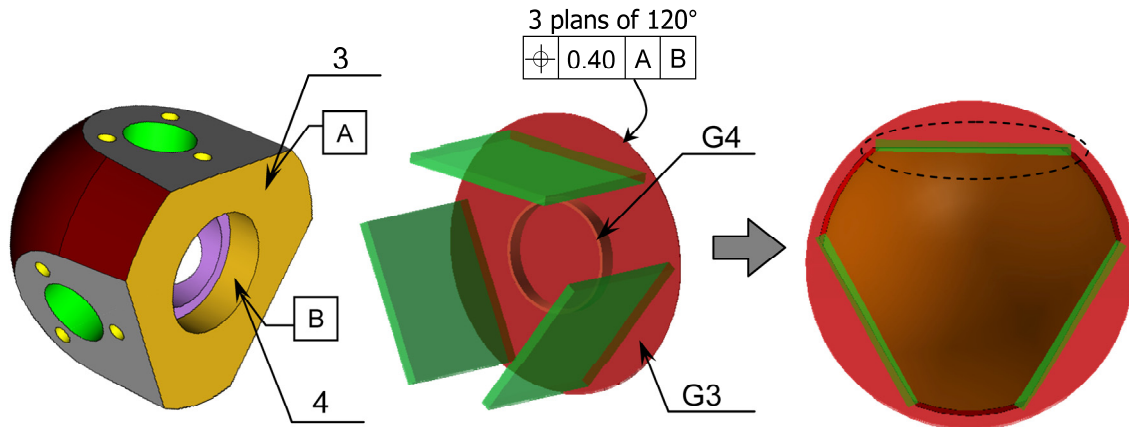


Figure 4-3: “Bolt” example, Gauge/MMP assembly

$$T_{P,G} = -T_{G,G_i} + T_{P,P_i} + T_{P_i,G_i}$$

MMP datum error
↑
Links

Gauge datum error = 0
↑
Links

(4-1)

Where:

$G_i$  are the positioning surfaces (datums) of the virtual gauge  $G$

$P_i$  are the positioning surfaces (datums) of the MMP according to the chosen standard (ISO or ASME)

#### 4.2.1 Case of a planar tolerance zone

In the case of a planar tolerance zone (Figure 4-4) TZ<sub>i</sub> and a tolerated plane  $i$ ,  $T_{TZ_i, P_i}$  represents the deviation between the real plane  $i$  and the median plane of the corresponding tolerance zone  $i$ .  $T_{TZ_i, P_i}$  is obtained by Eq. 4-2.

$$T_{TZ_i, P_i} = -T_{P,G} + T_{P,P_i} - T_{G,TZ_i}$$

MMP tolerated surface error
↑
Gauge TZ internal mobility

Positioning deviation
↑
Gauge TZ internal mobility

(4-2)



To calculate  $GapGP_k$  at the point  $V_v$ , first  $T_{Tz_i, P_i}$  should be expressed at point  $V_v$  and then projected along the verification directions  $\hat{n}^+$  and  $\hat{n}^-$  as indicated in Eq. 4-3. It should be mentioned that two  $GapGP$  are generated at each point  $V_v$ .

$$\begin{aligned}
 T_{Tz_i, P_i} &= \{\mathbf{R} \quad \mathbf{L}_{V_v}\}_{V_v, GCS} \\
 DisGP_k &= \left[ \hat{\mathbf{n}}^+ \cdot \mathbf{L}_{V_v} \right] \quad \text{for } k = 1 \text{ to number of } V_v \\
 GapGP_{k'} &= \frac{t}{2} - DisGP_k \\
 GapGP_{k'+1} &= \frac{t}{2} + DisGP_k
 \end{aligned} \tag{4-3}$$

In the example given in Figure 4-3, the  $GapGP_1$  and  $GapGP_2$  are expressed by Eq. 4-4.

$$\begin{aligned}
 GapGP_1 &= \frac{0.4}{2} - [20 (lry_{3G1} - lry_{3S2}) + ltx_{4G1} - ltx_{4S2} + 25 rx_5 - 20 ry_{3S2} - tx_{4S2} + tz_5 + 25 (-Ulr_{4G1} + Ulr_{4S2})] \\
 GapGP_2 &= \frac{0.4}{2} + [20 (lry_{3G1} - lry_{3S2}) + ltx_{4G1} - ltx_{4S2} + 25 rx_5 - 20 ry_{3S2} - tx_{4S2} + tz_5 + 25 (-Ulr_{4G1} + Ulr_{4S2})]
 \end{aligned} \tag{4-4}$$

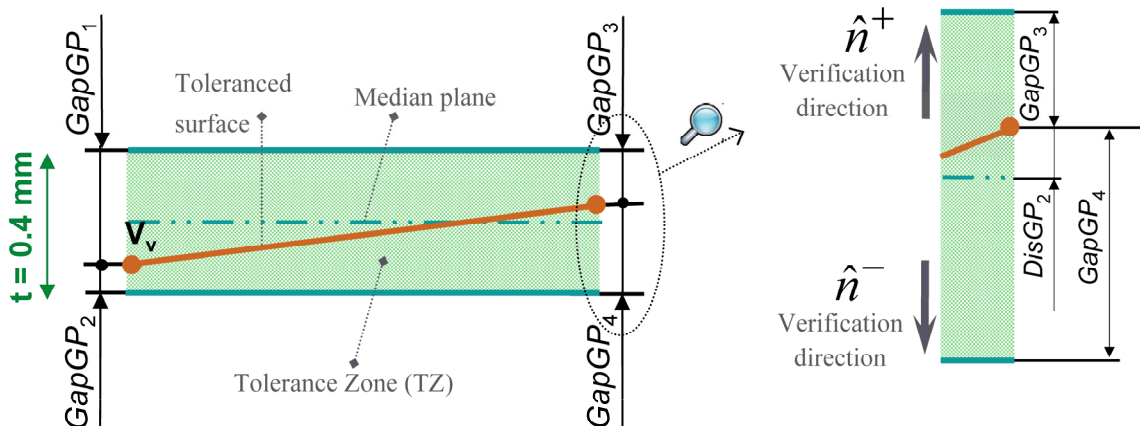


Figure 4-4:  $GapGP$  measurement in the case of planar TZ, case of “Bolt” example

Eq. 4-4 shows the influence of each parameter on the measured  $GapGP_k$ . It is important to note that certain parameters are hidden by the link parameters because the value of these link parameters depends on the other parameters. The verification point  $V_v$  is inside the tolerance zone if  $GapGP_k$  is positive or null. If all  $GapGP_k$  values for a specific tolerance are positive or null, the tolerance is thus verified.

### 4.2.2 Case of a cylindrical tolerance zone

For the case of a cylindrical zone (tolerance zone for an axis), the distances between the end points of the axis of the tolerated part and the cylindrical TZ are calculated by the means of non linear equations (See Figure 4-5). In this case, the distance between tolerance zone axis and part axis is measured in two points, the first point in the upper circle and the next one in lower circle.

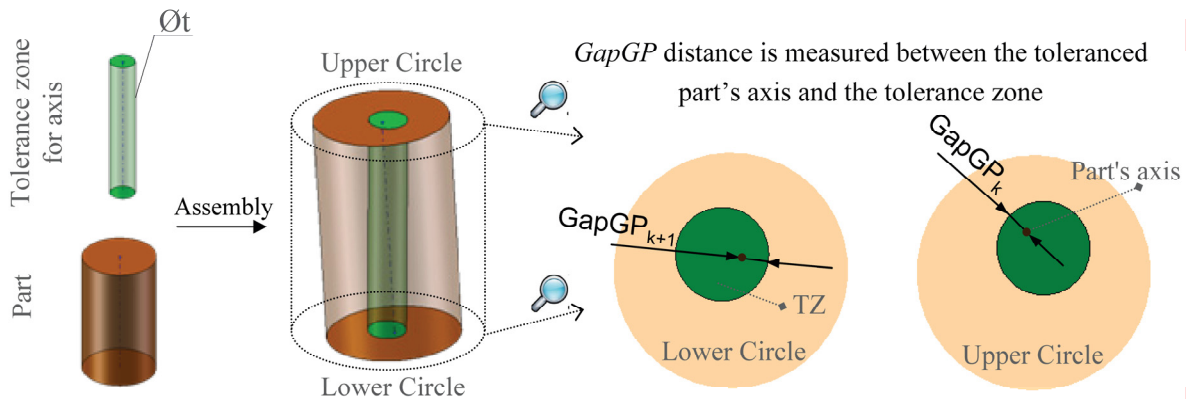


Figure 4-5: *GapGP* measurement in the case of cylindrical TZ

To find the equation which expresses the  $GapGP_k$  in this case, as underlined before, we have to first calculate  $T_{Tz_i, P_i}$  using Eq. 4-2. The second step consists in evaluating the deviation  $T_{Tz_i, P_i}$  onto a plane perpendicular to the tolerance zone axis ( $\hat{n}$ ) at the end points  $V_v$ . To calculate this,  $T_{Tz_i, P_i}$  is expressed at point  $V_v$  and then by using a double cross product  $DisGP$  is calculated as indicated in Eq. 4-5. (See Figure 4-5)

$$\begin{aligned}
 T_{Tz_i, P_i} &= \{ \mathbf{R} \quad \mathbf{L}_{V_v} \}_{V_v, GCS} \\
 DisGP_k &= \| \hat{n} \times \mathbf{L}_{V_v} \times \hat{n} \| \quad \text{for } k = 1 \text{ to number of } V_v \\
 GapGP_k &= \frac{t}{2} - DisGP_k \quad t = \text{Tolerance zone diameter}
 \end{aligned} \tag{4-5}$$

For the case of a tolerance zone for a cylinder with maximum material condition, we measure the distance of the tolerated cylinder boundary and the tolerance zone boundary in two circles. In this case the clearance is the subtraction of the radius of the tolerance zone and the radius of the tolerated cylinder as indicated in Eq. 4-6. See Figure 4-6.

$$\begin{aligned}
 \text{Clearance} &= r_1 - r_2 & r_1 &: \text{radius of TZ, fixed} & r_2 &: \text{radius of tolerated cylinder, variable} \\
 \text{GapGP}_k &= \text{Clearance} - \text{DisGP}_k
 \end{aligned}
 \tag{4-6}$$

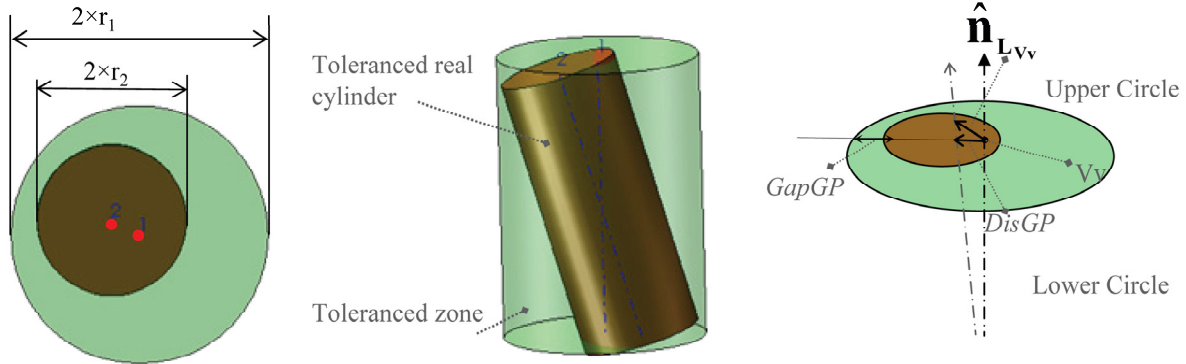


Figure 4–6: GapGP measurement in the case of a cylindrical tolerance zone with maximum material condition

As previously underlined, for all above mentioned tolerance zones, functional tolerance compliance is verified by the signed distance  $\text{GapGP}_k$ . For a given problem, the critical distance is the minimum distance denoted by  $\text{GapGP}_{\min}$  as developed in Eq. 4-7.

$$\text{GapGp}_{\min} = \min_{k=1,2,\dots} (\text{GapGP}_k)
 \tag{4-7}$$

If for a given part (MMP with certain values of defects or, in other hand one instance of the produced parts) the obtained  $\text{GapGP}_{\min}$  value is positive or null, the part is conform relative to the functional tolerance.

### 4.3 VIRTUAL GAUGE BEST POSITION

As previously mentioned, the Gauge/MMP assembly is not always complete and some relative displacements remain possible due to the material condition modifiers, incomplete datum frames or internal mobility due to the type of tolerance (e.g. orientation tolerance). See the example of Figure 4–2. These displacements may correspond to degrees of freedom (LGP<sub>DOF</sub>) of the Gauge/MMP assembly or to the parameters of a floating contact (LGP<sub>f</sub>) (internal mobility is not studied here). In the first case there is no limit for a DOF but, in the second case, the displacements are described by the link parameters LGP and their limits by the positioning algorithm CGP (generally non-penetration condition) complying with the

chosen tolerancing standard (ISO, ASME). Within the DOF and the limits of the  $LGP_f$  displacements, the most favorable position for the virtual gauge relative to the MMP has to be found.

In this position, the  $GapGP_{\min}$  has a maximum value. In other words, the virtual gauge will be displaced by an optimization algorithm that explores possible displacements until the best position relative to the MMP is found. In this position, all the  $GapGP_k$  will be measured for the functional tolerance verification. This procedure is expressed by Eq. 4-8.

$$\max_{LGP}^{CGP} (GapGP_{\min}) \quad (4-8)$$

#### 4.4 WORST CASE SEARCHING

The  $GapGP^*$  solution provided by Eq. 4-8 is also interpreted as a virtual measurement of an individual part. As previously stated, the method presented in this study for analyzing functional tolerance consists in finding the worst case (minimum value of the  $GapGP^*$ ) in order to guarantee that all the parts produced (even the worst) are in line with the functional tolerance.

A generic formulation of the problem, as proposed by Villeneuve et al [Villeneuve F. *et al*, 2005b], consists in solving the following objective functions:

$$\min_{DM, DH, LHP}^{CM, CH, CHP} \left( \max_{LGP}^{CGP} (GapGP_{\min}) \right) \quad (4-9)$$

These functions express the search for the worst case in terms of the functional tolerance under analysis. A process plan is considered able to satisfy the functional tolerance if the value determined in Eq. 4-9 remains positive or null while the MMP parameters vary in their limited variation domain. The search for the worst case is an optimization task that can be expressed as shown in Eq. 4-9. The objective function in this optimization is the  $GapGP^*$ . The variables are the CM, CH, and LHP. The limits of these variables are expressed by constraints (CM and CH) and the positioning algorithm (CHP).

## 4.5 CONCLUSION

This chapter showed how the MMP can be measured by the way of a virtual gauge (tolerance analysis). The different types of virtual gauge with or without DOF and internal mobility are reviewed. The mathematical expression of *GapGP* and especially the way that the best position of the virtual gauge is defined, are improved relative to the work of Vignat [Vignat F., 2005].

Worst case based toleranced analysis is based on searching for the worst part by using Eq. 4-9 which is a multi-layer optimization problem. This equation is not easy to solve and needs a multi-layer solution technique. In the next chapter the developed multi-layer solution technique will be explored. [Kamali Nejad M. *et al*, 2009b]

## 5 WORST CASE BASED TOLERANCE ANALYSIS (WCTA) USING OPTIMIZATION ALGORITHMS

This chapter presents firstly the reformulation of the worst case search problem and secondly proposes a comprehensive multi-layer optimization solution technique for solving the worst case search problem. At the end, the principal aspects of two optimization algorithms (Sequential quadratic method **SQP** and genetic algorithm **GA**) for finding the worst case will be explored.

### 5.1 REFORMULATION

Eq. 4-9 is a multi-layer constrained optimization problem. It checks whether a process plan is able to satisfy functional tolerance requirements. In order to provide a clearer mathematical representation of Eq. 4-9, a new formulation for worst case identification shall be put forward in this section. Secondly, a technique for solving the worst case search issue shall be discussed.

To simplify the technique adopted, the problem is broken down into two sub problems, (Eqs. 5-3 and 5-2) and variable substitution is applied, Eq. 5-1.

$$\begin{aligned}
 f: & \text{ functions expressing the } GapGP_k (k=1,2,\dots) \text{ equations} \\
 g: & \text{ positioning functions for MWP/fixture assemblies} \\
 h: & \text{ positioning functions for Gauge/MMP assemblies} \\
 m: & \text{ number of elementary MWP/fixture assemblies connection} \\
 n: & \text{ number of elementary Gauge/MMP assemblies connection} \\
 x = & \{DM, DH, LHP_f, LHP_{DOF}\} \\
 y = & LHP_s \\
 z = & \{LGP_f, LGP_{DOF}\} \\
 w = & LGP_s \quad \text{Where:}
 \end{aligned} \tag{5-1}$$

- $LHP_{DOF}$ ,  $LHP_s$  and  $LHP_f$  represent respectively the degrees of freedom, the slipping link parameters and the floating link parameters for the case of a MWP/fixture assembly.

- $LGP_{DOF}$ ,  $LGP_s$  and  $LGP_f$  represent respectively the degrees of freedom, the slipping link parameters and the floating link parameters for the case of a Gauge/MMP assembly.

The sub problems are expressed as:

**Sub I:**

$$\begin{aligned}
 \text{Worst case value} &= \min_x F(x,y) \\
 \text{Subject to: } &c(x,y) \geq 0 \\
 \text{Where: } &y = \{y_1, y_2, \dots, y_i\} \\
 \text{With: } &\forall i \in [1, m], y_i = \text{Solution of : } \max_{y_i} g_i(y_i) \\
 &\text{Subject to: } c(x,y) \geq 0
 \end{aligned} \tag{5-2}$$

**Sub II:**

$$\begin{aligned}
 F(x,y) &= \max_z \min_{\{f_i\}} \{f_i(x,y,z,w)\} \\
 \text{Subject to: } &c(x,y,z,w) \geq 0 \\
 \text{Where: } &w = \{w_1, w_2, \dots, w_i\} \\
 \text{With: } &\forall i \in [1, n], w_i = \text{Solution of : } \max_{w_i} h_i(w_i) \\
 &\text{Subject to: } c(x,y,z,w) \geq 0
 \end{aligned} \tag{5-3}$$

The task in Sub I is to find the worst possible part produced in a multi-stage machining process in relation to the tolerance being analyzed. The task in Sub II is to perform a virtual measurement of one individual part. In Sub II, the value of  $F(x, y)$  is calculated and supplied to Sub I. The overall structure of the solution procedure is shown in [Figure 5–1](#). The details regarding each sub problem will be provided in the corresponding sections. As shown in [Figure 5–1](#), the solution consists of two loops: an inner loop and an outer loop. The inner loop corresponds to Sub II (virtual measurement of one individual part) while the outer loop represents Sub I (worst case search).

To be able to solve the positioning algorithms (CHP and CGP), each sub problem is broken down into different layers. Each sub problem and the layers concerned will be explained in detail.

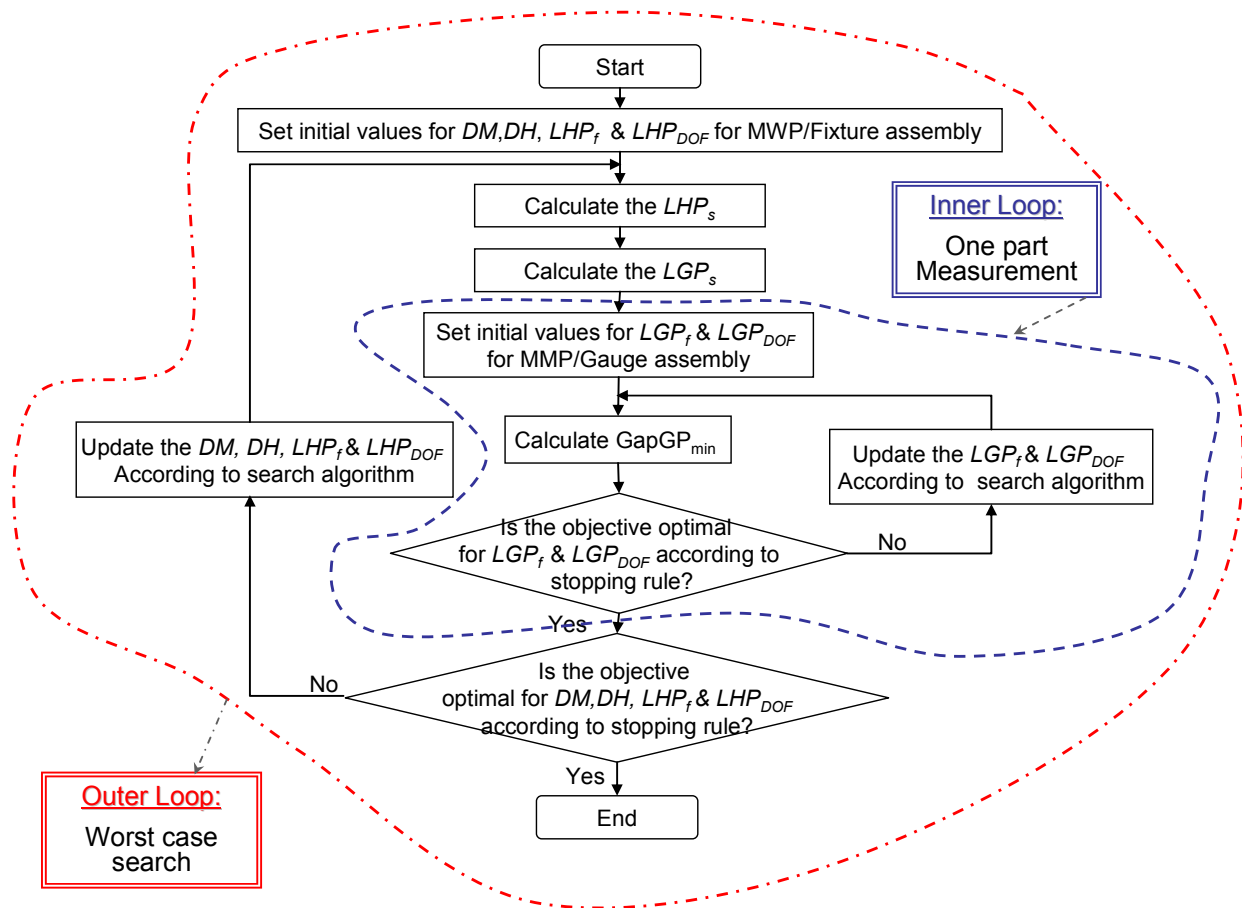


Figure 5–1: solution for worst case identification

## 5.2 SUB II (VIRTUAL MEASUREMENT OF ONE PART)

Sub II consists in measuring a part (MMP with certain values of defects or in other hand one instance of produced parts) produced in order to check its compliance with the functional tolerance. To do this, the gauge modeling the tolerance is first created and assembled with the given MMP (MMP with certain values for defects or one instance of the set of produced parts) as described in Chapter 4. The assembly process consists in making different hierarchical elementary connections. First of all, the slipping links parameters ( $LGP_s$ ) are calculated.

Once the assembly is ready, a signed distance ( $GapGP_k$ ) between the virtual gauge tolerance zone and the related MMP surface is calculated at the adequate number of verification points. The critical point, i.e. the smallest distance, is chosen ( $GapGP_{min}$ ). The number of verification points depends on the surface boundary geometry. In the case of a



convex polygonal surface boundary, the vertices are the verification points. In the case of a non polygonal surface boundary, the boundary has to be discretized in order to find the verification points.

The next step consists in finding a position of the virtual gauge (as described in section 4.3) where the  $GapGP_{min}$  reaches its maximum value, taking advantage of the possible DOF or floating link parameters ( $LGP_{DOF}$  or  $LGP_f$ ) of the Gauge/MMP assembly.

Solving sub II in its general form is not easy. A hierarchical solution needs to be developed. To do this, the iterative algorithm illustrated in Figure 5–1 can be used. It consists of the following steps:

**Step 1:** Calculate the slipping link parameters ( $LGP_s$ ). (With the assumption that the slipping link parameters are not dependent on the floating link parameters)

We treat the Gauge/MMP assembly (as well as the case of MWP/Fixture assembly) on the basis of elementary connections hierarchy. Due to the interpretations from the tolerance standard (ISO or ASME) for creating a virtual gauge, it is impossible to have a floating elementary connection before a slipping one. For example, in the example of “bolt” in Figure 4–2 (case 2) with maximum material condition, it is impossible to consider the floating cylinder-cylinder connection as the primary connection.

**Step 2:** Set the initial value for Gauge/MMP floating and DOF link parameters ( $LGP_f$  and  $LGP_{DOF}$ )

**Step 3:** Calculate  $GapGP_{min}$

**Step 4:** If stopping rules are not reached, update the floating and DOF link parameter values according to the search algorithm (i.e. GA or SQP) and go back to step 3

With this algorithm, the output will be a signed scalar that demonstrates whether compliance with the functional tolerance of the part being measured has been achieved or not. A positive or null value represents the achievement of compliance with the functional tolerance and a negative value means that the part does not comply with the functional tolerance.

## 5.2.1 Example

For illustration purposes, the virtual measuring process is applied to the “bolt” example defined in Figure 4–2 (case 1) and Figure 5–2. In order to check the localization functional tolerance without maximum material condition, a virtual gauge is created.

The Gauge and MMP assembly procedure consists in making two elementary connections according to ISO standard. The primary link connects plane G3 of the Gauge and plane 3 of the MMP. The secondary link is formed of a connection between cylinder G4 and cylinder 4. The primary link is a slipping link. The positioning function related to this link is the displacement of plane G3 in its normal direction. This can be expressed as the opposite (negative sign) of the following Gauge/MMP link parameter:  $-ltz_{3G1}^2$ . The non-penetration conditions are verified at four boundary points. See Table 5-1.

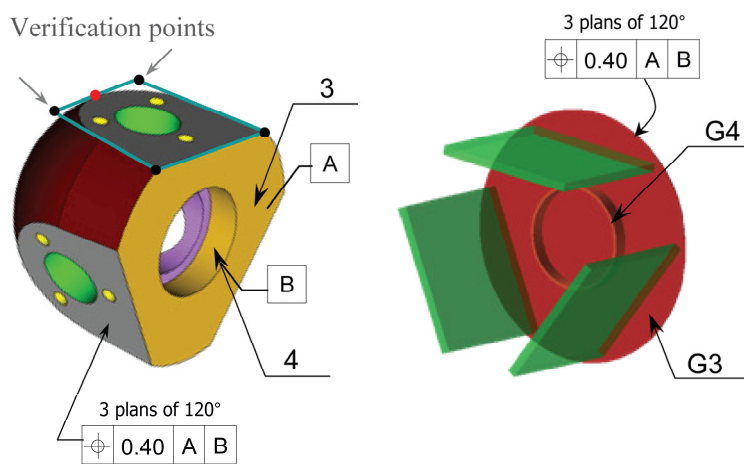


Figure 5–2: “Bolt” example, Virtual gauge and verification points

The secondary link is also a slipping link. The positioning function related to this link can be expressed as the diameter of cylinder G4:  $RN_{4G1}$ . In other words, cylinder G4 will expand until it reaches cylinder 4 (according to ISO). The non-penetration conditions are checked in the boundary circles (up and down) of the potential contact area. The driving link parameters, positioning functions and non-penetration conditions for this assembly are listed in Table 5-1. The values of the driving link parameters are calculated by applying an optimization algorithm for each elementary connection.

<sup>2</sup>  $ltz_{3G1}$  corresponds to surface number 3 of the gauge number 1

One DOF remains for the gauge in this assembly (rotation around Z axis:  $Ulrz_{4G1}$ ). According to ISO standards, this rotation is used to establish the best position for the virtual gauge. In other words, in order to center the toleranced surfaces inside the tolerance zone, in the best possible manner, the optimum  $LGP_{DOF}$  value has to be found. In this position,  $GapGP_{min}$  is at its maximum value.

The  $GapGP$  must be calculated for each of the three planes measured at 4 verification points. The contours of these planes are modified to this aim. The red point in Figure 5–2 is the middle point of the arc of the machined plane. Because of the geometry of the machined plane, this point is very important to verify. This point is replaced by two black points in Figure 5–2 for simplifying the  $GapGP$  equations. This means that there will be twelve verification points (3 planes  $\times$  4 verification points by each plane), resulting in twelve  $GapGP$  equations.

The output of Sub II for this example will be  $F(x, y) = \text{scalar}$  which denotes the value of  $GapGP_{min}$  for the measured part represented by the x and y vectors.

$$\left\{ \begin{array}{l} GapGp_1 = \frac{t}{2} + (-5 \times lry_{3G1} + ltx_{4G1} + 25 \times rx_5 + 5 \times ry_{3s2} - 25 \times ry_5 - tx_{4s2} + tz_5 - 25 \times Urz_{4G1} + 5 \times lry_{3s2}) \\ \vdots \\ GapGp_7 = \frac{t}{2} - (40 \times lry_{3G1} + ltx_{4G1} + 21 \times rx_5 - 40 \times ry_{3s2} + 20 \times ry_5 - tx_{4s2} + tz_5 - 21 \times Urz_{4G1} - 40 \times lry_{3s2}) \\ \vdots \end{array} \right. \quad (5-4)$$

### 5.2.2 Summary of sub II

To summarize, the input of Sub II is a manufactured part with deviations. This part denotes an instance of the set of parts produced represented by an instance of the MMP parameters. The part is input into Sub II as the x and y vectors that contain the deviations (DM, DH, and LHP). In Sub II, a virtual gauge is created and assembled with the MMP input. Through the assembling process, the slipping link parameter values are first calculated using the positioning algorithm (CGP). If there are still some DOF or floating link parameters, an optimization algorithm determines their values, which correspond to the most favorable

position of the virtual gauge relative to the MMP. Consequently, the maximum value of  $GapGP_{min}$  is calculated. The output of Sub II is therefore a scalar. If this scalar is positive or null, the part is compliant and, if not, the value of the tolerance violation is obtained. If the functional tolerance is violated, this algorithm can be used to identify the extent of the violation together with its root cause.

Tolerance analysis					
MMP			Gauge 1		
Surface	Surface defects	Constraints	Surface	Surface defects	Constraints
Plane 3	$rx_{P,P3}, ry_{P,P3}, tz_{P,P3}$	cf. <sup>3</sup>	Plane G4	-	-
Cylinder 4	$rx_{P,P4}, ry_{P,P4}$ $tx_{P,P4}, ty_{P,P4}$	cf.	Cylinder G4	-	-

Assembly				
Hierarchy	Driving Link parameters (LGP)	Type of link	Positioning algorithm (CGP)	
			Positioning function to maximize	Non-penetration condition
Primary LGP[1]	$lrx_{3G1}$ $lry_{3G1}$ $ltz_{3G1}$	Slipping	$-ltz_{3G1}$	$15 lrx_{3G1} - 20 lry_{3G1} + ltz_{3G1} \geq 0$ $-15 lrx_{3G1} - 20 lry_{3G1} + ltz_{3G1} \geq 0$ $-15 lrx_{3G1} + 20 lry_{3G1} + ltz_{3G1} \geq 0$ $15 lrx_{3G1} + 20 lry_{3G1} + ltz_{3G1} \geq 0$
Secondary LGP[2]	$ltx_{4G1}$ $lty_{4G1}$	Slipping	$RN_{4G1}$	$RN_4 - RN_{4G1} + r_4 - \sqrt{(ltx_{4G1} - \frac{H}{2} lry_{4G1})^2 + (lty_{4G1} + \frac{H}{2} lrx_{4G1})^2} \geq 0$ <sup>4</sup> $RN_4 - RN_{4G1} + r_4 - \sqrt{(ltx_{4G1} + \frac{H}{2} lry_{4G1})^2 + (lty_{4G1} - \frac{H}{2} lrx_{4G1})^2} \geq 0$

Table 5-1: "Bolt" example, Gauge/MMP assembly

This process permits to verify both dimensional and geometrical tolerance. As we do not consider the form deviation in our simulation method, form tolerances cannot be verified. See [Table 5-2](#).

<sup>3</sup> cf. correspond to the chosen quality constraint over the surface defects parameters. See [5.3.2](#)

<sup>4</sup> RN= Nominal radius, r= radius deviation , H= contact length

Tolerance type	Material condition	Complete assembly <sup>5</sup>	Incomplete assembly
Orientation  // ⊥	Without max material condition	✓	✓ Figure 4-1, Case 2
	With max material condition	✓	✓
Localization  ⊕ ⊙ ≡	Without max material condition	✓ Figure 4-1, Case 3 Figure 7-7	✓ Figure 4-2, Case 1
	With max material condition	✓	✓ Figure 4-2, Case 2

Table 5-2: Different type of tolerance that can be handled by the proposed solution technique

### 5.3 SUB I (VIRTUAL MANUFACTURING)

The task in Sub I is to find the worst possible part, in terms of tolerance, that a multi-stage machining process might produce. If the worst part in a series of manufactured parts complies with the functional tolerance, it is logical to conclude that all of the manufactured parts will comply. The measuring procedure for one manufactured part has already been described.

Sub I concerns the manufacturing process and hence deals with machining deviations (DM), fixture surface deviations (DH) and link parameters between MWP and the fixture (LHP). These are the target variables of the optimization task in Sub I. The target function in Sub I is the output value of Sub II.

There are different layers in Sub I and different constraints. The following paragraphs discuss firstly about the different possible layouts handled by CHP positioning algorithm and secondly about the algorithm used to identify the worst case and the strategies adopted to express the machining and fixtures constraints.

<sup>5</sup> Complete assembly refers to a virtual gauge without a DOF or with some limited DOF because of the material condition.

### 5.3.1 The fixture layouts handled by the CHP positioning algorithm

The CHP positioning algorithm is able to consider the common fixture layouts in turning and milling. The elementary connections which are presented in Table 3-2 can be used to this aim. These common elementary connections are extended in Table 5-3.

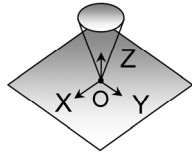
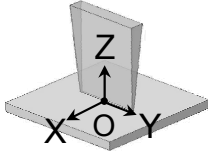
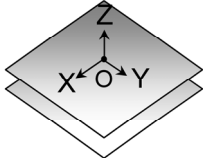
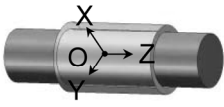
Elementary connection		Coordinate system	Blocking DOF
Punctual			1
Linear orientation	Straight		2
	Ring shape		
Plane-Plane			3
Cylinder-Cylinder	Jaws		5
	Location		2
	Short alignment		2
	Long alignment		4

Table 5-3: Elementary connection, local coordinate system (LLCS) and blocking DOF

In a turning or milling operation, one or a set of elementary connection will be used to put the part (MWP) in the fixture. As mentioned in [Paris H., 1992, Paris H. *et al*, 2005, Zirmi S. *et al*, 2007], the common positioning layout are as follows:

- Lay out 3-2-1c, this layout consists in: one plane-plane, one straight linear orientation and one punctual elementary connections

Different combination of the above mentioned elements are possible: Figure 5-3

- 1 × Plane-Plane + 3 × Punctual
- 6 × Punctual

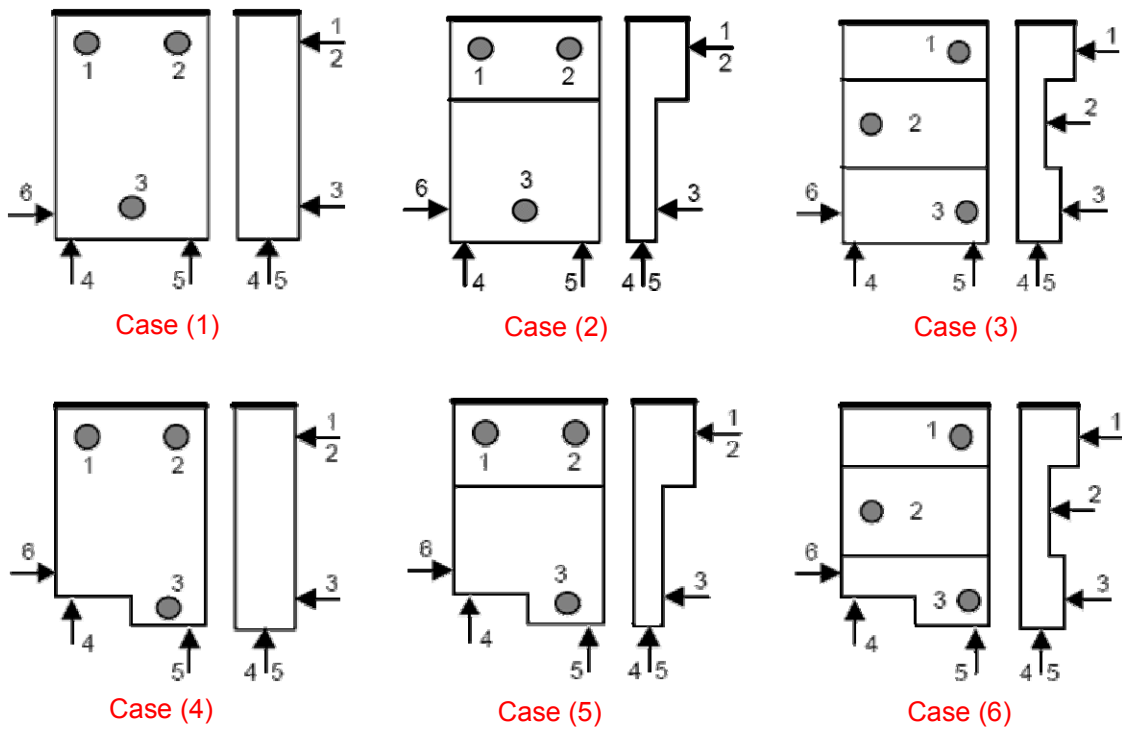


Figure 5-3: Positioning layout 3-2-1c

- Lay out 3-2-1r, this layout consists in: one plane-plane, one ring-shape linear orientation and one punctual elementary connection. [Figure 5-4](#).

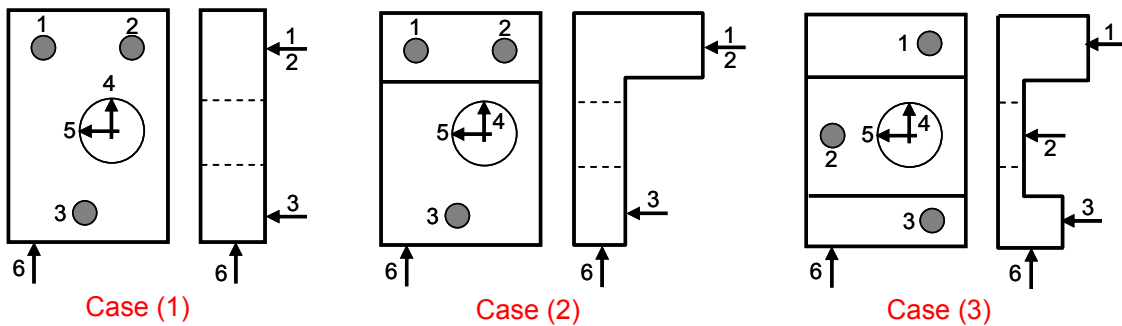


Figure 5-4: Positioning layout 3-2-1r

- Lay out 4-1-1, this layout consists in: one alignment (cylindrical) and two punctual elementary connections. [Figure 5-5](#).



Figure 5–5: Positioning lay out 4-1-1

With this short introduction of fixture layouts in turning and milling, it can be found that CHP positioning algorithm nearly covers 95% of common layouts. CHP can solve the over-constraint assemblies with the plane/plane or cylinder/cylinder elementary connections where the contact points between two surfaces are specified. This is one of the key point of this positioning algorithm. In the case of a sophisticated fixture layout, some simplifications should be applied in order to apply the CHP positioning algorithm.

### 5.3.2 Quality constraints

The machined surface deviation torsor parameters, known as machining deviation parameters (DM), are limited by constraints (CM) stemming from the machine tool's capabilities. The parameters of the fixture surface deviation torsor (DH) are also limited by constraints (CH) arising from the fixture quality. These constraints limit either one or a set of parameters. There are 3 main strategies for defining these constraints.

#### 5.3.2.1 Using the Measurement Results (dependent parameters)

In this strategy, a sufficient number of parts have to be produced and measured. The manufacturing conditions (temperature, machine tool, etc.) should be the same as for the simulation. The machined surface or positioning surface deviation ranges are obtained from the measurement data. Readers can refer to [Tichadou S. *et al*, 2007] for more details about how the measurements are performed. In this strategy, the measurement results will be modeled, assuming that the deviation parameters are not independent. Based on the measurement results obtained, the co-relation between the parameters is then sought (See



Figure 5–6). This strategy is very close to reality, but it is complicated to express the correlation between the parameters.

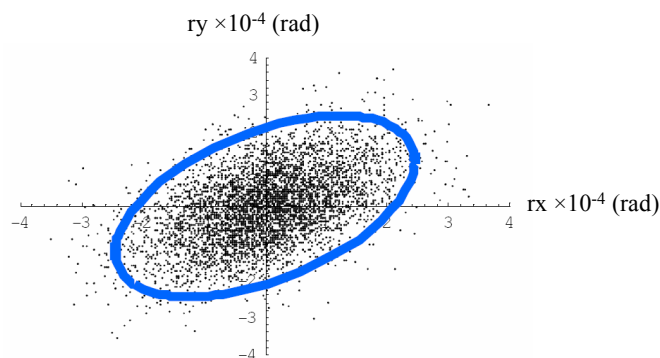


Figure 5–6: Co-relation between deviations parameters ( $rx$ ,  $ry$ )

With this strategy, the constraints obtained for the deviation parameters can be expressed as Eq. 5-5 for the example of Figure 5–6.

$$a \cdot rx^2 + b \cdot ry^2 + c \cdot rx \cdot ry \leq d \quad (5-5)$$

### 5.3.2.2 Using the Measurement Results (independent parameters)

As explained for the previous strategy, the parameter deviation ranges are obtained by measurements. As opposed to the previous strategy, the parameters here are assumed to be independent variables (for the purposes of simplification) with a distribution (that varies for the case of a normal distribution in the interval defined by  $[-3\sigma \quad +3\sigma]$ ). With this strategy, the constraints obtained will be as in Eq. 5-6 in the case of a plane SDT. The deviation variation range obtained is close to reality but considering independent parameters implies that these can simultaneously attain their extreme limits. This is highly improbable in reality.

$$\begin{aligned} \underline{rx} \leq rx \leq \overline{rx} & \quad \text{Where } \underline{rx} \text{ and } \overline{rx} \text{ are the lower and upper bounds of } rx \text{ respectively} \\ \underline{ry} \leq ry \leq \overline{ry} & \\ \underline{tz} \leq tz \leq \overline{tz} & \end{aligned} \quad (5-6)$$

### 5.3.2.3 Considering a variation Zone with dependent parameters

In this strategy, a standard (complying with ISO or ASME standard) variation zone is used to represent the deviation range of a surface or its feature (axis, center, etc.). Desrochers

proposes a 3-D representation of the variation zones [Desrochers A. *et al*, 1997]. A variation zone can be used in its generic form to present the potential variations along and about all the three Cartesian axes. The proposed representation comprises all standard variation zones, along with their corresponding SDT representation and geometrical constraints. The SDT parameter variations must be bound by the limits of the 3-D variation zones they represent. These boundary areas are hyper-surfaces of the space spanned by the six small displacement variables ( $rx, ry, rz, tx, ty, tz$ ). Illustrated below is the case of a planar variation zone showing how such constraints can be handled. In Figure 5–7, the variation zone is defined as the volume ranging between two parallel planes with a distance  $e$  between them. The ideal associated plane (shaded in Figure 5–7) must therefore lie inside this zone. The boundary points will be used to ensure that the associated surface remains within the variation zone. If four boundary points (A, B, C and D) are used on the associated plane with reference point O at the barycenter, it is possible to express their distances to the limiting planes, yielding to the linear set of inequalities in Eq. 5-7, where  $a, b$  and  $e$  are known.

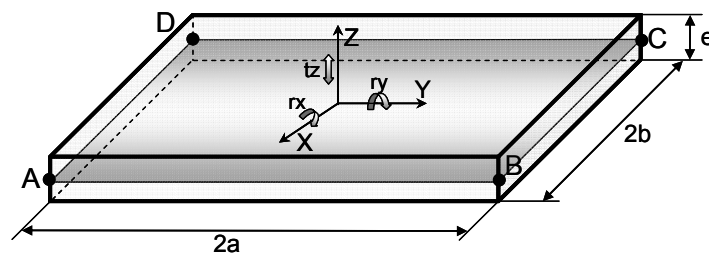


Figure 5–7: Planar variation zone

$$\begin{bmatrix} -e \\ 2 \\ -e \\ 2 \\ -e \\ 2 \\ -e \\ 2 \\ -e \\ 2 \end{bmatrix} \leq \begin{bmatrix} -a & b & 1 \\ -a & -b & 1 \\ a & -b & 1 \\ a & b & 1 \end{bmatrix} \cdot \begin{bmatrix} rx \\ ry \\ tz \end{bmatrix} \leq \begin{bmatrix} e \\ 2 \\ e \\ 2 \\ e \\ 2 \\ e \\ 2 \\ e \\ 2 \end{bmatrix} \quad (5-7)$$

In some works [Desrochers A., 2007, Desrochers A. *et al*, 2003a, Ghie W. *et al*, 2003] the standard variation zone described just before is used, but the variation range of each parameter is calculated when the others are set to zero (in other word, they are considered as the independent parameters). For example, if the SDT parameters of the plane illustrated in Figure 5–7 are considered as independent parameters, they can reach their maximum values

simultaneously. The associated surface therefore exceeds the variation zone. Because of this reason we do not use this type of constraint in our study. The constraints obtained with this strategy for plane SDT parameters variation limit can be expressed as Eq. 5-8.

$$\begin{aligned} \frac{-e}{a} &\leq rx \leq \frac{e}{a} \\ \frac{-e}{b} &\leq ry \leq \frac{e}{b} \\ \frac{-e}{2} &\leq tz \leq \frac{e}{2} \end{aligned} \quad (5-8)$$

### 5.3.3 Solution strategy

The search for the worst case in Sub I uses an iterative optimization algorithm. The algorithm illustrated in Figure 5-1 is applied to this end. The algorithm consists of the following steps:

**Step 1:** Set the initial value for DM, DH, floating and DOF link parameters ( $LHP_f$  and  $LHP_{DOF}$ )

**Step 2:** Calculate the MWP/Fixture slipping link parameters ( $LHP_s$ ) (with the assumption that the slipping link parameters are not dependent on the floating link parameters from previous setups)

**Step 3:** Calculate the  $GapGP_{min}$  with Sub II

**Step 4:** If the stopping rules are not reached, update DM, DH,  $LHP_f$  and  $LHP_{DOF}$  parameter values according to the search algorithm (i.e. SQP or GA) and go back to step 2

Based on the constraints associated with DM and DH, the proper optimization algorithm should be applied to step 4. Each Sub I iteration follows with many iterations in Sub II and its layers. If the gradient optimization method is used for step 4 in Sub I, the initial guess plays a very important role. If the wrong guess is chosen, there is a high risk of reaching a local minimum (instead of a global minimum).

Stochastic methods such as genetic algorithms can be applied to step 4 as well. The advantage of this kind of algorithm is that, by creating a big enough population, the probability of finding the global minimum point is higher. The drawback is the time needed to run such an algorithm.

## 5.4 OPTIMIZATION TECHNIQUES

This section discusses current global optimization algorithms. A specific optimization algorithm was not developed as part of this research work since the aim was to adopt current algorithms to solve the worst case search problem.

### 5.4.1 Sequential quadratic programming (SQP)

This method concerns the following problem:

$$\begin{aligned} \min f(x) \\ \text{Subject to : } C_i(x) \leq 0, l_i \leq x \leq u_i \end{aligned} \quad (5-9)$$

Where  $f : \mathfrak{R}^n \rightarrow \mathfrak{R}$  is a nonlinear function,  $c : \mathfrak{R}^n \rightarrow \mathfrak{R}^m$  represents a set of nonlinear constraints and it is assumed that  $-\infty \leq l_i \leq u_i \leq \infty$ , for  $i = 1, \dots, n$ . Algorithms based on the sequential quadratic programming (SQP) approach are some of the most effective methods for solving the problem illustrated in Eq. 5-9. Some interesting algorithms belonging to this class are given in [Byrd R. H. *et al*, 2000, Byrd R. H. *et al*, 1999, Gomes F. A. M. *et al*, 1999, Plantenga T., 1998]. A complete coverage of such methods can be found in [Nocedal J. *et al*, 1999].

Since SQP algorithms do not require iterations to be feasible, they have to take two conflicting objectives into account for each iteration: reducing infeasibility and reducing function  $f$ . Both objectives must be considered when deciding if the new iterate is to be accepted or rejected. To help with this choice, most algorithms combine optimality and feasibility into one single merit function. Filter methods, on the other hand, usually require only one of these two goals to be satisfied, avoiding the need to define their weighted sum. Both approaches have advantages and drawbacks. The Matlab [2007] optimization tool box was used in this research work. The tool box provides a mixture of these different approaches with the aim of attenuating their drawbacks and capitalizing on their best features.

In constrained optimization, the general aim is to transform the problem into an easier sub problem that can then be solved and used as the basis of an iterative process. A characteristic of a large class of early methods is the translation of the constrained problem to a basic unconstrained problem by using a penalty function for constraints that are near or

beyond the constraint boundary. In this way the constrained problem is solved using a sequence of parameterized unconstrained optimizations, which in the limit (of the sequence) converge to the constrained problem. These methods are now considered relatively inefficient and have been replaced by methods that have focused on the solution of the Kuhn-Tucker (KT) equations. The KT equations are necessary conditions for optimality of a constrained optimization problem. If the problem is a so-called convex programming problem, which means  $f(x)$  and  $C_i(x), i=1, \dots, m$  are convex functions, then the KT equations are both necessary and sufficient condition for a global solution point. For more details refer to Annex.

### 5.4.2 Genetic Algorithms

In the genetic algorithm, an initial population is created. It is possible to summarize this method as follows:

- 1- The algorithm begins by creating a random initial population.
- 2- The algorithm then creates a sequence of new populations, or generations. At each step, the algorithm uses the individuals in the current generation to create the next generation. To create the new generation, the algorithm performs the following steps:
  - Scores each member of the current population by computing its fitness value.
  - Scales the raw fitness scores to convert them into a more usable range of values.
  - Selects parents based on their fitness.
  - Produces children from the parents.
  - Children are produced either by making random changes to a single parent (mutation) or by combining the vector entries of a pair of parents (crossover).
  - Replaces the current population with the children to form the next generation.
- 3- The algorithm stops when one of the stopping criteria is met.

The Matlab GA tool box was used for optimization based on the GA method in this work. The GA uses the mutation and crossover functions to produce new individuals with each generation. The GA satisfies the linear and boundary constraints using mutation and crossover functions that only generate feasible points. The genetic algorithm uses the Augmented Lagrangian Genetic Algorithm (ALGA) to solve nonlinear constraint problems [Conn A. R. *et al*, 1991, Lewis R. M. *et al*, 2002].

The optimization problem solved by the ALGA algorithm is:

$$\begin{aligned}
 & \min_x f(x) \\
 & \text{Subject to :} \\
 & C_i(x) \leq 0, i = 1 \dots m \\
 & C_i(x) = 0, i = m + 1 \dots mt \\
 & Ax \leq b \\
 & A_{eq}x = b_{eq} \\
 & \mathbf{LB} \leq x \leq \mathbf{UB}
 \end{aligned} \tag{5-10}$$

Where  $C(x)$  represents the nonlinear inequality and equality constraints,  $m$  is the number of nonlinear inequality constraints, and  $mt$  is the total number of nonlinear constraints.

The Augmented Lagrangian Genetic Algorithm (ALGA) [Conn A. R. *et al*, 1991, Lewis R. M. *et al*, 2002] attempts to solve a nonlinear optimization problem with nonlinear constraints, linear constraints, and bounds. In this approach, bounds and linear constraints are handled separately from nonlinear constraints. A sub problem is formulated by combining the fitness function and nonlinear constraint function using the Lagrangian and the penalty parameters. A sequence of such optimization problems are approximately minimized using the genetic algorithm such that the linear constraints and bounds are satisfied.

A sub problem formulation is defined as:

$$\Theta(x, \lambda, s, \rho) = f(x) - \sum_{i=1}^m \lambda_i s_i \log(s_i - c_i(x)) + \sum_{i=m+1}^{mt} \lambda_i c_i(x) + \frac{\rho}{2} \sum_{i=m+1}^{mt} c_i(x)^2 \tag{5-11}$$

Where the components  $\lambda_i$  of the vector  $\lambda$  are nonnegative and are known as Lagrange multiplier estimates. The elements  $s_i$  of the vector  $s$  are nonnegative shifts and  $\rho$  is the positive penalty parameter. The algorithm begins by using an initial value for the penalty parameter.

The genetic algorithm minimizes a sequence of the sub problem, which is an approximation of the original problem. When the sub problem is minimized to a required accuracy and satisfies feasibility conditions, the Lagrangian estimates are updated. Otherwise, the penalty parameter is increased by a penalty factor. This results in a new sub problem

formulation and minimization problem. These steps are repeated until the stopping criteria are met.

## 5.5 CONCLUSION

In this chapter the worst case search problem is reformulated and is expressed with a comprehensive mathematical expression. For the purpose of developing a multi-layer optimization technique, the worst case search is broken down into two sub problems.

Furthermore three main strategies for defining the variation scope of surface defects parameters are proposed. Finally two current optimization techniques (SQP and GA) for solving each of the sub problems are introduced.

In chapter 7, the performance of these two optimization techniques for solving the worst case search problem when dealing with different quality constraints will be explored.

In the next chapter, another worst case search method for the purpose of tolerance analysis using the MMP will be explained.

## 6 WORST CASE BASED TOLERANCE ANALYSIS (WCTA) USING INTERVAL METHOD

The multi-layer optimization algorithm presented in chapter 5 needs long calculation that takes a lot of time. To overcome this problem, this chapter will present a combined approach (called interval method) built on two existing models for tolerance analysis: the MMP and the Jacobian-Torsor model. It should be pointed out that the notation of the MMP and the Jacobian-Torsor model has been homogenized in this section for better understanding.

### 6.1 MATRIX REPRESENTATION OF $GapGP_k$

As it is described in the previous chapter each  $GapGP_k$  is expressed as a function of the MMP parameters (DM, DH, LHP), and Gauge/MMP link parameters (LGP).

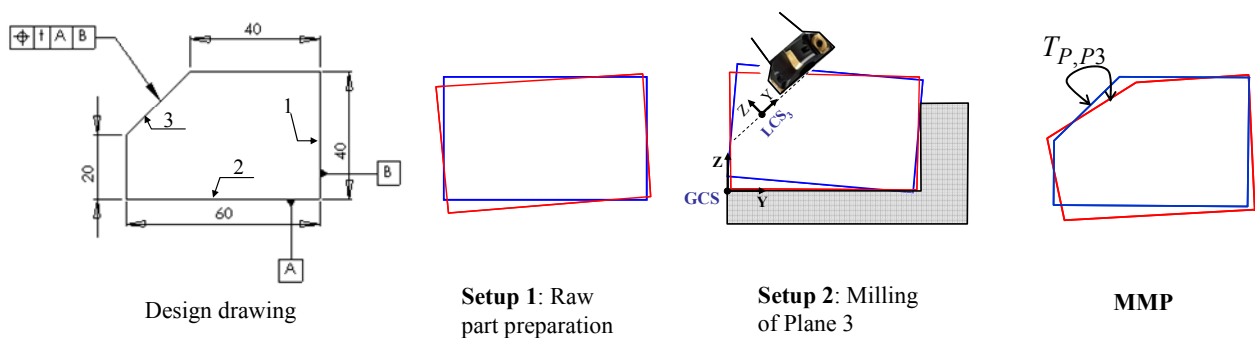


Figure 6–1: Manufacturing simulation, the MMP (nominal part in blue and actual part in red)

In this section we use the measurable distance “ $DisGP_k$ ” (See section 4.2) to be consistent with the Jacobian-Torsor approach. In the case of a planar tolerance zone,  $DisGP_k$  is a signed distance measured between the median plane of the virtual gauge tolerance zone and the MMP surface concerned. This distance is measured at the verification points along the boundary of the tolerated surface (Figure 6–2). These points are the vertices of the convex contour of the surface. In the case of a continuous contour, an appropriate discretization has to be performed.



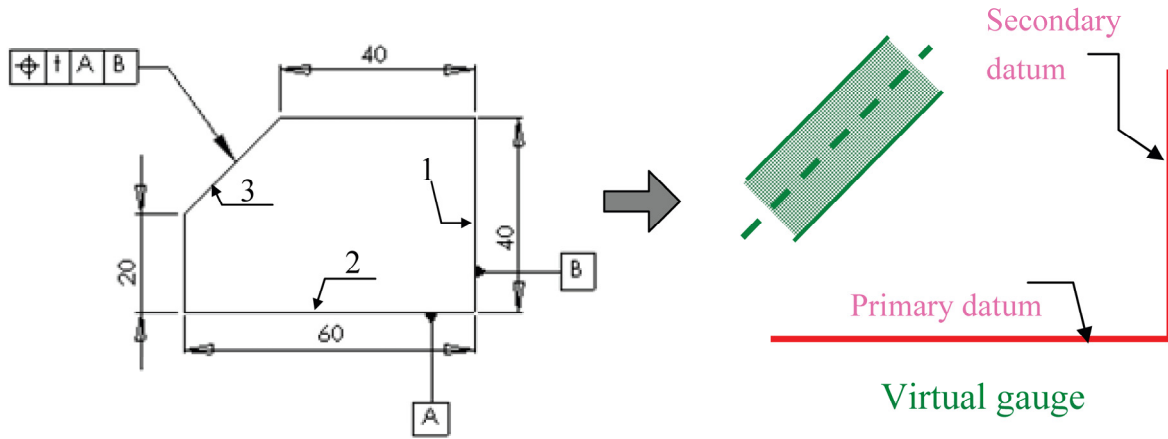


Figure 6-2: Virtual gauge, MMP and DisGP

Each  $DisGP_k$  is expressed as a function of the MMP parameters (DM, DH, LHP), and Gauge/MMP link parameters (LGP). For the example given in Figure 6-1, the  $DisGP_1$  equation is expressed by Eq. 6-1.

$$\begin{aligned}
 \mathbf{DisGP}_1 = & 21.21 (-lr_{x_{1G1}} + lr_{x_{1S2}}) + 0.7 (ltz_{1R1} - ltz_{1S2} - ltz_{2R1} + ltz_{2S2}) + \\
 & 21.21 rx_{1S2} - 14.14 rx_3 - 0.7 (tz_{1S2} - 0.7 tz_{2S2}) + tz_3
 \end{aligned} \tag{6-1}$$

Eq. 6-1 shows the influence of each parameter on the measured  $DisGP_k$ . It is important to note that certain parameters are hidden by the link parameters because the value of these link parameters depends on other parameters. Using  $DisGP_k$  equations it is thus possible to write a coefficient matrix for each active surface (machined or positioning surfaces) as well as for the links. In the current example, the coefficient matrix for the machined surface 3 is given in Eq. 6-2. The first line of this matrix expresses the geometrical relation between surface 3 and the  $DisGP_1$  measured. The second line concerns  $DisGP_2$ .

$$\begin{bmatrix} DisGP_1 \\ DisGP_2 \end{bmatrix} = \dots + \begin{bmatrix} -14.4 & 0 & 0 & 0 & 0 & 1 \\ 14.4 & 0 & 0 & 0 & 0 & 1 \end{bmatrix} \bullet \begin{bmatrix} rx_3 \\ ry_3 \\ rz_3 \\ tx_3 \\ ty_3 \\ tz_3 \end{bmatrix} + \dots \tag{6-2}$$

It is possible to calculate  $GapGP_k$  from  $DisGP_k$  in each verification point (See section 4.2). For the case of a planar tolerance zone  $GapGP_k$  can be obtained from  $DisGP_k$  value according to Eq. 6-3

$$\begin{aligned} GapGP_{k'} &= \frac{t}{2} - DisGP_k \\ &\text{(For } k=1 \text{ to number of verification point)} \\ GapGP_{k'+1} &= \frac{t}{2} + DisGP_k \end{aligned} \quad (6-3)$$

## 6.2 THE JACOBIAN-TORSOR MODEL

Ghie et al [Ghie W. *et al*, 2007] propose a unified Jacobian-torsor model for computer-aided tolerancing to perform tolerance analysis and tolerance synthesis in either deterministic or statistical situations [Desrochers A. *et al*, 2003b, Laperrière L. *et al*, 2002]. This model combines the benefits of both the Jacobian [Laperrière L. *et al*, 1999] and the torsor approaches developed for tolerancing. The proposed unified model is formulated using interval-based arithmetic. This model can be represented as:

$$[FR] = [J] [FEs] \quad (6-4)$$

Where:

[FR] : Functional requirements ( gap, clearance)

[FEs] : Functional Element uncertainties (tolerance, contacts, etc.)

[J] : Jacobian matrix expressing a geometrical relation between [FR] and [FEs].

The methodology associated with tolerance analysis comprises four basic steps. The first step identifies the kinematic tolerance chain, which passes through each functional element known to affect the functional requirement under study. Functional elements (FE) can be points, curves or surfaces belonging to a part in the assembly, or kinematic contacts between two surfaces belonging to two different parts between which there is physical or potential contact. The second step associates torsors (or screw parameters) with each functional element in the kinematic chain. These torsors express the degree of freedom and the small displacements (deviations) that the elements are allowed to have in relation to the bounds. The third step uses Jacobian matrices to reflect the relative position and orientation of the various FEs within the chosen kinematic chain. Finally, the fourth step combines the torsor model with the Jacobian model to form a matrix equation whose solution, using interval algebra, provides the bounds of the functional requirements (FR) being analyzed.

Interval analysis was introduced in R.E Moore’s book “interval analysis” in 1966 as a tool for automatically controlling the errors in a computed result. Such errors may be input errors, rounding errors occurring during computation, and truncation errors from using a numerical approximation to the mathematical problem. Nowadays, interval arithmetic is used in the theory of graphs, robotics and the theory of control. In this work, interval arithmetic will be used to associate bounds on the components of small displacement torsors. It is used to determine two terminal limits: a lower limit and an upper limit between which the actual surfaces must lie. The advantage of the interval method lies in the fact that all the results are guaranteed and given in the form of a closed interval taking into account possible numerical errors. A real interval  $A$  is a bounded, closed subset of the real numbers defined as:

$$A = [\underline{a} \quad \bar{a}] = \{a \in \mathfrak{R} / \underline{a} \leq a \leq \bar{a}\} \quad \text{Where } \underline{a}, \bar{a} \in \mathfrak{R} \text{ and } \underline{a} \leq \bar{a} \quad (6-5)$$

Consider  $A = [\underline{a} \quad \bar{a}]$  and  $B = [\underline{b} \quad \bar{b}]$ . It is possible to define four basic operators as:

$$\begin{aligned} A + B &= [\underline{a} + \underline{b} \quad \bar{a} + \bar{b}] \\ A - B &= [\underline{a} - \bar{b} \quad \bar{a} - \underline{b}] \\ A * B &= [\min(\underline{a}\underline{b}, \underline{a}\bar{b}, \bar{a}\underline{b}, \bar{a}\bar{b}) \quad \max(\underline{a}\underline{b}, \underline{a}\bar{b}, \bar{a}\underline{b}, \bar{a}\bar{b})] \\ \frac{A}{B} &= A * \left[ \frac{1}{\underline{b}} \quad \frac{1}{\bar{b}} \right] \end{aligned}$$

An interval vector is defined as a vector with interval components and the space of all  $n$  dimensional interval vectors is denoted by  $\mathfrak{R}$ . Similarly, an interval matrix is a matrix with interval components and the space of all  $m \times n$  matrices is denoted by  $\mathfrak{R}^{m \times n}$ . A point matrix or point vector has components whose radius is zero, otherwise it is said to be a thick matrix or thick vector. Interval arithmetic is also applied to matrix operations (multiplication, subtraction, etc.) such that the above rules are followed. [Hansen E. *et al*, 2004]

Eq. 6-4 can be expressed using an SDT with intervals where  $(\underline{rx}, \underline{ry}, \underline{rz}, \underline{tx}, \underline{ty}, \underline{tz})$  and  $(\bar{rx}, \bar{ry}, \bar{rz}, \bar{tx}, \bar{ty}, \bar{tz})$  signify the lower and upper limits of the small displacements  $rx$ ,  $ry$ ,  $rz$ ,  $tx$ ,  $ty$  and  $tz$  accordingly.

$$\begin{bmatrix} \underline{rx} & \overline{rx} \\ \underline{ry} & \overline{ry} \\ \underline{rz} & \overline{rz} \\ \underline{tx} & \overline{tx} \\ \underline{ty} & \overline{ty} \\ \underline{tz} & \overline{tz} \end{bmatrix}_{FR} = \left[ [J_1 \ J_2 \ J_3 \ J_4 \ J_5 \ J_6]_{FE1} \ \dots \ [J_{6n-5} \ J_{6n-4} \ J_{6n-3} \ J_{6n-2} \ J_{6n-1} \ J_{6n}]_{FE_n} \right] \bullet \begin{bmatrix} \underline{rx} & \overline{rx} \\ \underline{ry} & \overline{ry} \\ \underline{rz} & \overline{rz} \\ \underline{tx} & \overline{tx} \\ \underline{ty} & \overline{ty} \\ \underline{tz} & \overline{tz} \end{bmatrix}_{FE1} \bullet \begin{bmatrix} \underline{rx} & \overline{rx} \\ \underline{ry} & \overline{ry} \\ \underline{rz} & \overline{rz} \\ \underline{tx} & \overline{tx} \\ \underline{ty} & \overline{ty} \\ \underline{tz} & \overline{tz} \end{bmatrix}_{FE_n} \quad (6-6)$$

### 6.3 INTERVAL METHOD FOR TOLERANCE ANALYSIS

This section presents a new formulation for error stack-up mechanism in a multi-stage machining operation and worst-case based functional tolerance analysis. This formulation combines the MMP and the Jacobian-Torsor model. The functional elements will first be introduced and then the formulation presented.

#### 6.3.1 The functional elements(FE) of the interval method

Basically, three types of uncertainties are considered as functional element (FE) deviations: machined surface deviations, fixture surface deviations and links. In other words, each active surface involved in the machining operation and the links are the functional elements. The possible deviations of the functional elements are expressed by small displacement torsors with intervals. All the functional element torsor parameters are the combined approach parameters. According to the type of functional element and its geometry, some of the small displacement torsor parameters may be null.

##### 6.3.1.1 Surface deviation representation using an SDT with intervals

The SDT parameter range can be represented by intervals. As outlined before, this SDT with interval will be used for representing the fixture surface deviation, datum surface deviation and machined surface deviation. Eq. 6-7 shows the SDT with intervals for the  $i^{th}$

functional element. It should be underlined that all components of  $[FE_i]$  are assumed as independent variables.

$$[FE_i] = \left\{ \begin{array}{l} \underline{rx} \leq rx \leq \overline{rx} \quad \underline{tx} \leq tx \leq \overline{tx} \\ \underline{ry} \leq ry \leq \overline{ry} \quad \underline{ty} \leq ty \leq \overline{ty} \\ \underline{rz} \leq rz \leq \overline{rz} \quad \underline{tz} \leq tz \leq \overline{tz} \end{array} \right\} = \left\{ \begin{array}{l} \left[ \underline{rx} \quad \overline{rx} \right] \quad \left[ \underline{tx} \quad \overline{tx} \right] \\ \left[ \underline{ry} \quad \overline{ry} \right] \quad \left[ \underline{ty} \quad \overline{ty} \right] \\ \left[ \underline{rz} \quad \overline{rz} \right] \quad \left[ \underline{tz} \quad \overline{tz} \right] \end{array} \right\}_{FEi} = \left\{ \begin{array}{l} \left[ \underline{rx} \quad \overline{rx} \right] \\ \left[ \underline{ry} \quad \overline{ry} \right] \\ \left[ \underline{rz} \quad \overline{rz} \right] \\ \left[ \underline{tx} \quad \overline{tx} \right] \\ \left[ \underline{ty} \quad \overline{ty} \right] \\ \left[ \underline{tz} \quad \overline{tz} \right] \end{array} \right\}_{FEi} \quad (6-7)$$

### 6.3.1.2 Link representation using an SDT with intervals

The range of variation of the driving link parameters can be expressed using intervals. To obtain the variation interval of the driving link parameters, it is necessary to identify the different possible contacts for a link. For that we used the method described in 3.3.2. This expresses the variation interval of the driving link parameters using an optimization problem. If the driving link parameters are considered as independent variables, their extreme bounds can be defined as shown in Eq. 6-8

#### Case of MWP/Fixture:

$$\overline{l^*} = \frac{CH, CM, CHP}{Max} (l^*) \quad \underline{l^*} = \frac{CH, CM, CHP}{Min} (l^*) \\ \underline{l^*} = \frac{DH, DM, LHP}{Max} (l^*) \quad \overline{l^*} = \frac{DH, DM, LHP}{Min} (l^*) \quad (6-8)$$

Where  $l^*$  is the link parameter considered and  $* \in \{rx_{kSj}, ry_{kSj}, rz_{kSj}, tx_{kSj}, ty_{kSj}, tz_{kSj}\}$   
 $k$  = surface number and  $j$  = setup number

#### Case of Gauge/MMP:

$$\overline{l^*} = \frac{CM, CGP}{Max} (l^*) \quad \underline{l^*} = \frac{CM, CGP}{Min} (l^*) \\ \underline{l^*} = \frac{DM, LGP}{Max} (l^*) \quad \overline{l^*} = \frac{DM, LGP}{Min} (l^*) \quad (6-9)$$

Where  $l^*$  is the link parameter considered and  $* \in \{rx_{kGj}, ry_{kGj}, rz_{kGj}, tx_{kGj}, ty_{kGj}, tz_{kGj}\}$   
 $k$  = surface number and  $j$  = gauge number

The driving link lower limit and upper limit values obtained will then be replaced in the link torses as shown in Eq. 6-10.

$$[FE_i] = \left\{ \begin{array}{cc} [\underline{lr_x} & \overline{lr_x}] & [\underline{lt_x} & \overline{lt_x}] \\ [\underline{lr_y} & \overline{lr_y}] & [\underline{lt_y} & \overline{lt_y}] \\ [\underline{lr_z} & \overline{lr_z}] & [\underline{lt_z} & \overline{lt_z}] \end{array} \right\}_{FE_i} = \begin{array}{c} [\underline{lr_x} & \overline{lr_x}] \\ [\underline{lr_y} & \overline{lr_y}] \\ [\underline{lr_z} & \overline{lr_z}] \\ [\underline{lt_x} & \overline{lt_x}] \\ [\underline{lt_y} & \overline{lt_y}] \\ [\underline{lt_z} & \overline{lt_z}] \end{array}_{FE_i} \quad 6 \quad (6-10)$$

As previously outlined, according to the type of connection (floating or slipping), the link parameter values (LHP) are determined by a specific algorithm (CHP) that takes into account the constraints and, in certain cases, a positioning function.

This method for obtaining the link parameter variation intervals can be applied to the case of the MWP/Fixture or Gauge/MMP. To illustrate this, two examples (2D and 3D) of the MWP/Fixture assembly are given.

### 6.3.1.3 Example

In the example in [Figure 6-1](#), the MWP/Fixture assembly procedure involves two elementary connections: a primary and a secondary link. In the primary link, surface 1 of the MWP and surface 1S2 of the fixture are connected. This link is a slipping link, meaning that the positioning algorithm consists in maximizing the positioning function under non-penetration conditions. The non-penetration conditions are checked at two boundary points. See [Table 6-1](#).

The secondary link is formed of the connection between surface 2 and surface 2S2. Given that two degrees of freedom have already been blocked by the primary link, there will be one driving link parameter for this secondary link. As previously underlined, an automatic algorithm has been developed to find the driving link parameters. See [Table 6-1](#)

The variation intervals of these link parameters (that are obtained by Eq. [6-8](#)) are indicated in [Table 6-1](#). These values are obtained considering the surface defects indicated in the last row of this table for the fixture and datum surface deviations. The nominal connection happens when all the related surfaces are perfect (without any deviations). The worst connection happens when all the related surfaces have maximum deviations.

<sup>6</sup> The indices are eliminated for simplification.

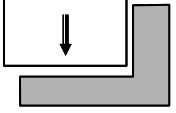
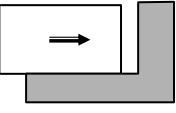
Setup 2					
Fixture			MWP		
Surface	Surface defects (DH)	Constraints (CH)	Surface	Surface defects (DM)	Constraints (CM)
Plane 1S2	$rx_{1S2}, tz_{1S2}$	cf. last row	Plane1	$rx_1, tz_1$	cf. last row
Plane 2S2	$rx_{2S2}, tz_{2S2}$	cf. last row	Plane2	$rx_2, tz_2$	cf. last row
Assembly					
Hierarchy	Driving link parameters LHP	Type of link	Positioning algorithm (CHP)		
			Positioning function to be maximized	Non-penetration conditions	
Primary	$lr_{x_{1S2}}, ltz_{1S2}$	Slipping	$-ltz_{1S2}$	$-30 lr_{x_{1S2}} + ltz_{1S2} \geq 0$ $30 lr_{x_{1S2}} + ltz_{1S2} \geq 0$	
Secondary	$ltz_{2S2}$	Slipping	$-ltz_{2S2}$	$20 lr_{x_{1S2}} + ltz_{2S2} - 20 (rx_1 - rx_{1S2} - rx_2 + rx_{2S2}) \geq 0$ $-20 lr_{x_{1S2}} + ltz_{2S2} + 20 (rx_1 - rx_{1S2} - rx_2 + rx_{2S2}) \geq 0$	
MWP		Fixture		Links	
Plane 1	Plane 2	Plane 1S2	Plane 2S2	Primary	Secondary
$\begin{bmatrix} [-0.003 & 0.003] \\ 0 \\ 0 \\ 0 \\ 0 \\ [-0.1 & 0.1] \end{bmatrix}$	$\begin{bmatrix} [-0.005 & 0.005] \\ 0 \\ 0 \\ 0 \\ 0 \\ [-0.1 & 0.1] \end{bmatrix}$	$\begin{bmatrix} [-0.003 & 0.003] \\ 0 \\ 0 \\ 0 \\ 0 \\ [-0.1 & 0.1] \end{bmatrix}$	$\begin{bmatrix} [-0.005 & 0.005] \\ 0 \\ 0 \\ 0 \\ 0 \\ [-0.1 & 0.1] \end{bmatrix}$	$\begin{bmatrix} [0 & +0] \\ U \\ U \\ U \\ U \\ [0 & +0] \end{bmatrix}$	$\begin{bmatrix} [0 & +0] \\ U \\ U \\ U \\ U \\ [0 & 0.176] \end{bmatrix}$

Table 6-1: MWP/Fixture Assembly based on the example in Figure 6-1

The MWP/Fixture assembly illustrated in Figure 6-3 will be used in a 4-axis milling machine for machining planes 5, 6 and 7. The positioning procedure involves making two elementary connections. The primary link is formed of a connection between plane 3 of MWP and 3S2 of the fixture. In the secondary link, cylinder 4 and cylinder 4S2 will be used for a short alignment of MWP. The primary link is a slipping link and the secondary link is a floating link. Any type of adjustment can be considered for the secondary link (e.g. H7/g6 referring to ISO standard for hole and shaft assembly). The link parameters and non-penetration condition for this assembly are given in Table 6-2. One degree of freedom (DOF) remains for the MWP in this assembly (rotation around the Z axis). The variation interval of the link parameters when considering an H7g6 adjustment for the secondary link is given in

Table 6-2. The fixture and datum surface deviations considered for this example are indicated in the last row of this table.

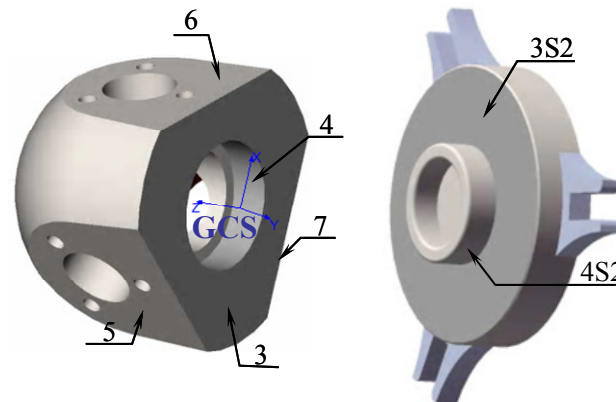


Figure 6–3: MWP/Fixture assembly with a floating link, “Bolt” example

## 6.4 TOLERANCE ANALYSIS

The new method for manufactured part tolerance analysis developed in this chapter is based on a modified version of the Jacobian-Torsor model, which is then combined with the MMP. The manufacturing simulation method used in this combined approach is the MMP method as described in chapter 3. Focusing on a specific process plan, the MMP collects the errors propagated in successive machining operations. For measuring the MMP, a virtual gauge is created using the functional tolerance (based on ISO or ASME standards). This is then assembled with the MMP. The accumulated defects on the final manufactured part can be modeled by the signed distance between the virtual gauge and the MMP ( $DisGP_k$ ) and calculated according to Eq. 6-11.

$$[DisGP] = [A] [FEs] \quad (6-11)$$

Where:

[DisGP] : signed distance between virtual gauge and MMP

[FEs] : Functional Element SDT or link torsor

[A] : Coefficient matrix expressing a geometrical relation between [DisGP] and [FEs]

The idea consists in considering the worst possible case for each functional element and studying the error stack-up on the final manufactured part. The contribution of each functional element will be established using the ( $A_i$ ) coefficient matrix. Machined surface and fixture surface (FE) uncertainties are expressed using the SDT with intervals. Each torsor component



will be considered independently of the others. The links will be expressed using the link torsor with intervals. Eq. 6-11 can be extended by replacing the functional element torsors.

Setup 2					
Fixture			MWP		
Surface	Surface defects (DH)	Constraints (CH)	Surface	Surface defects (DM)	Constraints (CM)
Plane 3S2	$rx_{3S2}, ry_{3S2}, tz_{3S2}$	cf. last row	Plane 3	$rx_3, ry_3, tz_3$	cf. last row
Cylinder 4S2	$rx_{4S2}, ry_{4S2}, tx_{4S2}, ty_{4S2}$	cf. last row	Cylinder 4	$rx_4, ry_4, tx_4, ty_4$	cf. last row.
Assembly					
Hierarchy	Link parameters (LHP)	Type of link	Positioning Algorithm(CHP)		
			Positioning function to be maximized	Non-penetration condition	
Primary	$lrx_{3S2}, lry_{3S2}, ltz_{3S2}$	Slipping	$-ltz_{3S2}$	$15 lrx_{3S2} - 20 lry_{3S2} + ltz_{3S2} \geq 0$ $-15 lrx_{3S2} - 20 lry_{3S2} + ltz_{3S2} \geq 0$ $-15 lrx_{3S2} + 20 lry_{3S2} + ltz_{3S2} \geq 0$ $15 lrx_{3S2} + 20 lry_{3S2} + ltz_{3S2} \geq 0$	
Secondary	$ltx_{4S2}, lty_{4S2}$	Floating	-	$RN_4 - RN_{4S2} + r_4 - r_{4S2} - \sqrt{(ltx_{4S2} - \frac{H}{2} lry_{4S2})^2 + (lty_{4S2} + \frac{H}{2} lrx_{4S2})^2} \geq 0$ <sup>7</sup> $RN_4 - RN_{4S2} + r_4 - r_{4S2} - \sqrt{(ltx_{4S2} + \frac{H}{2} lry_{4S2})^2 + (lty_{4S2} - \frac{H}{2} lrx_{4S2})^2} \geq 0$	
MWP		Fixture		Links	
Plane 3	Cylinder 4	Plane 3S2	Cylinder 4S2	Primary	Secondary
$\begin{bmatrix} [-0.0005 & 0.0005] \\ [-0.0003 & 0.0003] \\ 0 \\ 0 \\ 0 \\ [-0.0051 & 0.0051] \end{bmatrix}$	$\begin{bmatrix} [-0.0003 & 0.0003] \\ [-0.0003 & 0.0003] \\ 0 \\ [0 & +0] \\ [0 & +0] \\ 0 \end{bmatrix}$ Radius deviation: $[-0.01 & 0.01]$	$\begin{bmatrix} [-0.0013 & 0.0013] \\ [-0.0007 & 0.0007] \\ 0 \\ 0 \\ 0 \\ [-0.015 & 0.015] \end{bmatrix}$	$\begin{bmatrix} [-0.0008 & 0.0008] \\ [-0.0008 & 0.0008] \\ 0 \\ [0 & +0] \\ [0 & +0] \\ 0 \end{bmatrix}$ Radius deviation: $[-5e^{-4} & 5e^{-4}]$	$\begin{bmatrix} [0 & +0] \\ [0 & +0] \\ U \\ U \\ U \\ [0 & +0] \end{bmatrix}$	$\begin{bmatrix} \text{Dependent} \\ \text{dependent} \\ U \\ [-0.05 & 0.05] \\ [-0.05 & 0.05] \\ U \end{bmatrix}$

Table 6-2: Assembly procedure for the “Bolt” example in Figure 6–3

<sup>7</sup> RN= Nominal radius, r= radius deviation , H= contact length



$$\begin{aligned}
GapGP_{k'} &= \left[ \inf\{DisGP_k\} + \left(\frac{t}{2}\right) \quad \sup\{DisGP_k\} + \left(\frac{t}{2}\right) \right] \\
GapGP_{k'+1} &= \left[ \left(\frac{t}{2}\right) - \sup\{DisGP_k\} \quad \left(\frac{t}{2}\right) - \inf\{DisGP_k\} \right]
\end{aligned} \tag{6-14}$$

For  $k=1$  to number of verification points

The process compliance condition can be expressed by using *GapGP* interval as indicated in Eq. 6-15.

$$GapGP_k \subseteq \mathfrak{R}^+ \quad \text{For } k = 1 \text{ to number of } GapGP \text{ distances} \tag{6-15}$$

## 6.5 VIRTUAL GAUGE BEST POSITION

As described in section 4.3, based on the type of tolerance, datum system and material condition, DOF or internal mobility or limited displacement for the virtual gauge related to MMP sometimes remain. In section 4.3, it is described how the best position of a virtual gauge is found related to MMP by the way of optimization methods. In this section, the method for finding the best position of virtual gauge, when using interval method for the purpose of tolerance analysis, is described.

Actually, Eq. 6-11 can be decomposed as indicated in Eq. 6-16.

$$DisGP = \underbrace{[A'] \cdot [FE]}_{\text{Fixed}} + \underbrace{[A''] \cdot [DOF]}_{\text{variable}} \tag{6-16}$$

The first term on the right-hand side of Eq. 6-16 is fixed and it represents the contribution of all the functional element uncertainties in  $DisGP_k$  values. The second term represents the contribution of the DOF and the limited displacements of the gauge in  $DisGP_k$  values. By using the algorithm proposed in Figure 6-4, the optimal value of the DOF and the limited displacements of the gauge are calculated. In this algorithm the aim is to minimize the objective function which is the radius of  $DisGP_{max}$  interval. Optimization techniques, like SQP, work well to this aim.

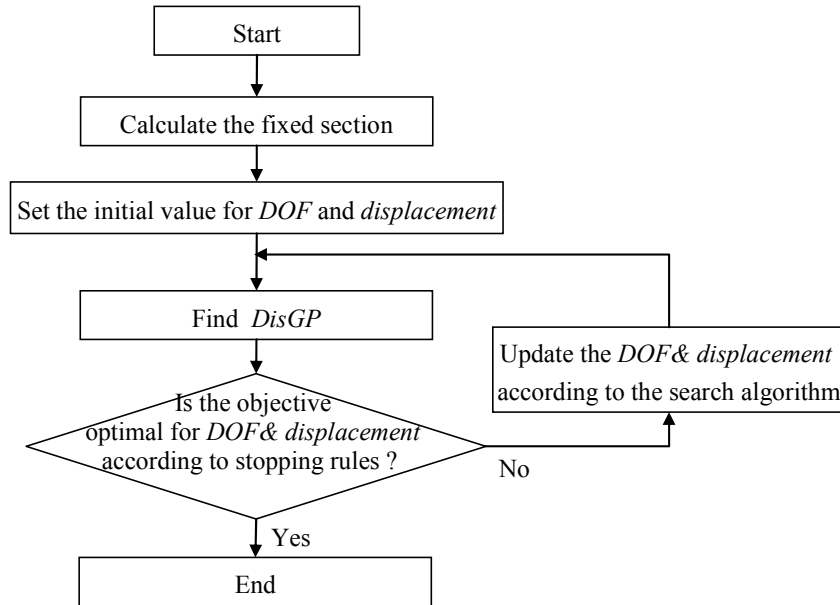


Figure 6–4: Proposed algorithm for finding the best position of virtual gauge

## 6.6 CONCLUSION

This chapter presented the interval method for the worst case based tolerance analysis using the MMP in a multi-stage machining process. This method blends the benefits of the Model of Manufactured Part and the Jacobian-Torsor model. This method additionally, allows performing the calculation very rapidly compared to the optimization methods.

In this method, interval arithmetic is used to associate bounds on the components of the small displacement torsors. It is used to determine two terminal limits: a lower limit and an upper limit. The advantage of the interval method lies in the fact that all the results are guaranteed and given in the form of a closed interval taking into account possible numerical errors. Furthermore it is more rapid than the optimization approach.

If a process is found to be nonconform, it is possible to find the root cause of the errors leading to tolerance violation. Based on Eq. 6-12, the contribution of each functional element is known; hence it is easy to find out which FE leads to process nonconformity, e.g. the fixture tools. It is possible to summarize the tolerance analysis based on this combined approach in four basic steps. The first step involves collecting information about machine tool and fixture quality. The second step involves creating the MMP, writing the MWP/Fixture positioning algorithm (CHP), creating the virtual gauge and its positioning algorithm (CGP),

and then finding the coefficient matrices. In the third step, the extreme bounds of the MWP/Fixture and Gauge /MMP link parameters are calculated using Eq. 6-8. Finally, the fourth step uses Eq. 6-12 to calculate the  $DisGP_k$  variation intervals at the verification points. The results obtained are then compared with the functional tolerance as part of the tolerance analysis.

## 7 STOCHASTIC TOLERANCE ANALYSIS AND CASE STUDY

In this chapter the performance of the two aforementioned worst case search methods (Multi layer optimization and interval approach) will be compared with each other and with a stochastic approach. As it is outlined in chapter 2, worst case tolerance analysis is exaggeratedly pessimist. The worst part might never been produced therefore, clearly, there is a need to take into consideration the probabilistic behavior of the manufacturing processes.

In stochastic methods, a large number of parts are randomly (due to the manufacturing errors) created and then the compliance of each generated part is verified with the functional tolerance. Firstly the stochastic approach for tolerance analysis using the MMP will be explored and secondly the three approaches will be applied to two 3D examples.

### 7.1 STOCHASTIC APPROACH FOR TOLERANCE ANALYSIS USING THE MMP

The stochastic method for tolerance analysis using the MMP uses Monte Carlo (MC) simulation. The method associated with MC consists in producing enough number of parts to check whether they all comply with the functional tolerance [Vignat F. *et al*, 2008]. The various parameters occurring in the analysis equation are randomly generated. The objective is to generate a distribution for the significant characteristics of the considered surfaces inside a domain limited by constraints. For example, the machined surface deviations related to nominal machine tool (DM) are limited by constraints (CM) stemming from the machine tool capabilities and fixture surface deviations (DH) are limited by constraints (CH) stemming from fixture precision. These constraints limit either one or a set of parameters. The parts are virtually produced according to the defects generation procedure. The defects generation procedure should be compatible with the chosen quality constraints described in 5.3.2.

The generated parts are put forward to Sub II (see section 5.2) where each part will be verified in term of functional tolerance.

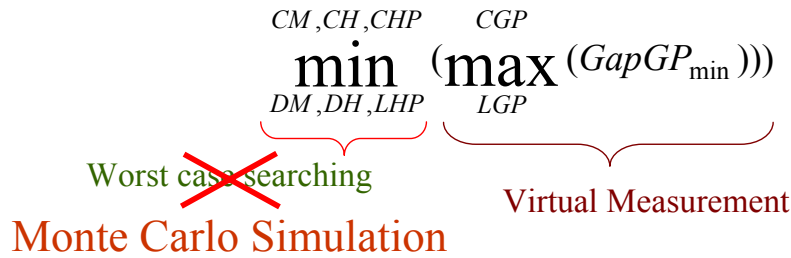


Figure 7–1: Monte Carlo simulation

### 7.1.1 Defect generation procedure

In stochastic method, worst case searching procedure (Sub I) is replaced with a MC simulation .See [Figure 7–1](#). In MC simulation, virtual parts (which represent different instances of production time) are produced by the defects generation procedure according to the chosen quality constraints. In this section, the defects generation procedure is described to show how it is possible to handle 3 different strategies described in section [5.3.2](#). Depending on the type of chosen strategy, the defects should be generated with a compatible defect generation method.

#### 7.1.1.1 Using Measurement Results (independent variables)

As described in section [5.3.2.1](#), the parameters can be considered as independent or dependent. For the case with independent parameters, each parameter is generated within its range using a classical generator like extended cellular automata generator [Kier L. B. *et al*, 2005].

#### 7.1.1.2 Using Measurement Results (dependent variables) and Variation zone

Concerning the two above mentioned strategies, the parameters are dependent. For generating the most uniform distributed defect parameters, two cases are distinguished:

##### Case one:

When it is possible to make a non-correlated variable substitution, the classical generator described in section [7.1.1.1](#) is applied to the substituted variables and the reverse

substitution is applied. Each set of generated defects should be verified as to whether they respect the quality constraints imposed by the chosen strategy.

For example, in a cylindrical variation zone, a variable substitution is made so that 4 variables are generated without correlation according to Eq. 7-1. The 4 defect parameters describing the cylinder “real” position are then calculated using Eq. 7-2.

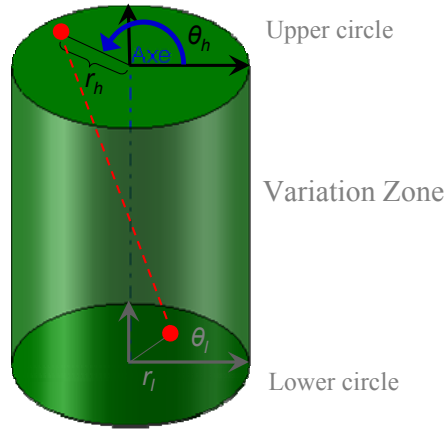


Figure 7–2: Defect generation for the case of a cylindrical variation zone (dependent parameters)

$$r_h = \left\{ x \left| \begin{array}{l} 0 \leq x \leq r_{\text{variation zone}} \\ \text{probability density } F_r(x) = \left( \frac{x}{r_{\text{variation zone}}} \right)^2 \end{array} \right. \right\}$$

$$r_l = \left\{ x \left| \begin{array}{l} 0 \leq x \leq r_{\text{variation zone}} \\ \text{probability density } F_r(x) = \left( \frac{x}{r_{\text{variation zone}}} \right)^2 \end{array} \right. \right\} \quad (7-1)$$

$$\theta_h = \left\{ x \left| \begin{array}{l} 0 \leq x \leq 2\pi \\ \text{with probability density } F_\theta(x) = \left( \frac{x}{2\pi} \right) \end{array} \right. \right\}$$

$$\theta_l = \left\{ x \left| \begin{array}{l} 0 \leq x \leq 2\pi \\ \text{with probability density } F_\theta(x) = \left( \frac{x}{2\pi} \right) \end{array} \right. \right\}$$

$$rx = -r_h \sin(\theta_h) + r_l \sin(\theta_l)$$

$$ry = r_h \cos(\theta_h) - r_l \cos(\theta_l)$$

(7-2)

$$tx = \frac{r_h \cos(\theta_h) + r_l \cos(\theta_l)}{2}$$

$$ty = \frac{r_h \sin(\theta_h) + r_l \sin(\theta_l)}{2}$$



**Case two:**

In this case the parameters are still dependent and it is not possible to make a non-correlated variable substitution because of the complexity of the correlations (e.g. ellipse). A new larger variation zone is created that circumscribes the previous one (e.g. a rectangle). This allows using the classical random described in section 7.1.1.1 or those of case 1. Consequently each set of generated defects will be kept if it meets the constraint of principle domain. This procedure should be repeated until reaching the needed number of defects sets.

For the example illustrated in Figure 7-3, the constraints obtained for the measurement results for deviation parameters can be expressed as Eq. 7-3 which represents the blue ellipse.

$$a \cdot rx^2 + b \cdot ry^2 + c \cdot rx \cdot ry \leq d \quad (7-3)$$

For random generation of defects we replace the blue ellipse with a larger domain which is represented by the red rectangle in Figure 7-3.

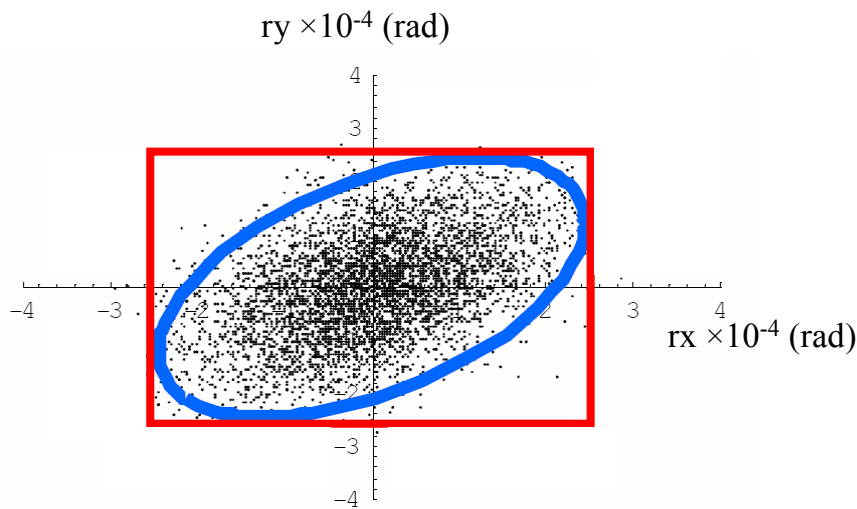


Figure 7-3: random generation of defects-Case two

The defects are generated with respect to the constraints imposed by the new domain, Eq.7-4, by a classical random generator and for each set of generated defects, it will be kept if it meets the d constraints imposed by the principle domain (the blue ellipse in this case).

$$\begin{aligned} -3 \times 10^{-4} &\leq rx \leq 3 \times 10^{-4} \\ -3 \times 10^{-4} &\leq ry \leq 3 \times 10^{-4} \end{aligned} \quad (7-4)$$

Regarding a planar variation zone, each nominal vertex of the convex boundary of the plane is randomly generated along the normal of the nominal plane. The values are randomly generated between  $-\frac{e}{2}$  and  $\frac{e}{2}$  with a uniform density. See Figure 7-4. A plane is then positioned from the generated vertices using a mean square root criteria. The 3 parameters  $r_x$ ,  $r_y$  and  $t_z$  are then calculated from the plane characteristics. After the generation of the set of parameters, a verification of the constraints is performed. If one of the constraints is not verified, the set is rejected. The procedure is repeated until the required number of valid sets is reached.

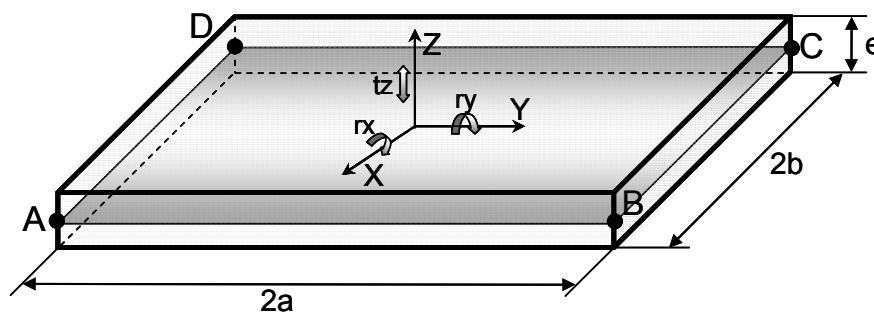


Figure 7-4: Planar variation zone

### 7.1.2 Floating link values generation

Among the link values (LHP), as it is outlined before, there are two types of link parameters: slipping ( $LHP_s$ ) and floating ( $LHP_f$ ). The  $LHP_s$  link values are determined by CHP algorithms (positioning function in line with NPC) thus for each instance of the defects parameters value, a unique set of LHPs can be calculated.  $LHP_f$  have to be generated with respect to CHP which is just the NPC for the case of a floating connection. In other word, there is a range of variation for  $LHP_f$  parameters which satisfies these NPC.

For determining the floating link parameters  $LHP_f$ , it should be considered that they have to respect the positioning algorithm (CHP). The second requirement, for the determination of the link values, is that their density has to be controlled (uniform or other distribution) in the variation scope allowed by CHP.

For example, in Figure 7-5, the primary link is formed of a connection between plane 3 of MWP and 3S2 of the fixture. In the secondary link, cylinder 4 and cylinder 4S2 will be used for a short alignment of MWP relative to the fixture with H7g6 adjustment according to

ISO standard. The primary link is a slipping link and the secondary link is a floating link. See section 6.3.1.3 for more details.

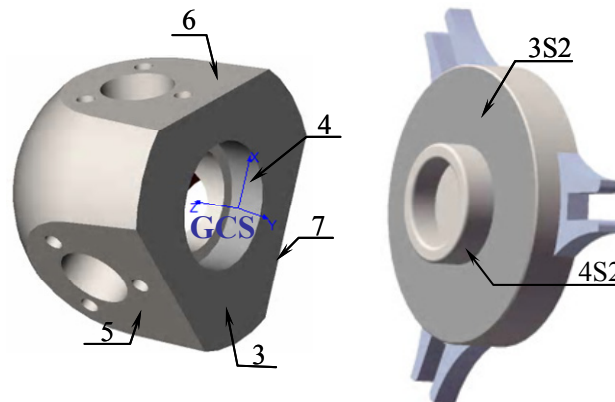


Figure 7-5: MWP/Fixture assembly with a floating link

The primary link parameter values are calculated by maximization of positioning function with respect to NPC. The secondary link parameters ( $ltx_{4S2}$ ,  $lty_{4S2}$ ) have to be generated by the defect generation procedure that respect the limits imposed by NPC between the MWP and the fixture. In order to fulfill these requirements, the generation of these parameters is made according to the following algorithm. [Vignat F. *et al*, 2008]

- Calculate the maximum centering clearance  $r_c$  (based on H7g6 adjustment)
- Randomly generate:
  - $\theta$  between 0 and  $2\pi$  and  $r$  between 0 and  $r_c$  as in Eq. 7-1
- Calculate  $ltx_{4S2}$ ,  $lty_{4S2}$  according to Eq. 7-5
- Verify the non-penetration between the MWP and the fixture
  - If verified, keep the link values
  - Otherwise reduce  $r_c$  and redo the generation

$$\begin{aligned} ltx_{4S2} &= r \cos(\theta) \\ lty_{4S2} &= r \sin(\theta) \end{aligned} \tag{7-5}$$

This generation procedure complies with both of the requirements; all of the generated links satisfies the CHP algorithm and Figure 7-6 shows that the distribution uniformly fills the allowed domain.

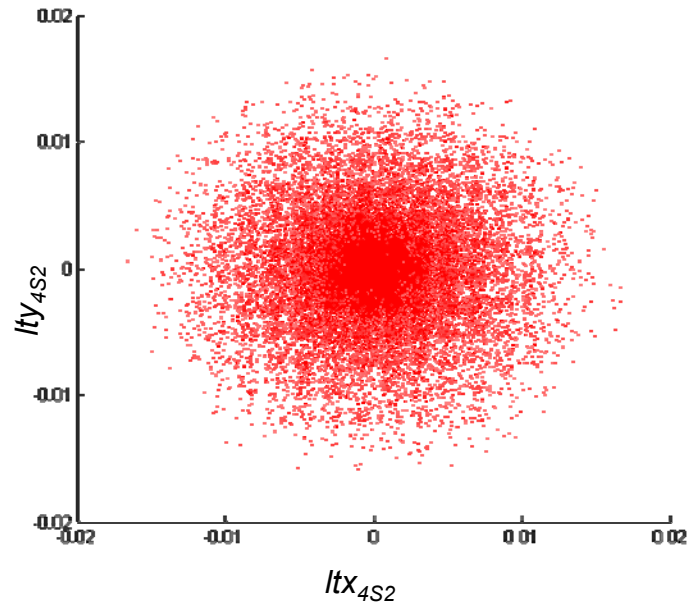


Figure 7–6: Distribution of link parameters in the allowed domain

## 7.2 EXAMPLES AND COMPARISON

In this section, the three aforementioned techniques for tolerance analysis with the MMP will be applied to two 3D examples and their characteristics will be explored.

### 7.2.1 “Double inclined plane” example

The part illustrated in Figure 7–7 will be used to perform a tolerance analysis of the double inclined machined plane with the before mentioned techniques.

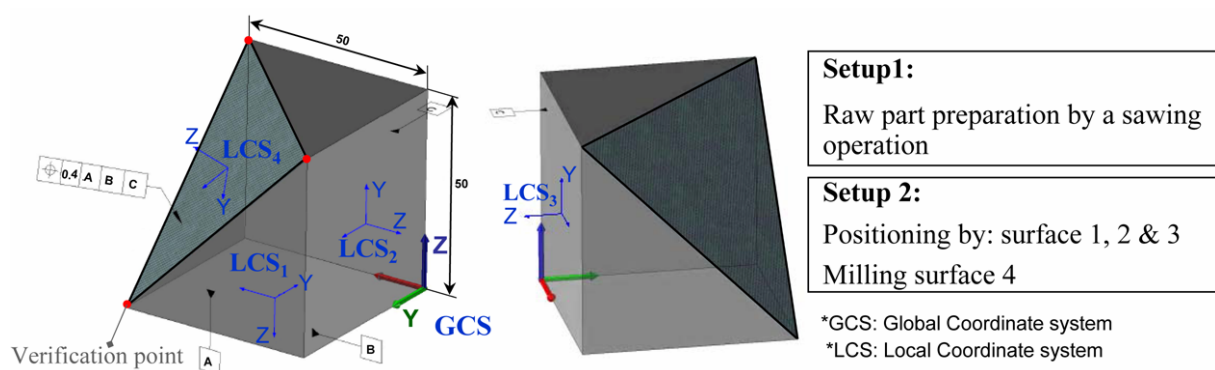


Figure 7–7: Definition of “Double inclined plane” example

Setup 1 of the process plan consists in preparing the raw blocks through a sawing operation. This results in the MWP that will go through setup 2. Concerning the MWP/Fixture assembly in setup 2, the positioning surfaces of the MWP are plane 1, plane 2 and plane 3 and the positioning surfaces of the fixture are plane 1S2, plane 2S2 and plane 3S2. The assembly procedure for MWP/Fixture assembly comprises three hierarchical slipping connections whose link parameters (LHP) and positioning algorithm (CHP) are given in [Table 7-1](#). In setup 2, plane 4 is machined on a milling machine.

In the first section, the quality constraints with independent parameters will be studied and in the second section the quality constraints with dependent parameters will be treated. Actually, quality constraints with independent parameters can be treated by all three aforementioned solution methods, but the quality constraints with dependent parameters can only be treated by optimization technique and MC simulation.

### **7.2.1.1 First section-independent parameters-interval approach**

The approach is limited by the fact that it considers the parameters independently. The example will be dealt with using the four tolerance analysis steps described in [6.4](#).

#### **Step 1:**

In this section the quality constraints “Using the Measurement Results (independent parameters)” are considered and the MWP positioning surface deviation range, the machining errors and the fixture surface deviation range are obtained from a database created over the measurement results (the ranges are available in [Table 7-3](#) ). This section will not describe how to create the database (details about database creation can be found in [Tichadou S. *et al*, 2007]).

#### **Step 2:**

For each elementary connection, the link parameters (LHP) and the positioning algorithm (CHP) are given in [Table 7-1](#). The MMP will be obtained following the simulation of the manufacturing process by using the simulation method described in [chapter 3](#).

#### **Step 3:**

In this step the extreme bounds of the link parameters related to the MWP/Fixture and Gauge/MMP assembly are calculated using [Eq. 6-8](#). The results are given in [Table 7-3](#).

Setup2					
Fixture			Part (MWP)		
Surface	Surface deviation (DH)	Constraints (CH)	Surface	Surface deviation (DM)	Constraints (CM)
Plane 1S2	$rx_{1S2}, ry_{1S2}, tz_{1S2}$	c.f.	Plane 1	$rx_1, ry_1, tz_1$	c.f.
Plane 2S2	$rx_{2S2}, ry_{2S2}, tz_{2S2}$	c.f.	Plane 2	$rx_2, ry_2, tz_2$	c.f.
Plane 3S2	$rx_{3S2}, ry_{3S2}, tz_{3S2}$	c.f.	Plane 3	$rx_3, ry_3, tz_3$	c.f.
Part/Fixture assembly					
Hierarchy	link parameters (LHP)	Type of link	Positioning algorithm (CHP)		
			Positioning function to	Non-penetration condition	
Primary	$lr_{x1S2}$ $lr_{y1S2}$ $ltz_{1S2}$	Slipping	$-ltz_{1S2}$	$-25 lr_{x1S2} + 25 lr_{y1S2} + ltz_{1S2} \geq 0$ $-25 lr_{x1S2} - 25 lr_{y1S2} + ltz_{1S2} \geq 0$ $25 lr_{x1S2} - 25 lr_{y1S2} + ltz_{1S2} \geq 0$ $25 lr_{x1S2} + 25 lr_{y1S2} + ltz_{1S2} \geq 0$	
Secondary	$lr_{y2S2}$ $ltz_{2S2}$	Slipping	$-ltz_{2S2}$	$25 lr_{x1S2} + 25 lr_{y2S2} + ltz_{2S2} - 25 rx_1 + 25 rx_{1S2} + 25 rx_2 - 25 rx_{2S2} \geq 0$ $25 lr_{x1S2} - 25 lr_{y2S2} + ltz_{2S2} - 25 rx_1 + 25 rx_{1S2} + 25 rx_2 - 25 rx_{2S2} \geq 0$ $-25 lr_{x1S2} - 25 lr_{y2S2} + ltz_{2S2} + 25 rx_1 - 25 rx_{1S2} - 25 rx_2 + 25 rx_{2S2} \geq 0$ $-25 lr_{x1S2} + 25 lr_{y2S2} + ltz_{2S2} + 25 rx_1 - 25 rx_{1S2} - 25 rx_2 + 25 rx_{2S2} \geq 0$	
Tertiary	$ltz_{3S2}$	Slipping	$-ltz_{3S2}$	$(-25 lr_{y1S2} - 25 lr_{y2S2} + ltz_{3S2} + 25 rx_3 + 25 rx_{3S2} - 25 ry_1 - 25 ry_{1S2} - 25 ry_2 - 25 ry_{2S2} - 25 ry_3 + 25 ry_{3S2}) \geq 0$ $(25 lr_{y1S2} - 25 lr_{y2S2} + ltz_{3S2} + 25 rx_3 + 25 rx_{3S2} + 25 ry_1 + 25 ry_{1S2} - 25 ry_2 - 25 ry_{2S2} + 25 ry_3 - 25 ry_{3S2}) \geq 0$ $(25 lr_{y1S2} + 25 lr_{y2S2} + ltz_{3S2} - 25 rx_3 - 25 rx_{3S2} + 25 ry_1 + 25 ry_{1S2} + 25 ry_2 + 25 ry_{2S2} + 25 ry_3 - 25 ry_{3S2}) \geq 0$ $(-25 lr_{y1S2} + 25 lr_{y2S2} + ltz_{3S2} - 25 rx_3 - 25 rx_{3S2} - 25 ry_1 - 25 ry_{1S2} + 25 ry_2 + 25 ry_{2S2} - 25 ry_3 + 25 ry_{3S2}) \geq 0$	

Table 7-1: Fixture/MWP assembly for the “Double inclined plane”

**Step4**

In the last step, the  $DisGP_k$  variation intervals are calculated using Eq 6-11. There are 3 verification points for machined plane 4. There will therefore be three  $DisGP_k$ . See Table 7-2.

**Results and discussion**

The results given in Table 7-2 are obtained using the Matlab INTLAB (interval laboratory) [Rump S. M., 2007] toolbox. As seen in this table, the critical points are  $DisGP_2$  and  $DisGP_3$ . To be able to validate this process plan in terms of functional tolerance compliance, the variation interval obtained for  $DisGP_i$  must be compared with the localization tolerance value ( $t=0.4$ ). This proves that the process plan and fixture tools applied are able to satisfy the functional tolerance.

$$DisGP_{k(k=1,2,3)} \subseteq \begin{bmatrix} -0.4 & 0.4 \\ 2 & 2 \end{bmatrix} \quad (7-6)$$

These results can be expressed with *GapGP* intervals as well:

Machined surface	verification point	Verification points	Results (mm)	
			DisGP	GapGP
Plane 4	1	(50, 50, 0)	[-0.1856 0.0991]	[0.11 0.38]
				[0.02 0.29]
	2	(0, 50, 50)	[-0.1728 0.0863]	[0.03 0.28]
				[0.12 0.37]
	3	(50, 0, 50)	[-0.1901 0.1036]	[0.01 0.30]
				[0.10 0.39]

Table 7-2: Interval approach results for “Double inclined plane” example with *DisGP* and *GapGP* expression

### 7.2.1.2 First Section-independent parameters-optimization approach

The ranges of variables are those expressed previously in Table 7-3 and used for the interval approach. The assembly process of MWP/fixture and the one of Gauge/MMP are explained just before.

To be able to validate the process plan for satisfying the localization tolerance of plane 4, the worst case is sought. In Sub II, there is no degree of freedom or floating link for the Gauge/MMP assembly.

The MATLAB software was used for programming with a Pentium®, 3.2 GHz. Both optimization algorithms (GA and SQP) were applied to minimize Sub I. Figure 7–8 represents the results obtained using the SQP and Figure 7–9 represents those obtained using GA.

### 7.2.1.3 First section-independent parameters-MC simulation

By using the defect generation method explained in 7.1.1.1 (independent parameters), 100000 parts are virtually created within the ranges mentioned in Table 7-3. The created parts are then put forward to sub II for measurement. The distribution of  $GapGP_{min}$  and the worst part found by MC are mentioned in Figure 7–10.

Functional elements			Coefficient matrix [A]	Defects range	Functional elements			Coefficient matrix [A]	Defects range
Prepared Surfaces by sawing	Plane 1	$rx_1$	$[0]_{3 \times 6}$	$\begin{bmatrix} -0.0005 & 0.0005 \\ -0.0003 & 0.0003 \\ 0 \\ 0 \\ 0 \\ -0.0051 & 0.0051 \end{bmatrix}$	Fixture Surface Deviations	Plane 1S2	$rx_{1S2}$	$\begin{bmatrix} -2887 & 2887 & 0 & 0 & 0 & -0.58 \\ 0 & -2887 & 0 & 0 & 0 & -0.58 \\ 2887 & 0 & 0 & 0 & 0 & -0.58 \end{bmatrix}$	$\begin{bmatrix} -0.0013 & 0.0013 \\ -0.0007 & 0.0007 \\ 0 \\ 0 \\ 0 \\ -0.015 & 0.015 \end{bmatrix}$
		$ry_{1S2}$		$\begin{bmatrix} -0.0013 & 0.0013 \\ -0.0007 & 0.0007 \\ 0 \\ 0 \\ 0 \\ -0.015 & 0.015 \end{bmatrix}$					
		$tz_{1S2}$		$\begin{bmatrix} -0.0013 & 0.0013 \\ -0.0007 & 0.0007 \\ 0 \\ 0 \\ 0 \\ -0.015 & 0.015 \end{bmatrix}$					
	Plane 2	$rx_2$	$[0]_{3 \times 6}$	$\begin{bmatrix} -0.0005 & 0.0005 \\ -0.0003 & 0.0003 \\ 0 \\ 0 \\ 0 \\ -0.0051 & 0.0051 \end{bmatrix}$		Plane 2S2	$rx_{2S2}$	$\begin{bmatrix} 0 & 0 & 0 & 0 & 0 & -0.58 \\ 0 & -28.87 & 0 & 0 & 0 & -0.58 \\ 0 & 28.87 & 0 & 0 & 0 & -0.58 \end{bmatrix}$	$\begin{bmatrix} -0.0013 & 0.0013 \\ -0.0007 & 0.0007 \\ 0 \\ 0 \\ 0 \\ -0.015 & 0.015 \end{bmatrix}$
		$ry_{2S2}$		$\begin{bmatrix} -0.0013 & 0.0013 \\ -0.0007 & 0.0007 \\ 0 \\ 0 \\ 0 \\ -0.015 & 0.015 \end{bmatrix}$					
		$tz_{2S2}$		$\begin{bmatrix} -0.0013 & 0.0013 \\ -0.0007 & 0.0007 \\ 0 \\ 0 \\ 0 \\ -0.015 & 0.015 \end{bmatrix}$					
	Plane 3	$rx_3$	$[0]_{3 \times 6}$	$\begin{bmatrix} -0.0005 & 0.0005 \\ -0.0003 & 0.0003 \\ 0 \\ 0 \\ 0 \\ -0.0051 & 0.0051 \end{bmatrix}$		Plane 3S2	$rx_{3S2}$	$\begin{bmatrix} 0 & 0 & 0 & 0 & 0 & -0.58 \\ 0 & 0 & 0 & 0 & 0 & -0.58 \\ 0 & 0 & 0 & 0 & 0 & -0.58 \end{bmatrix}$	$\begin{bmatrix} -0.0013 & 0.0013 \\ 0.0007 & 0.0007 \\ 0 \\ 0 \\ 0 \\ -0.015 & 0.015 \end{bmatrix}$
		$ry_{3S2}$		$\begin{bmatrix} -0.0013 & 0.0013 \\ 0.0007 & 0.0007 \\ 0 \\ 0 \\ 0 \\ -0.015 & 0.015 \end{bmatrix}$					
		$tz_{3S2}$		$\begin{bmatrix} -0.0013 & 0.0013 \\ 0.0007 & 0.0007 \\ 0 \\ 0 \\ 0 \\ -0.015 & 0.015 \end{bmatrix}$					
Machined surface	Plane 4	$rx_4$	$\begin{bmatrix} 40.82 & 0 & 0 & 0 & 0 & 1 \\ -20.41 & 35.36 & 0 & 0 & 0 & 1 \\ -20.41 & -35.36 & 0 & 0 & 0 & 1 \end{bmatrix}$	$\begin{bmatrix} -0.0003 & 0.0003 \\ -0.0003 & 0.0003 \\ 0 \\ 0 \\ 0 \\ -0.0031 & 0.0031 \end{bmatrix}$					
MWP/Fixture Links	Primary	$lrx_{1S2}$	$\begin{bmatrix} -28.87 & 28.87 & 0 & 0 & 0 & -0.58 \\ 0 & -28.87 & 0 & 0 & 0 & -0.58 \\ 28.87 & 0 & 0 & 0 & 0 & -0.58 \end{bmatrix}$	$\begin{bmatrix} 0 & +0 \\ 0 & +0 \\ 0 \\ 0 \\ 0 & +0 \end{bmatrix}$	Primary	$lrx_{1G1}$	$\begin{bmatrix} 28.87 & -28.87 & 0 & 0 & 0 & 0.58 \\ 0 & 28.87 & 0 & 0 & 0 & 0.58 \\ -28.87 & -28.87 & 0 & 0 & 0 & 0.58 \end{bmatrix}$	$\begin{bmatrix} 0 & +0 \\ 0 & +0 \\ 0 \\ 0 \\ 0 & +0 \end{bmatrix}$	
		$lry_{1S2}$		$\begin{bmatrix} 0 & 0 & 0 & 0 & 0 & -0.58 \\ 0 & -28.87 & 0 & 0 & 0 & -0.58 \\ 0 & 28.87 & 0 & 0 & 0 & -0.58 \end{bmatrix}$		$\begin{bmatrix} 0 & +0 \\ 0 & +0 \\ 0 \\ 0 \\ 0 & +0 \end{bmatrix}$			
		$ltz_{1S2}$		$\begin{bmatrix} 0 & 0 & 0 & 0 & 0 & -0.58 \\ 0 & -28.87 & 0 & 0 & 0 & -0.58 \\ 0 & 28.87 & 0 & 0 & 0 & -0.58 \end{bmatrix}$		$\begin{bmatrix} 0 & +0 \\ 0 & +0 \\ 0 \\ 0 \\ 0 & +0 \end{bmatrix}$			
	Secondary	$lry_{2S2}$	$\begin{bmatrix} 0 & 0 & 0 & 0 & 0 & -0.58 \\ 0 & -28.87 & 0 & 0 & 0 & -0.58 \\ 0 & 28.87 & 0 & 0 & 0 & -0.58 \end{bmatrix}$	$\begin{bmatrix} 0 & +0 \\ 0 & +0 \\ 0 \\ 0 \\ 0 & 0.0901 \end{bmatrix}$	Secondary	$lry_{2G1}$	$\begin{bmatrix} 0 & 0 & 0 & 0 & 0 & 0.58 \\ 0 & 28.87 & 0 & 0 & 0 & 0.58 \\ 0 & -28.87 & 0 & 0 & 0 & 0.58 \end{bmatrix}$	$\begin{bmatrix} 0 & +0 \\ 0 & +0 \\ 0 \\ 0 \\ 0 & 0.0251 \end{bmatrix}$	
		$ltz_{2S2}$		$\begin{bmatrix} 0 & 0 & 0 & 0 & 0 & -0.58 \\ 0 & -28.87 & 0 & 0 & 0 & -0.58 \\ 0 & 28.87 & 0 & 0 & 0 & -0.58 \end{bmatrix}$		$\begin{bmatrix} 0 & +0 \\ 0 & +0 \\ 0 \\ 0 \\ 0 & 0.0251 \end{bmatrix}$			
		$ltz_{3S2}$		$\begin{bmatrix} 0 & 0 & 0 & 0 & 0 & -0.58 \\ 0 & 0 & 0 & 0 & 0 & -0.58 \\ 0 & 0 & 0 & 0 & 0 & -0.58 \end{bmatrix}$		$\begin{bmatrix} 0 \\ 0 \\ 0 \\ 0 \\ 0 & 0.1201 \end{bmatrix}$			
Tertiary	$ltz_{3G1}$	$\begin{bmatrix} 0 & 0 & 0 & 0 & 0 & 0.58 \\ 0 & 0 & 0 & 0 & 0 & 0.58 \\ 0 & 0 & 0 & 0 & 0 & 0.58 \end{bmatrix}$	$\begin{bmatrix} 0 \\ 0 \\ 0 \\ 0 \\ 0 & 0.0351 \end{bmatrix}$						

Table 7-3: “Double inclined plane” example, range of defect parameters, Coefficient matrices and functional elements torsor with intervals

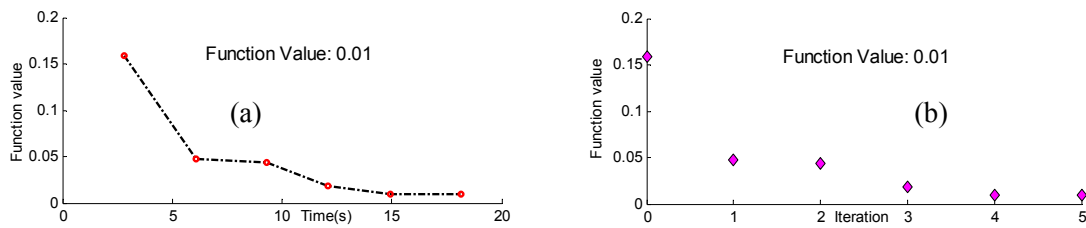


Figure 7-8 : Optimization by SQP, First section, with GapGP expression

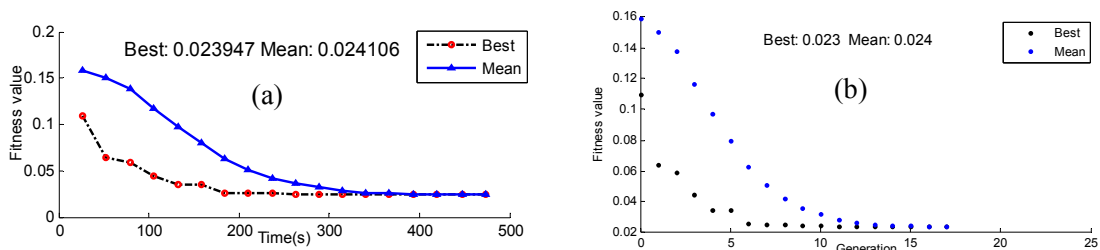


Figure 7-9 : Optimization by GA, First section, with GapGP expression



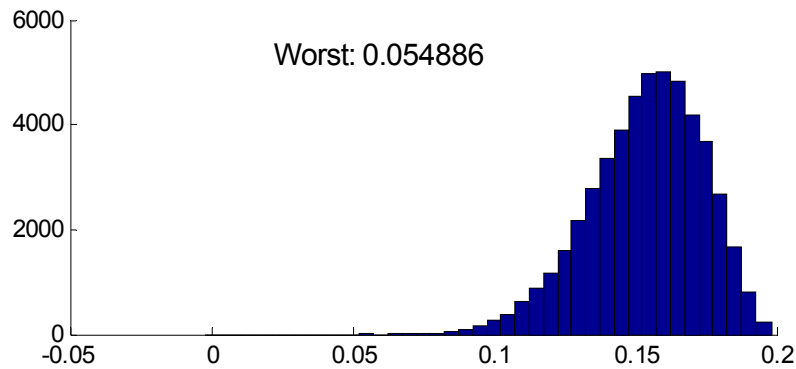


Figure 7–10: Mc results for first-section

### Discussion

The GA is very sensitive to parameter settings such as crossover rate, mutation rate and population size (in this example, we used a population size of 200, a crossover rate of 0.8 and a Gaussian mutation rate). If these parameters are correctly adjusted, enough population is created and random phenomena are used, the point obtained is almost sure to be a global minimum.

The advantage of the GA is that it does not need an initial point to start the optimization process. A little change in GA parameter setting may change the final solution obtained. The disadvantage of GA is that it needs a lot of time to converge.

SQP does not always converge towards a global minimum. The end result depends highly on the initial guess point. If the initial point is correctly defined, the SQP is able to reach the minimum quickly. [Figure 7–11](#) shows the performance of SQP with different initial guess points.

To over step this problem, SQP should be executed with different initial points. Some hybrid algorithms exist in which a population containing a large number of initial points is created to be use to start up the SQP.

In the case of the “double inclined plane”, the results obtained confirm that the process plan is valid in terms of satisfying the functional tolerance. There is a small difference between the results obtained from GA and SQP. In both algorithms, there is no proof that the point obtained is the global minimum. The time required for the GA to find this point is nearly 30 times greater than that required using SQP.

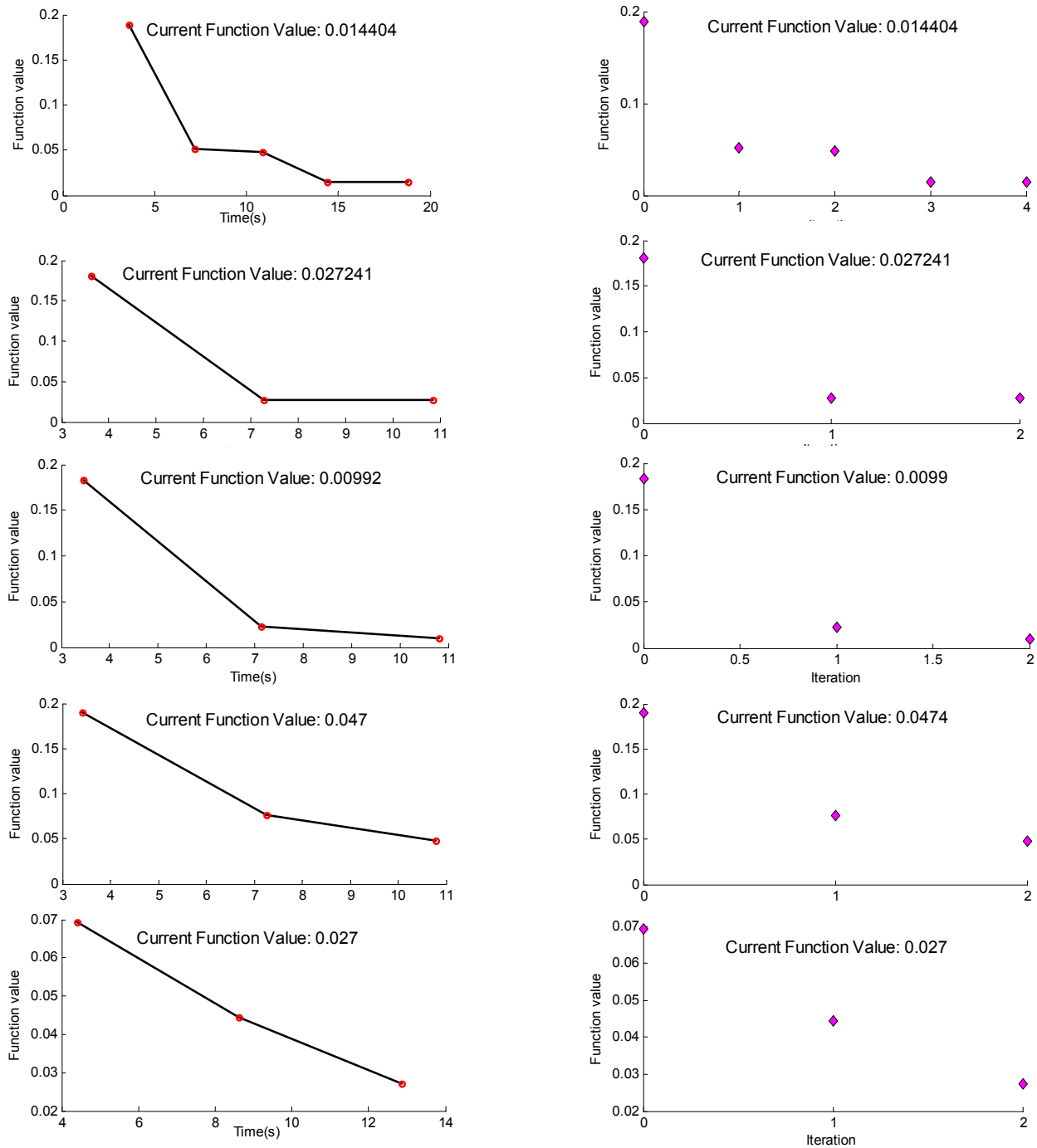


Figure 7–11: Performance of SQP with different initial guess points, with GapGP expression

The interval method converges to the global minimum if all the defects parameters (DM and DH) and the links (LHP and LGP) are assumed as independent variables. As it could be found from Table 7-4, the value obtained from combined approach and optimization techniques are the same in the case of such quality constraints. When using the quality constraints type “Using the Measurement Results (independent parameters)” it is more

meaningful to use interval method because it is more rapid compared with optimization techniques (in the case of the current example the elapsed time is less than 1 seconds). It can quickly give the process planner an initial idea about the quality of the manufactured parts with the chosen process plan.

Results	Optimization		Interval method	MC simulation
	SQP	GA		
GapGP <sub>min</sub> (mm)	0.01	0.024	[0.01 0.30]	0.054
DisGP <sub>max</sub> (mm)	0.190	0.176	0.190	0.146

Table 7-4: GapGP<sub>min</sub> and DisGP<sub>min</sub> obtained for first section

As it could be found from Table 7-4 and Table 7-5, the difference between MC simulation and other approaches is more significant. This difference can be explained. Considering a simple example (Figure 7-12) in which the dimension  $c$  is the result of the dimensions  $a$  and  $b$ , the worst case of dimension  $c$  is calculated from  $\Delta c$  obtained by Eq. 7-7 (as it is mentioned in section 2.3.1)

$$\Delta c = \Delta a + \Delta b \quad (7-7)$$

In statistical analysis, we assumed a distribution to each of  $a$  and  $b$  dimensions and then the variance of dimension  $c$  is calculated by Eq. 7-8. (With the assumption that  $a$  and  $b$  are independent)

$$\sigma^2_c = \sigma^2_a + \sigma^2_b \quad (7-8)$$

In MC simulation, we use uniform distribution. The variance of a uniformly distributed variable  $a$  is found from Eq. 7-9.

$$\sigma^2_a = \frac{\Delta_a^2}{12} \quad (7-9)$$

By replacing Eq. 7-9 in Eq. 7-8, and considering the fact that the sum of two uniform distributed variables is approximately normally distributed<sup>8</sup>, it is possible to find  $\Delta c$ :

<sup>8</sup> In fact by increasing the number of variables, the sum of uniform distributed variables get closer to normal distribution

$$\sigma_c^2 = \frac{\Delta_a^2}{12} + \frac{\Delta_b^2}{12}$$

$$\Delta_c = 6 \times \sqrt{\sigma_c^2} \quad \text{with the assumption that } c \text{ is normally distributed} \quad (7-10)$$

$$\Delta_c = \sqrt{3} \times \sqrt{\Delta_a^2 + \Delta_b^2}$$

In the case of  $n$  times dimension  $a$  with a same distribution and variance Eq. 7-7 and Eq. 7-10 become as Eq. 7-11.

$$\Delta_c = n \times \Delta_a \quad \text{Worst case} \quad (7-11)$$

$$\Delta_c = \sqrt{3n} \times \Delta_a \quad \text{Statistical analysis}$$

Eq. 7-11 shows that the worst values calculated for resulting dimension  $c$  by using worst case approach and statistical approach will get far from each other by increasing the number of participant dimensions. In the case of the “double inclined plane” example, there are nearly 21 participant parameters in *DisGP* so the worst value obtained by MC simulation is different from the one obtained by worst case approach.

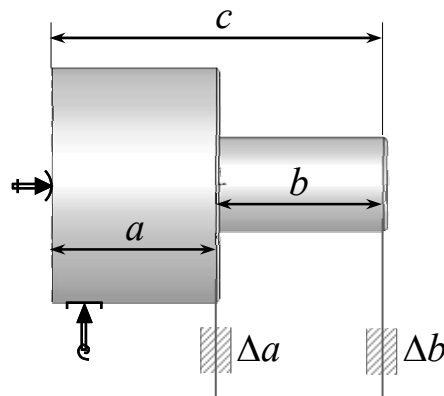


Figure 7–12: A part with two machined surfaces

#### 7.2.1.4 Second section with dependent variables (Variation zone)

In this section, the MC simulation and optimization techniques are compared when dealing with dependent quality constraints. Interval approach doesn't cover this type of quality constraint. In this section the same process plan will be treated but the variation range of DM and DH parameters are defined by the variation zones as indicated in Table 7-6.

The defects parameters variations, as mentioned in chapter 5.3.2.3, must be bound by the limits of the 3-D variation zones they represent. The MATLAB software was used for programming with a Pentium®, 3.2 GHz.

### 7.2.1.5 Second section-dependent variables-optimization approach

Both optimization algorithms (GA and SQP) were applied to minimize Sub I. Figure 7–13 represents the results obtained using SQP and Figure 7–14 represents those obtained using GA.

### 7.2.1.6 Second section-dependent variables- MC simulation

For MC simulation, 100000 parts are produced virtually according to the quality constrains described in Table 7-6 by the defect generation procedure described in section 7.1.1.2. The next step is to check the proportion of them that meet the functional tolerance. The  $GapGP$  are virtually measured between the part and the tolerance zone by using Sub II. The  $GapGP_{min}$  is then selected and will be retained as a result of the control. The distribution of the  $GapGP_{min}$  values obtained for the 100000 parts is represented by the histogram Figure 7–15.

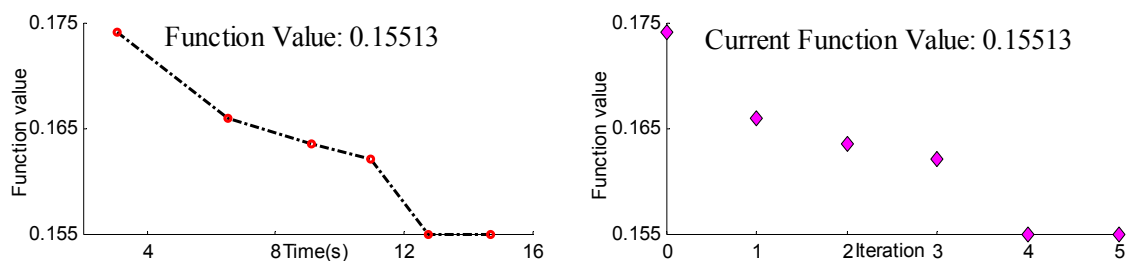


Figure 7–13: Optimization by SQP, Second section, with GapGP expression

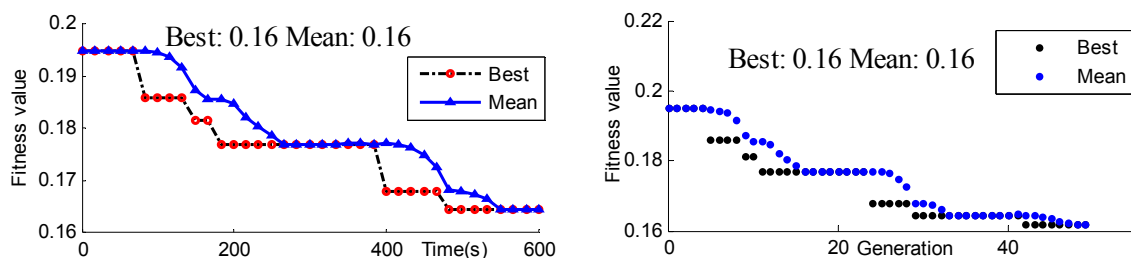


Figure 7–14: Optimization by GA, Second section, with GapGP expression

Section one (Independent variables)- Final point						
Surface deviation			SQP	GA	MC	
Setup 1	Prepared Surfaces by sawing	Plane 1	$rx_1$	0,0005	0,0004	-0,0001
			$ry_1$	-0,0001	0,0002	0,0003
			$tz_1$	0	0,0009	-0,0022
		Plane 2	$rx_2$	0,0005	0,0005	-0,0002
			$ry_2$	-0,0003	0,0003	0
			$tz_2$	0	-0,0051	0,0046
		Plane 3	$rx_3$	0,0005	0,0005	0,0004
			$ry_3$	-0,0001	-0,0003	-0,0002
			$tz_3$	0	0	-0,0012
Setup 2	Fixture surface deviation	Plane 1S2	$rx_{1S2}$	-0,0013	0,0013	0,0013
			$ry_{1S2}$	-0,0007	-0,0007	-0,0004
			$tz_{1S2}$	0,015	0,015	0,0145
		Plane 2S2	$rx_{2S2}$	0,0013	-0,0013	-0,0011
			$ry_{2S2}$	-0,0007	-0,0007	-0,0007
			$tz_{2S2}$	0,015	0,0141	0,0116
		Plane 3S2	$rx_{3S2}$	0,0013	0,0013	0,0013
			$ry_{3S2}$	0,0007	0,0007	0,0006
			$tz_{3S2}$	0,015	0,015	0,0017
	Machined surface	Plane 4	$rx_4$	0,0003	0	-0,0002
			$ry_4$	0,0003	0	-0,0002
			$tz_4$	-0,0031	-0,003	0,0004

Table 7-5: Final points obtained for first section

Setup 1		
Prepared Surfaces by sawing (Machining)		
No	Surface defects	variation scope
Plane 1	$rx_1, ry_1, tz_1$	Planar variation zone 0.01 (mm)
Plane 2	$rx_1, ry_1, tz_1$	Planar variation zone 0.01 (mm)
Plane 3	$rx_3, ry_3, tz_3$	Planar variation zone 0.01 (mm)
Set up 2		
Fixture surface deviation (Positioning)		
No	Surface defects	variation scope
Plane 1S2	$rx_{1S2}, ry_{1S2}, tz_{1S2}$	Planar variation zone 0.02 (mm)
Plane 2S2	$rx_{2S2}, ry_{2S2}, tz_{2S2}$	Planar variation zone 0.02 (mm)
Plane 3 S2	$rx_{3S2}, ry_{3S2}, tz_{3S2}$	Planar variation zone 0.02 (mm)
Machining		
Plane 4	$rx_4, ry_4, tz_4$	Planar variation zone 0.006 (mm)

Table 7-6: Second section-Deviation range for “Double inclined plane” manufacturing process

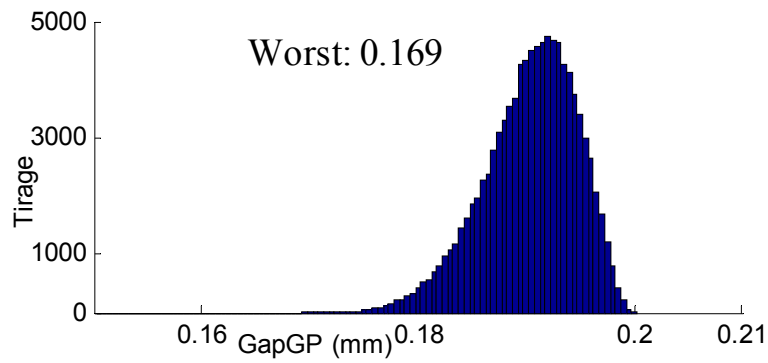


Figure 7–15: MC simulation results, Second section

Results	Optimization		MC simulation
	SQP	GA	
<b>GapGP<sub>min</sub> (mm)</b>	0.15	0.16	0.17
<b>DisGP<sub>max</sub> (mm)</b>	0.05	0.04	0.03

Table 7-7: GapGP<sub>min</sub> and DisGP<sub>max</sub> obtained for second section

### Discussion

The first point is that the values obtained in the second section by means of optimization techniques are higher than those obtained in the first section. This is because of the fact that in the first section all the defects parameters of a plane could have their extreme values simultaneously whereas in the case of the second section, in fact they are limited by the bounds of 3D variation zone of similar size and they can not reach their extreme value simultaneously.

Actually the 3D bounded variation zone is closer to tolerance standard. The value obtained by MC, reflects accurately the real production. From Table 7-7 it can be found that the worst value obtained for GapGP<sub>min</sub> is a little far from those obtained by optimization techniques. This raised from the fact that in real production the worst part might never been produced. In other word, when using the optimization technique, the worst part is searched but with MC simulation, the defects are generated randomly so the probability to find the worst part is very low.

Second section (Independent variables)- Final point						
Surface deviation			SQP	GA	MC	
Setup 1	Prepared Surfaces by sawing	Plane 1	$r_{X,P,1}$	0,0001	0	0
			$r_{Y,P,1}$	0	0	0
			$t_{Z,P,1}$	-0,0002	-0,0046	0,0009
		Plane 2	$r_{X,P,2}$	0,0001	0	0
			$r_{Y,P,2}$	0,0001	0	0
			$t_{Z,P,2}$	0,0013	-0,0046	-0,0001
		Plane 3	$r_{X,P,3}$	0	0	0
			$r_{Y,P,3}$	0,0002	0,0001	0
			$t_{Z,P,3}$	0,0007	0,0012	0,0019
Setup 2	Fixture surface deviation	Plane 1S2	$r_{X1S2}$	0	0	-0,0003
			$r_{Y1S2}$	0,0004	0,0004	0
			$t_{Z1S2}$	0	-0,0001	0,0017
		Plane 2S2	$r_{X2S2}$	0	0	0,0002
			$r_{Y2S2}$	0,0004	0,0003	-0,0002
			$t_{Z2S2}$	0	-0,0018	0,0025
		Plane 3S2	$r_{X3S2}$	-0,0001	-0,0003	0,0001
			$r_{Y3S2}$	0	0	0,0001
			$t_{Z3S2}$	0,0083	0,0001	0,0008
	Machined surface	Plane 4	$r_{X4}$	0,0001	-0,0001	0
			$r_{Y4}$	0	0	0,0001
			$t_{Z4}$	-0,001	-0,0006	-0,0003

Table 7-8: Final points obtained for second section

On the other hand, the difference between the MC result and those of optimization (See Table 7-7) depends on the number of *GapGP* equation parameters. This difference increases with the number of parameters. See section 7.2.1.3.

The problem of converging optimization techniques to a local minimum point exists in second section as well. The technique used in this example for finding a good initial guess point for SQP algorithms consists of running a MC simulation with a small number of parts (in this example 10000) then choosing the worst part of this small population as the start point for SQP. This method is called “hybrid optimization method”. Another combination of two approaches to make a hybrid technique can be for example SQP and GA. In this case a GA algorithm with a small number of populations will be used to find a start point for SQP. See Table 7-8 for final points.



## 7.2.2 “Bolt” example

In this section, we treat another 3D example with a floating cylinder-cylinder connection in MWP/Fixture assembly. In this example, the parameters are considered as independent variables. Figure 7–16 shows the functional tolerance for the “bolt” example. In the first setup, plane 3 and cylinder 4 are machined using a turning operation. The surfaces obtained are then used for positioning in setup 2. Setup 2 consists of a milling operation with a 4-axis milling machine. The machined surfaces are Planes 5, 6 and 7. See Table 7-9.

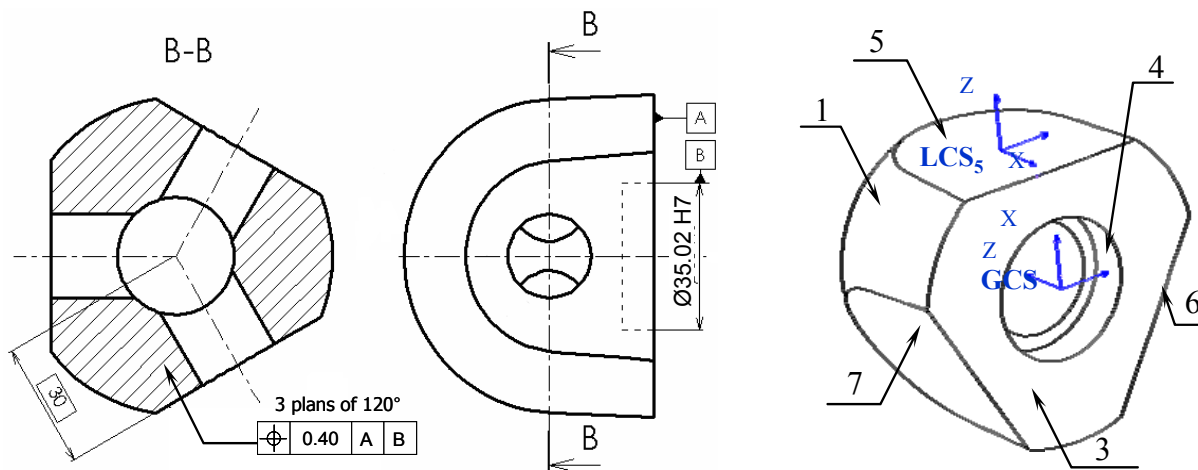


Figure 7–16: “Bolt” example: functional tolerance

### 7.2.2.1 MWP/Fixture assembly

The MWP/Fixture assembly illustrated in Figure 7–5 will be used in a 4-axis milling machine for machining planes 5, 6 and 7. The positioning procedure of MWP and fixture involves making two elementary connections. The primary link is formed of a connection between plane 3 of MWP and 3S2 of the fixture. In the secondary link, cylinder 4 and cylinder 4S2 will be used for a short alignment of MWP relative to fixture. The primary link is a slipping link and the secondary link is a floating link. Any type of adjustment can be considered for the secondary link (e.g. H7/g6 referring to ISO standard for hole and shaft assembly). See Figure 7–17

<b>Setup 1</b>	
Positioning	undetermined
Machining	Plane 3 and cylinder 4
<b>Setup 2</b>	
Positioning	-Plane on 4 -Centering in cylinder 4 (height 5mm)
Machining	Planes 5, 6 and 7

Table 7-9: Proposed process plan for the “Bolt”

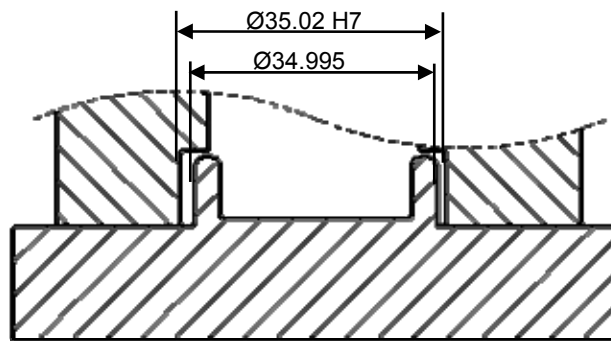


Figure 7-17: “Bolt” example, MWP/Fixture secondary link adjustment

The link parameters and non-penetration condition for this assembly are given in [Table 6-2](#). One degree of freedom (DOF) remains for the MWP in this assembly (rotation around the Z axis).

### 7.2.2.2 Parameters variation range

The fixture surface deviation, the positioning surface deviation of the MWP in setup 2 and the machined surface deviation ranges are based on the result of measurements and the parameters are considered to be independent. The parameter variation ranges are shown in [Table 7-10](#).

### 7.2.2.3 Gauge/MMP assembly

In order to inspect the location functional tolerance, a virtual gauge is created. See [Figure 5-2](#). The assembly procedure of gauge and MMP consists in making two elementary connections according to ISO standards. The primary link connects plane G3 of the Gauge and plane 3 of the MMP. The secondary link is formed of a connection between cylinder G4

and cylinder 4. The primary link is a slipping link. The positioning function related to this link is the displacement of plane G3 in its normal direction. This can be expressed as the opposite (negative sign) of the following Gauge/MMP link parameter:  $-ltz_{3G1}$ <sup>9</sup>. The non-penetration conditions are verified at four boundary points. See [Table 7-12](#).

The secondary link is also a slipping link. The positioning function related to this link can be expressed as the diameter of cylinder G4:  $RN_{4G1}$ . In other words, cylinder G4 will expand until it reaches in contact with the cylinder 4 (according to ISO). The non-penetration conditions are checked along the boundary circles (up and down) of the potential contact area which is cylindrical. The driving link parameters, positioning functions and non-penetration conditions for this assembly are listed in [Table 5-1](#).

One DOF remains for the gauge in this assembly (rotation around Z axis:  $Ulrz_{4G1}$ ). According to ISO standards, this rotation is used to establish the best position for the virtual gauge. In other words, in order to center the tolerated surfaces inside the tolerance zone, in the best possible manner, the optimum DOF value has to be found. In this position,  $GapGP_{min}$  is at its maximum value. The  $GapGP$  is for each of the three planes measured at 4 verification points. This means that there will be twelve verification points in all, resulting in twelve  $GapGP$  equations. See section [5.2.1](#)

#### **7.2.2.4 Optimization approach**

Matlab software is used for programming the search for the worst case with a Pentium®, 3.2 GHz. the SQP algorithm is applied for the optimization task in Sub II. Both algorithms (SQP and GA) are used for the optimization task in Sub I. The results are illustrated in [Figure 7-18](#) and [Figure 7-19](#) respectively. In these figures the values of quality constraints violation are mentioned. As it could be found from these values, the solution obtained respects the quality constraints (the range of defects parameters).

#### **7.2.2.5 Interval approach**

The interval of the fixture surface deviation, the positioning surface deviation of the MWP in setup 2, the machined surface deviation and the link parameters (when considering a

---

<sup>9</sup>  $ltz_{3G1}$  refers to the surface number 3 and gauge number 1

H7g6 adjustment for the secondary link) are given in Table 7-11. In this table the coefficient matrix concerning each of the aforementioned parameters are presented.

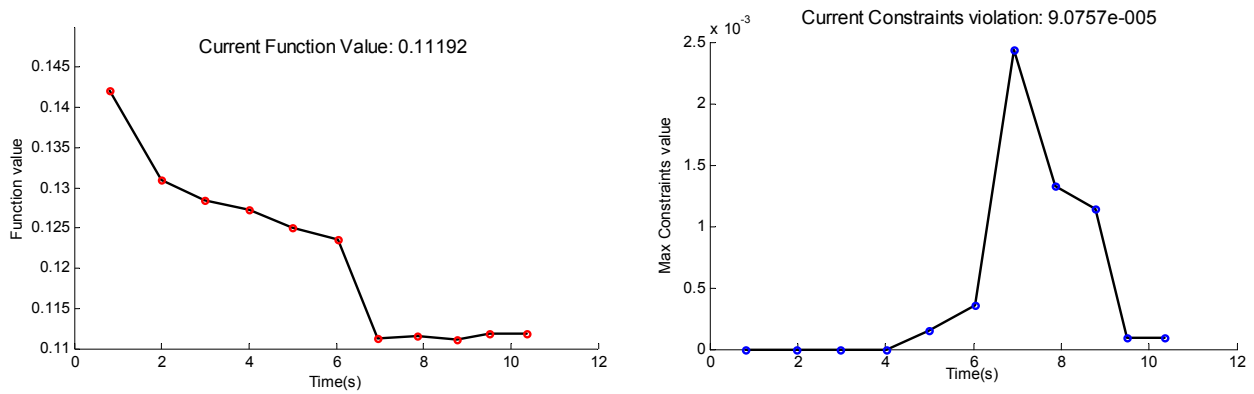


Figure 7-18: Optimization with SQP, with GapGP expression

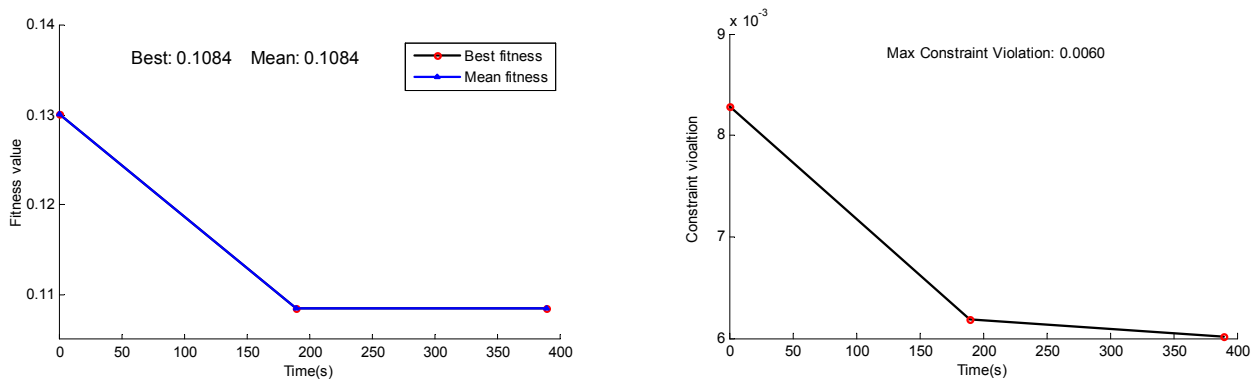


Figure 7-19: Optimization with GA, with GapGP expression

As outlined before, one DOF remains for the gauge in this assembly (rotation around Z axis:  $Ulrz_{4G1}$ ). The best position of the virtual gauge related to the MMP will be established by this DOF. (See section 4.3). The results obtained are mentioned in Table 7-12 by the GapGP and DisGP expression.

Setup 1		
Machining (prepared surfaced by turning)		
No	Surface defects	variation scope
Plane 3	$rx_{P,P3}$	$-5.10^{-4} < rx_{P,P3} < 5.10^{-4}$
	$ry_{P,P3}$	$-3.10^{-4} < ry_{P,P3} < 3.10^{-4}$
	$tz_{P,P3}$	$-5.10^{-3} < tz_{P,P3} < 5.10^{-3}$
Cylinder 4	$rx_{P,P4}$	$-8.10^{-4} < rx_{P,P4} < 8.10^{-4}$
	$ry_{P,P4}$	$-8.10^{-4} < ry_{P,P4} < 8.10^{-4}$
	$tx_{P,P4}$	$tx_{P,P4} = ty_{P,P4} \approx 0$
	$ty_{P,P4}$	$tx_{P,P4} = ty_{P,P4} \approx 0$
	$ra_4$	$-0.01 < \text{radius variation } ra_4 < 0.01$
Setup 2		
Positioning		
No	Surface defects	Variation scope
Plane 3S2	$rx_{3S2}$	$-13.10^{-4} < rx_{3S2} < 13.10^{-4}$
	$ry_{3S2}$	$10^{-3} < ry_{3S2} < 10^{-3}$
	$tz_{3S2}$	$10^{-2} < tz_{3S2} < 10^{-2}$
Cylinder 4S2	$rx_{4S2}$	$-8.10^{-4} < rx_{4S2} < 8.10^{-4}$
	$ry_{4S2}$	$-8.10^{-4} < ry_{4S2} < 8.10^{-4}$
	$tx_{4S2}$	$tx_{4S2} = ty_{4S2} \approx 0$
	$ty_{4S2}$	$tx_{4S2} = ty_{4S2} \approx 0$
	$ra_{4S2}$	$-5.10^{-4} < \text{radius variation } ra_{4S2} < 5.10^{-4}$
Machining		
Plane 5	$rx_5$	$-3.10^{-4} < rx_5 < 3.10^{-4}$
	$ry_5$	$-3.10^{-4} < ry_5 < 3.10^{-4}$
	$tz_5$	$-31.10^{-4} < tz_5 < 31.10^{-4}$
Plane 6	$rx_6$	$-3.10^{-4} < rx_6 < 3.10^{-4}$
	$ry_6$	$-3.10^{-4} < ry_6 < 3.10^{-4}$
	$tz_6$	$-31.10^{-4} < tz_6 < 31.10^{-4}$
Plane 7	$rx_7$	$-3.10^{-4} < rx_7 < 3.10^{-4}$
	$ry_7$	$-3.10^{-4} < ry_7 < 3.10^{-4}$
	$tz_7$	$-31.10^{-4} < tz_7 < 31.10^{-4}$

Table 7-10: Deviation range for “bolt” manufacturing process

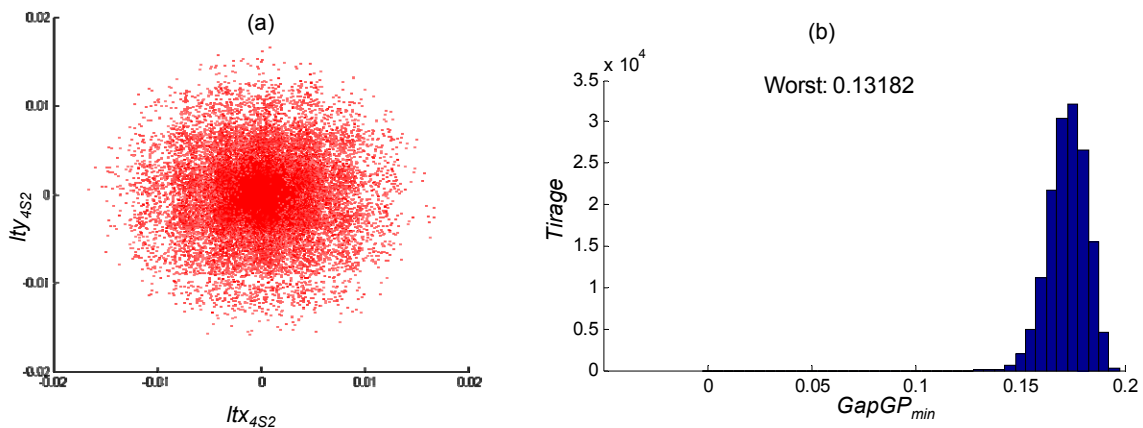


Figure 7-20: MC simulation for “bolt” example



Machined surface	Verification point	DisGP	GapGP
Plane 5	1	[-0.0536 0.0536]	[0.1464 0.2536]
			[0.1464 0.2536]
	2	[-0.0536 0.0536]	[0.1464 0.2536]
			[0.1464 0.2536]
	3	[-0.0709 0.0709]	[0.1291 0.2709]
			[0.1291 0.2709]
	4	[-0.0709 0.0709]	[0.1291 0.2709]
			[0.1291 0.2709]
Plane 5	5	[-0.0824 0.0824]	[0.1176 0.2824]
			[0.1176 0.2824]
	6	[-0.0674 0.0674]	[0.1326 0.2674]
			[0.1326 0.2674]
	7	[-0.0902 0.0902]	[0.1098 0.2902]
			[0.1098 0.2902]
	8	[-0.1028 0.1028]	[0.0972 0.3028]
			[0.0972 0.3028]
Plane 5	9	[-0.0674 0.0674]	[0.1326 0.2674]
			[0.1326 0.2674]
	10	[-0.0824 0.0824]	[0.1176 0.2824]
			[0.1176 0.2824]
	11	[-0.1028 0.1028]	[0.0972 0.3028]
			[0.0972 0.3028]
	12	[-0.0902 0.0902]	[0.1098 0.2902]
			[0.1098 0.2902]

Table 7-12: Interval approach results for “Bolt” example with DisGP and GapGP expression

### 7.2.2.6 MC simulation

To perform MC simulation concerning with example, 150000 parts are virtually produced by using the independent parameters strategy within the ranges mentioned in Table 7-10. The defect generation procedure uses a simple random generator for producing surface deviations. Concerning the secondary floating link parameters of MWP/Fixture in setup 2, the algorithm presented in section 7.1.1.2 is used to generate the link value with respect to the NPC between MWP and fixture. Figure 7–20(a) shows that the generated parameters respect the NPC and their distribution uniformly fills the allowed domain.

The virtual generated parts are put forward to Sub II in order to verify their conformity. Figure 7–20(b) shows the distribution of  $GapGP_{min}$  values obtained over 150000 parts.

Results	Optimization		Interval method	MC simulation
	SQP	GA		
$GapGP_{min}$ (mm)	0.1119	0.1084	[0.097 0.302]	0.131
$DisGP_{max}$ (mm)	0.0881	0.0916	[0.0103 0.102]	0.069

Table 7-13: Worst  $GapGP_{min}$  and  $DisGP_{max}$  obtained for “Bolt” example

### 7.2.2.7 Discussion

This example shows a MMP/Fixture assembly with a floating link and a virtual gauge with one DOF. Through this example, the performance of our three solution techniques developed for tolerance analysis when dealing with floating link and virtual gauge with DOF is explored.

Table 7-13 shows the result obtained by each of the solution technique. The worst  $GapGP_{min}$  value obtained is positive. This proves that the applied process plan and fixture tools are able to satisfy the functional tolerance.

Comparing SQP and GA, it is worth mentioning that the initial point is very important for optimization with SQP. The algorithms are run with the same initial point. This point has to be feasible and be close to the global solution. This means that an algorithm able to find a suitable initial point needs to be developed. This research used the GA with a small population size to obtain an initial point.

With the same initial point, the GA running time is 40 times greater than that of SQP but (as it can be found from the results) the probability that the point obtained by GA to be a global minimum is higher than those obtained by SQP. The GA parameters (mutation rate, crossover rate, etc) play a very important role in reaching the global optimum point.

The minimum value for  $GapGP_{min}$  is obtained by interval method. Normally when using the independent parameters (as it is outlined in previous example) the value obtained by interval approach and optimization approach should be the same. This is not the case in this example.



The fact is that, in interval approach, when there is a floating elementary connection, the floating link parameters are considered as independent variables for calculating their extreme bounds; therefore they all can take the maximum possible value allowed by the variation range. See Figure 7–21. This not the cases when using the optimization approach. In the “Bolt example”, there is a floating connection with two driving link parameters between cylinder 4 (MWP) and cylinder 4S2. As it can be found from Figure 7–21, the variation interval for each driving link parameter when the other parameters are set to zero is  $[-0.023 \ 0.023]$ . This is the link parameter variation interval that will be used in the interval approach. In the optimization approach, these two driving link parameters are not considered independent. In other word, they can not have their maximum value simultaneously. This is why the result obtained by the optimization approach is greater than that obtained by the interval approach.

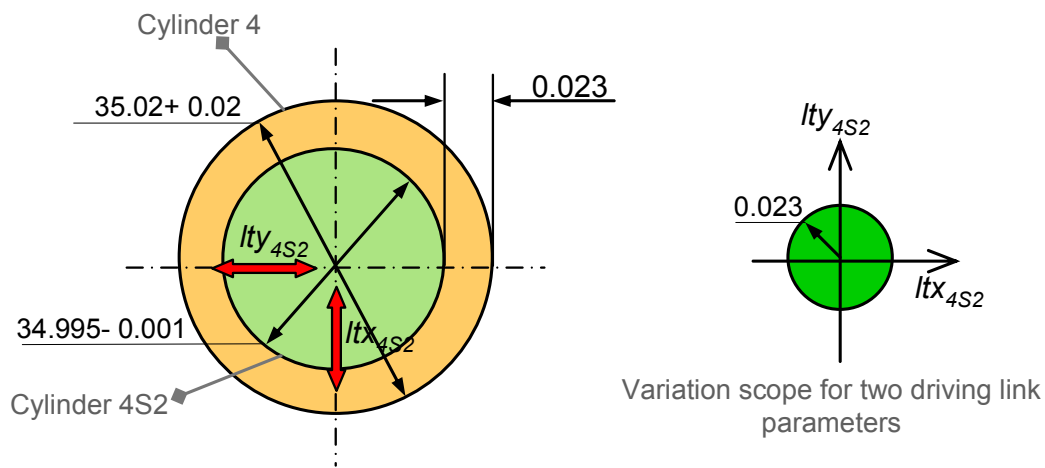
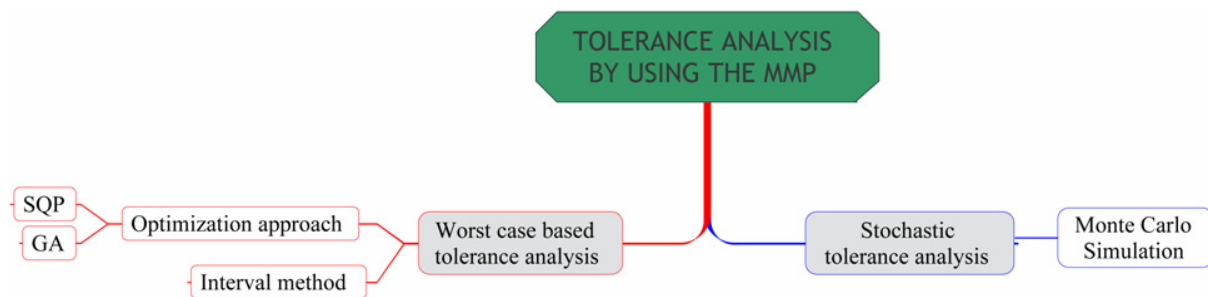


Figure 7–21: “Bolt”, Clearance for MWP/Fixture secondary link

## 8 CONCLUSION AND PERSPECTIVES

This manuscript contributes to developing the solution techniques associated with the Model of manufactured Part (MMP) developed by Villeneuve and Vignat [Vignat F. *et al*, 2007b, Villeneuve F. *et al*, 2005a] for modeling the different geometrical deviation impacts on the part produced (error stack-up) in a multi-stage machining process. The MMP cumulates the impacts of various sources of manufacturing errors hence enabling tolerance analysis. The MMP, beside the developed solution techniques, allows the manufacturing engineers to evaluate a candidate process plan from a geometrical point of view.

The solution techniques developed are classified into two categories: Search for finding the worst-case (worst part produced) and stochastic method. See [Figure 8–1](#).



*Figure 8–1: The developed solution techniques for tolerance analysis by using the MMP*

In this manuscript, in chapter 2, a comprehensive review of the available literature about tolerance analysis especially in multi-stage machining operation is given. The advantages and drawbacks of existing methods are discussed.

In Chapter 3, the simulation method leading to MMP (Model of Manufactured Part) proposed by [Vignat F. *et al*, 2007b, Villeneuve F. *et al*, 2005a] for the case of machining process is reminded. Some modifications have been applied to this method in terms of notation. The mathematical expression of the method has been improved as well.

In chapter 4, the application of MMP for the purpose of tolerance analysis in machining is explored. The virtual gauge and the measurement procedure of the MMP by it are explained in detail by means of two measurable distances (*GapGP* and *DisGP*). The initial formulation

of the worst case search problem which had been proposed by Vignat and Villeneuve for the first time is reminded [Vignat F. *et al*, 2005].

In chapter 5, the initial worst case searching formula proposed in chapter 4 is deeply reformulated and it is broken down into two sub problems. A multi-layer solution technique based on the optimization algorithms is then developed. Three different strategies for defining the variation scope of surface defects parameters are proposed. The developed solution technique nearly covers 95% of the current fixture layouts. Two current optimization techniques (SQP and GA) are applied for solving each of the proposed sub problems [Kamali Nejad M. *et al*, 2008a, Kamali Nejad M. *et al*, 2009b].

In chapter 6 the interval method is presented. This method is built on two existing models (the MMP and the Jacobian-Torsor). It is then showed how it can be applied to worst-case based functional tolerance analysis in multi-stage machining operations [Kamali Nejad M. *et al*, 2009a, Kamali Nejad M. *et al*, 2008b].

The approach is nonetheless limited by the fact that it considers the parameters independently. This means that they can reach their extreme values simultaneously, which is why the method cannot be applied to dependent parameters. Although yet unsolved, this limit could be overstepped by modifying the coefficient matrix. Use of the optimization problem for calculating the link parameter variation intervals should also be underlined. This tells us the worst link value for the assemblies. The link parameter variation intervals can be calculated for each elementary link in a hierarchical assembly by considering the general fixture layouts with different positioning links (Punctual, Plane/Plane and Cylinder/Cylinder).

In chapter 7, a stochastic approach for functional tolerance analysis by using the MMP is proposed. This approach uses Monte Carlo (MC) simulation. The defect generation procedure in MC simulation is adjusted by the strategies explained for defining the variation scope of the surface defects parameters.

The performance of the aforementioned tolerance analysis approaches are explored and compared with each other through two 3D examples with different strategies for defining the variation scope of surface defects parameters. The advantages and disadvantages of each approach is discussed. For example, SQP needs an initial point for start-up. Finding a good initial point is not always easy. Interval method is very fast but it can not handle the

dependent parameters. MC simulation is closer to reality but it needs a long computation time and in can not be used for WCTA.

## 8.1 PERSPECTIVES

Three main perspectives axis can be envisaged:

The first axis consists in developing an automatic data exchange interface between CAD software (used for defining the geometry of a part), Mathematica® (used for calculating the *GapGP* equations) and Matlab® (used for solution techniques). As things currently stand, the data exchange between these software is done manually for performing the computations which is time consuming. This interface could cover the automatic generation of Matlab® codes for multi-layer optimization techniques or eventually the coefficient matrices in the interval method. A whole integrated box could give to the process planner a very good evaluation tool with different solution techniques and quality strategies.

The second axis would be testing the performance of global optimization or hybrid optimization techniques dealing with the worst case search problem to be sure of obtaining the global solution. The possible methods can be optimization by using intervals analysis, ant colony optimization algorithm (ACO) or simulated annealing. The performance of the hybrid optimization techniques (e.g. GA in line with SQP) is also an interesting research subject.

The third axis would be performing some measurements to find the variation range of the defect parameters and establishing the correlation that exists between these parameters. This measurement is not easy and needs to evaluate very small values as the defects. Sometimes the defects values are smaller than the precision of the measuring machines. This work is started by Tichadou and Kamli Nejad [Tichadou S. *et al*, 2007, Tichadou S. *et al*, 2005] and currently is being followed by Bui Minh in Annecy.



## 9 REFERENCES

- [2007]Matlab, Available online at: <http://www.mathworks.com> (accessed 30 June 2007)
- [Asme Y14.5m, 1994] ASME Y14.5M (1994) "Dimensioning and Tolerancing ANSI Y14.5M." New York.
- [Ayadi B. *et al*, 2008]Ayadi B, Anselmetti B, Bouaziz Z et al (2008), "Three-dimensional modelling of manufacturing tolerancing using the ascendant approach," *The International Journal of Advanced Manufacturing Technology*, vol. 39: pp. 279-90.
- [Ballot E. *et al*, 1998]Ballot E, Bourdet P (1998), "A computation method for the consequences of geometric errors in mechanisms.,"In: ElMaraghy H. A., Ed., *Geometric Design Tolerancing: Theories, Standards and Applications*, pp. 197-207, presented at: 5th CIRP Seminar on Computer-Aided Tolerancing, Toronto, Canada.
- [Bjørke Ø., 1989] Bjørke Ø (1989) "Computer-Aided Tolerancing." 2nd ed, ASME press, New York.
- [Bourdet P. *et al*, 1995] Bourdet P, Ballot E (1995), "Geometric behavior laws for computer-aided tolerancing,"In: Kimura F., Ed., pp. 119-31, presented at: 4th CIRP Design Seminar on Computer-Aided Tolerancing.
- [Bourdet P. *et al*, 1996] Bourdet P, Mathieu L, Lartigue C et al (1996), "The concept of the small displacement taylor in metrology," In: *Advanced Mathematical Tools in Metrology II, Series Advances in Mathematics for Applied Sciences*: World Scientific, pp. 10-122.
- [Broyden C. G., 1970] Broyden C G (1970), "The Convergence of a Class of Double-rank Minimization Algorithms," *Journal of Applied Mathematics*, vol. 6: pp. 222-31.
- [Byrd R. H. *et al*, 2000] Byrd R H, Gilbert J C, Nocedal J (2000), "A trust region method based on interior point techniques for nonlinear programming," *Mathematical Programming*, vol. 89: pp. 149-85.
- [Byrd R. H. *et al*, 1999] Byrd R H, Hribar M E, Nocedal J (1999), "An interior point algorithm for large-scale nonlinear programming," *Siam Journal on Optimization*, vol. 9: pp. 877-900.
- [Cai W. *et al*, 1997] Cai W, Hu S J, Yuan J X (1997), "A variational method of robust fixture configuration design for 3-D workpieces," *Journal of Manufacturing Science and Engineering-Transactions of the ASME*, vol. 119: pp. 593-602.
- [Camelio J. *et al*, 2004] Camelio J, Jack Hu S, Zhong W (2004), "Diagnosis of multiple fixture faults in machining processes using designated component analysis," *Journal of Manufacturing Systems*, vol. 23: pp. 309-15.
- [Chase K. W. *et al*, 1995] Chase K W, Gao J, Magleby S P (1995), "General 2-D tolerance analysis of mechanical assemblies with small kinematic adjustments," *Journal of Design and Manufacture*, vol. 5: pp. 263-74.
- [Chase K. W. *et al*, 1996] Chase K W, Gao J, P M S et al (1996), "Including Geometric Feature Variations in Tolerance Analysis of Mechanical Assemblies," *IIE transactions*, vol. 28: pp. 795-807.

- [Chase K. W. *et al*, 1997a] Chase K W, Magleby S P (1997a), "A comprehensive system for computer-Aided Tolerance Analysis of 2-D and 3-D Mechanical Assemblies," presented at: 5th International Seminar on Computer-Aided Tolerancing, Toronto, Canada.
- [Chase K. W. *et al*, 1997b] Chase K W, Magleby S P, Glancy C G (1997b), "Tolerance Analysis of 2-D and 3-D Mechanical Assemblies with Small Kinematic Adjustments," In: *Advanced Tolerancing Techniques* Zhang H. C. Ed.: Wiley, pp. 103-38.
- [Chase K. W. *et al*, 1991] Chase K W, Parkinson A R (1991), "A survey of research in the application of tolerance analysis to the design of mechanical assemblies," *Research in Engineering Design*, vol. 3: pp. 23-37.
- [Chen J. S. *et al*, 1993] Chen J S, Yuan J X, Ni J *et al* (1993), "REAL-TIME COMPENSATION FOR TIME-VARIANT VOLUMETRIC ERRORS ON A MACHINING CENTER," *Journal of Engineering for Industry-Transactions of the ASME*, vol. 115: pp. 472-79.
- [Choudhuri S. A. *et al*, 1999] Choudhuri S A, De Meter E C (1999), "Tolerance analysis of machining fixture locators," *Journal of Manufacturing Science and Engineering-Transactions of the ASME*, vol. 121: pp. 273-81.
- [Clément A. *et al*, 1997] Clément A, Valade C, Rivière A (1997), "13 oriented constraints for dimensioning, tolerancing and inspection," In: *Advanced Mathematical Tools in Metrology* vol. III, Ciarlini P. and Cox M. G. *et al* Eds: World Scientific, pp. 24-42.
- [Conn A. R. *et al*, 1991] Conn A R, Gould N I M, Toint P L (1991), "A Globally Convergent Augmented Lagrangian Algorithm for Optimization with General Constraints and Simple Bounds," *Siam Journal on Numerical Analysis*, vol. 28: pp. 545-72.
- [Craig M., 1996] Craig M (1996), "Dimensional management versus tolerance assignment," *Assembly Automation*, vol. 16: pp. 12-&.
- [Dantan J.-Y., 2000] Dantan J-Y (2000) "Synthèse des spécifications géométriques : modélisation par Calibre à Mobilités Internes. " Ph.D Thesis. L'UNIVERSITE BORDEAUX 1 Mécanique.
- [Dantan J.-Y. *et al*, 2002] Dantan J-Y, Ballu A (2002), "Assembly specification by Gauge with Internal Mobilities (GIM)-A specification semantics deduced from tolerance synthesis," *Journal of Manufacturing Systems*, vol. 21: pp. 218-35.
- [Dantan J.-Y. *et al*, 2008] Dantan J-Y, Ballu A, Mathieu L (2008), "Geometrical product specifications -- model for product life cycle," *Computer-Aided Design*, vol. 40: pp. 493-501.
- [Desrochers A., 1999] Desrochers A (1999), "Modeling three-dimensional tolerance zones using screw parameters," pp., presented at: CD-ROM proceeding of 25th ASME Design Automation Conference Las-Vegas.
- [Desrochers A., 2003] Desrochers A (2003), "A CAD/CAM representation model applied to tolerance transfer methods," *Journal of Mechanical Design*, vol. 125: pp. 14-22.

- [Desrochers A., 2007] Desrochers A (2007), "Geometrical variations management in a multi-disciplinary environment with the Jacobian-Torsor model," In: Davidson J. K., Ed., Models for Computer Aided Tolerancing in Design and Manufacturing, pp. 75-84, presented at: 9th CIRP International Seminar on Computer-Aided Tolerancing, Arizona.
- [Desrochers A. *et al*, 1994] Desrochers A, Clement A (1994), "A DIMENSIONING AND TOLERANCING ASSISTANCE MODEL FOR CAD-CAM SYSTEMS," *International Journal of Advanced Manufacturing Technology*, vol. 9: pp. 352-61.
- [Desrochers A. *et al*, 2003a] Desrochers A, Ghie W, Laperriere L (2003a), "Application of a Unified Jacobian---Torsor Model for Tolerance Analysis," *Journal of Computing and Information Science in Engineering*, vol. 3: pp. 2-14.
- [Desrochers A. *et al*, 2003b] Desrochers A, Ghie W, Laperriere L (2003b), "Application of a unified Jacobian-Torsor model for tolerance analysis," *Transactions-of-the-ASME-Journal-of-Computing-and-Information-Science-in-Engineering.*, vol. 3: pp. 12.
- [Desrochers A. *et al*, 1995] Desrochers A, Maranzana R (1995), "Constrained dimensioning and tolerancing assistance for mechanisms," presented at: 4th CIRP Design Seminar on Computer-Aided Tolerancing
- [Desrochers A. *et al*, 1997] Desrochers A, Riviere A (1997), "A matrix approach to the representation of tolerance zones and clearances," *International Journal of Advanced Manufacturing Technology*, vol. 13: pp. 630-36.
- [Evans D. H., 1974] Evans D H (1974), "Statistical tolerancing: the state of the art, Part I: background," *Journal of Quality Technology*, vol. 6: pp.
- [Fleming A., 1988] Fleming A (1988), "Geometric Relationships between Toleranced Features," *Artificial Intelligence*, vol. 37: pp. 403-12.
- [Fletcher R., 1970] Fletcher R (1970), "A new approach to variable metric algorithms," *The Computer Journal*, vol. 13: pp.
- [Forouraghi B., 2002] Forouraghi B (2002), "Worst-case tolerance design and quality assurance via genetic algorithms," *Journal of Optimization Theory and Applications*, vol. 113: pp. 251-68.
- [Fortini E. T., 1967] Fortini E T (1967) "Dimensioning for Interchangeable Manufacture." Industrial Press, New York.
- [Gao J. *et al*, 1995] Gao J, Chase K W, Magleby S P (1995), "Comparison of assembly tolerance analysis by direct linearization and modified Monte Carlo simulation methods," pp. 353-60, presented at: ASME Design Engineering Technical Conferences, Boston, MA.
- [Gao J. *et al*, 1998] Gao J, Chase K W, Magleby S P (1998), "Generalized 3-D tolerance analysis of mechanical assemblies with small kinematic adjustments," *IIE Transactions*, vol. 30: pp. 367-77.
- [Ghie W. *et al*, 2003] Ghie W, Laperriere L, Desrochers A (2003), "A unified Jacobian-torsor model for analysis in computer aided tolerancing," In: Gogu G. and Coutellier D. *et al*, Eds, Recent Advances in Integrated Design and Manufacturing in Mechanical Engineering, pp. 63-72, presented at: 4th International Conference on Integrated



Design and Manufacturing in Mechanical Engineering, Clermont Fernand, FRANCE.

- [Ghie W. *et al*, 2007] Ghie W, Laperriere L, Desrochers A (2007), "Re-design of mechanical assemblies using the unified Jacobian-Torsor model for tolerance analysis," In: Davidson J. K., Ed., *Models for Computer Aided Tolerancing in Design and Manufacturing*, pp. 95-104, presented at: 9th CIRP International Seminar on Computer-Aided Tolerancing, Arizona.
- [Giordano M. *et al*, 1993] Giordano M, Duret D (1993), "Clearance space and deviation space: Application to three-dimensional chain of dimensions and positions," presented at: 3rd CIRP Design Seminar on Computer-Aided Tolerancing (CAT)
- [Giordano M. *et al*, 1992] Giordano M, Duret D, Tichadou S et al (1992), "Clearance space in volumic dimensioning," *Annals of the CIRP*, vol. 41: pp. 565-68.
- [Giordano M. *et al*, 1999] Giordano M, Pairel E, Samper S (1999), "Mathematical representation of tolerance zones," In: Houten F. v. and Kals H., Eds, pp. 177-86, presented at: 6th CIRP International Seminar on Computer-Aided Tolerancing, Un Enschede, The Netherlands.
- [Goldfarb D., 1970] Goldfarb D (1970), "A Family of Variable Metric Updates Derived by Variational Means," *Mathematics of Computing*, vol. 24: pp. 23-26.
- [Gomes F. A. M. *et al*, 1999] Gomes F A M, Maciel M C, Martinez J M (1999), "Nonlinear programming algorithms using trust regions and augmented Lagrangians with nonmonotone penalty parameters," *Mathematical Programming*, vol. 84: pp. 161-200.
- [Hansen E. *et al*, 2004] Hansen E, Walster G W (2004) "Global optimization using interval analysis." Marcel Dekker,
- [Hong Y. S. *et al*, 2002] Hong Y S, Chang T C (2002), "A comprehensive review of tolerancing research," *International Journal of Production Research*, vol. 40: pp. 2425-59.
- [Huang Q. *et al*, 2003] Huang Q, Shi J J (2003), "Part dimensional error and its propagation modeling in multi-operational machining processes," *Journal of Manufacturing Science and Engineering-Transactions of the ASME*, vol. 125: pp. 255-62.
- [Huang S. H. *et al*, 2004] Huang S H, Liu Q, Musa R (2004), "Tolerance-based process plan evaluation using Monte Carlo simulation," *International Journal of Production Research*, vol. 42: pp. 4871-91.
- [Islam M. N., 2004] Islam M N (2004), "Functional dimensioning and tolerancing software for concurrent engineering applications," *Computers in Industry*, vol. 54: pp. 169-90.
- [Juster N. P., 1992] Juster N P (1992), "Modelling and representation of dimensions and tolerances: a survey," *Computer-Aided Design*, vol. 24: pp. 3-17.
- [Kamali Nejad M. *et al*, 2008a] Kamali Nejad M, Desrochers A, Vignat F et al (2008a), "Tolerance Analysis in Machining, An Approach Combining The Model of Manufactured Part and The Jacobian-torsor Model," pp., presented at: ASME 28th Computers and Information in Engineering Conference (CIE), New York City, US

- [Kamali Nejad M. *et al*, 2009a] Kamali nejad M, Vignat F, Desrochers A et al (2009a), "3D Simulation of manufacturing defects for tolerance analysis," *Accepted for Journal of Computing and Information Science in Engineering*
- [Kamali Nejad M. *et al*, 2008b] Kamali Nejad M, Vignat F, Villeneuve F (2008b), "Tolerance Analysis in Multi-Operational Machining Process Based on the Model of Manufactured Part " presented at: 5th International Conference on Digital Enterprise Technology, Nantes, France.
- [Kamali Nejad M. *et al*, 2009b] Kamali Nejad M, Vignat F, Villeneuve F (2009b), "Simulation of the geometrical defects of manufacturing," *The International Journal of Advanced Manufacturing Technology*
- [Kier L. B. *et al*, 2005] Kier L B, Seybold P G, Cheng C-K (2005), "Cellular Automata," In: *Modeling Chemical Systems Using Cellular Automata*: Springer Netherlands, pp. 9-38.
- [Kirschling G., 1991] Kirschling G (1991) "Quality Assurance and Tolerance." Springer, Berlin.
- [Lafond P. *et al*, 1999] Lafond P, Laperrière L (1999), "Jacobian-based Modeling of Dispersions Affecting Pre-Defined Functional Requirements of Mechanical Assemblies," International Symposium on Assembly and Task Planning, pp., presented at: IEEE International Symposium on Assembly and Task Planning, Porto, Portugal.
- [Laperrière L. *et al*, 2000] Laperrière L, ElMaraghy H A (2000), "Tolerance analysis and synthesis using Jacobian transforms," *Cirp Annals 2000: Manufacturing Technology* 359-62.
- [Laperrière L. *et al*, 2002] Laperrière L, Ghie W, Desrochers A (2002), "Statistical and deterministic tolerance analysis and synthesis using a unified Jacobian-torsor model," *Cirp Annals-Manufacturing Technology*, vol. 51: pp. 417-20.
- [Laperrière L. *et al*, 2001] Laperrière L, Kabore T (2001), "Monte Carlo simulation of tolerance synthesis equations," *International Journal of Production Research*, vol. 39: pp. 2395-406.
- [Laperrière L. *et al*, 1998] Laperrière L, Lafond P (1998), "Modeling dispersions affecting pre-defined functional requirements of mechanical assemblies using Jacobian transforms," presented at: Integrated Design and Manufacturing in Mechanical Engineering, 2nd IDMME Conference, Compiègne, France.
- [Laperrière L. *et al*, 1999] Laperrière L, Lafond P (1999), "Modeling Tolerances and Dispersions of Mechanical Assemblies Using Virtual Joints," ASME Design Engineering Technical Conferences, pp., presented at: 5th ASME Design Automation Conference, Las Vegas, Nevada.
- [Larsen G. C., 1991] Larsen G C (1991) "A Generalized Approach to Kinematic Modeling for Tolerance Analysis of Mechanical Assemblies " M.Sc Thesis. Brigham Young University Mechanical Engineering.
- [Legoff O. *et al*, 2004] Legoff O, Tichadou S, Hascoet J Y (2004), "Manufacturing errors modelling: two three-dimensional approaches," *Proceedings of the Institution*

- of Mechanical Engineers Part B-Journal of Engineering Manufacture*, vol. 218: pp. 1869-73.
- [Lewis R. M. *et al*, 2002] Lewis R M, Torczon V (2002), "A globally convergent augmented Lagrangian pattern search algorithm for optimization with general constraints and simple bounds," *Siam Journal on Optimization*, vol. 12: pp. 1075-89.
- [Liggett J. V., 1992] Liggett J V (1992) "Dimensional Variation Management Handbook: A Guide for Quality, Design, and Manufacturing Engineers." Prentice Hall,
- [Lin E. E. *et al*, 2001] Lin E E, Zhang H C (2001), "Theoretical tolerance stackup analysis based on tolerance zone analysis," *International Journal of Advanced Manufacturing Technology*, vol. 17: pp. 257-62.
- [Lin S.-S. *et al*, 1997] Lin S-S, Wang H-P, Zhang C (1997), "Statistical tolerance analysis based on beta distributions," *Journal of Manufacturing Systems*, vol. 16: pp. 150-58.
- [Loose J. P. *et al*, 2007] Loose J P, Zhou S Y, Ceglarek D (2007), "Kinematic analysis of dimensional variation propagation for multistage machining processes with general fixture layouts," *Ieee Transactions on Automation Science and Engineering*, vol. 4: pp. 141-52.
- [Louati J. *et al*, 2006] Louati J, Ayadi B, Bouaziz Z *et al* (2006), "Three-dimensional modelling of geometric defaults to optimize a manufactured part setting," *The International Journal of Advanced Manufacturing Technology*, vol. 29: pp. 342-48.
- [Martinsen K., 1993] Martinsen K (1993), "Vectorial Tolerancing for All Types of Surfaces," *ASME Advances in Design Automation*, vol. 2: pp. 187-98.
- [Mathieu L. *et al*, 2005] Mathieu L, Ballu A (2005), "A model for a coherent and complete tolerancing process," presented at: 9th CIRP International Seminar on Computer-Aided Tolerancing, Arizona.
- [Mathieu L. *et al*, 2007] Mathieu L, Ballu A (2007), "A Model for a Coherent and Complete Tolerancing Process," In: *Models for Computer Aided Tolerancing in Design and Manufacturing*, pp. 35-44.
- [Mathieu L. *et al*, 1997] Mathieu L, Clement A, Bourdet P (1997), "Modeling, Representation and processing of tolerances, tolerance inspection: a survey of current hypothesis," presented at: 5th CIRP International Seminar on Computer-Aided Tolerancing, Toronto, Canada.
- [Musa R. A. *et al*, 2004] Musa R A, Huang S H, Rong Y K (2004), "Simulation-based tolerance stackup analysis in machining," *Transactions of the North American Manufacturing Research Institution of SME*, vol. Vol 32: pp. 533-40.
- [Nguyen D. S. *et al*, 2009] Nguyen D S, Vignat F, Brissaud D (2009), "Applying Monte-Carlo Methods to Geometric Deviations Simulation within Product Life Cycle," presented at: 11th CIRP International Seminar on Computer-Aided Tolerancing, Annecy, France
- [Nigam S. D. *et al*, 1995] Nigam S D, Turner J U (1995), "REVIEW OF STATISTICAL APPROACHES TO TOLERANCE ANALYSIS," *Computer-Aided Design*, vol. 27: pp. 6-15.
- [Nocedal J. *et al*, 1999] Nocedal J, Wright S J (1999) "Numerical Optimization." Springer, New york.

- [Pairel E., 2007] Pairel E (2007), "Three-dimensional verification of geometric tolerances with the "fitting gauge" model," *Journal of Computing and Information Science in Engineering*, vol. 7: pp. 26-30.
- [Pairel E. *et al*, 2007] Pairel E, Hernandez P, Giordano M (2007), "Virtual gauge representation for geometric tolerances in CAD-CAM systems," In: Davidson J. K., Ed., *Models for Computer Aided Tolerancing in Design and Manufacturing* pp. 3-12, presented at: 9th CIRP International Seminar on Computer-Aided Tolerancing, Arizona.
- [Paris H., 1992] Paris H (1992) "Contribution a la conception automatique des gammes d'usinage: le probleme du posage et du bridage des pieces " Ph.d Thesis. Universite Joseph Fourier Mecanique
- [Paris H. *et al*, 2005] Paris H, Brissaud D (2005), "Process planning strategy based on fixturing indicator evaluation," *International Journal of Advanced Manufacturing Technology*, vol. 25: pp. 913-22.
- [Plantenga T., 1998] Plantenga T (1998), "A trust region method for nonlinear programming based on primal interior-point techniques," *Siam Journal on Scientific Computing*, vol. 20: pp. 282-305.
- [Portman V. T. *et al*, 1987] Portman V T, Shuster V G (1987), "Computerized Synthesis of a Theoretical Model of a Three-Plane Dimension Chain," vol. 7: *Soviet Engineering Research*, pp. 57-60.
- [Portman V. T. *et al*, 1995] Portman V T, Weill R D (1995), "Modelling Spatial Dimensional Chains for CAD/CAM Applications," presented at: 4th CIRP Seminar on Computer Aided Tolerancing, Tokyo, Japan.
- [Powell M., 1978a] Powell M (1978a), "The Convergence of Variable Metric Methods for Nonlinearly Constrained Optimization Calculations," In: *Nonlinear Programming 3*, Mangasarian O. L. and Meyer R. R. *et al* Eds: Academic Press.
- [Powell M., 1978b] Powell M (1978b), "A fast algorithm for nonlinearly constrained optimization calculations," In: *Numerical Analysis*, pp. 144-57.
- [Powell M., 1979] Powell M (1979), "Variable metric methods for constrained optimization," In: *Computing Methods in Applied Sciences and Engineering, 1977, I*, pp. 62-72.
- [Prabhakaran G. *et al*, 2007] Prabhakaran G, Padmanaban K P, Krishnakumar R (2007), "Machining fixture layout optimization using FEM and evolutionary techniques," *International Journal of Advanced Manufacturing Technology*, vol. 32: pp. 1090-103.
- [Radouani M. *et al*, 2000] Radouani M, Saka A, Carrard M (2000), "Le dimensionnement et le tolérancement vectoriels VD&T : outil de CAO : Etude comparative entre GD&T et VD&T," *Journal européen des systèmes automatisés*, vol. 34: pp. 293-304.
- [Ramesh R. *et al*, 2000a] Ramesh R, Mannan M A, Poo A N (2000a), "Error compensation in machine tools - a review Part I: geometric, cutting-force induced and fixture-dependent errors," *International Journal of Machine Tools & Manufacture*, vol. 40: pp. 1235-56.

- [Ramesh R. *et al*, 2000b] Ramesh R, Mannan M A, Poo A N (2000b), "Error compensation in machine tools - a review Part II: thermal errors," *International Journal of Machine Tools & Manufacture*, vol. 40: pp. 1257-84.
- [Requicha A. A. G., 1993] Requicha A A G (1993), "Mathematical definitions of tolerance specifications," *Manufacturing Review*, vol. 4: pp. 269-74.
- [Rivest L. *et al*, 1994] Rivest L, Fortin C, Morel C (1994), "Tolerancing a Solid Model with a Kinematic Formulation," *Computer-Aided Design*, vol. 26: pp. 465-76.
- [Robison R. H., 1989] Robison R H (1989) "A Practical Method for Three-Dimensional Tolerance Analysis Using a Solid Modeler " Ph.D Thesis. Brigham Young University Mechanical Engineering.
- [Roy U. *et al*, 1991] Roy U, Liu C R, Woo T C (1991), "Review of Dimensioning and Tolerancing - Representation and Processing," *Computer-Aided Design*, vol. 23: pp. 466-83.
- [Rump S. M., 2007] INTLAB - INTerval LABoratory, Available online at: <http://www.ti3.tu-harburg.de/rump/intlab/> (accessed
- [Salomons O. W. *et al*, 1996a] Salomons O W, Haalboom F J, Poerink H J J et al (1996a), "A computer aided tolerancing tool II: Tolerance analysis," *Computers in Industry*, vol. 31: pp. 175-86.
- [Salomons O. W. *et al*, 1996b] Salomons O W, Poerink H J J, Haalboom F J et al (1996b), "A computer aided tolerancing tool I: Tolerance specification," *Computers in Industry*, vol. 31: pp. 161-74.
- [Samper S. *et al*, 2006] Samper S, Petit J-P, Giordano M (2006), "Computer Aided Tolerancing - Solver and Post Processor Analysis," In: *Advances in Design*, pp. 487-97.
- [Schittkowski K., 1985] Schittkowski K (1985), "NLQPL: A FORTRAN-Subroutine, Solving Constrained Nonlinear Programming Problems," *Annals of Operations Research*, vol. 5: pp. 485-500.
- [Shan A. *et al*, 1999] Shan A, Roth R N, Wilson R J (1999), "A new approach to statistical geometrical tolerance analysis," *International Journal of Advanced Manufacturing Technology*, vol. 15: pp. 222-30.
- [Shan A. *et al*, 2003] Shan A, Roth R N, Wilson R J (2003), "Genetic algorithms in statistical tolerancing," *Mathematical and Computer Modelling*, vol. 38: pp. 1427-36.
- [Shanno D. F., 1970] Shanno D F (1970), "Conditioning of Quasi-Newton Methods for Function Minimization," *Mathematics of Computing*, vol. 24: pp. 647-56.
- [Shen Z. *et al*, 2005] Shen Z, Ameta G, Shah J J et al (2005), "A comparative study of tolerance analysis methods," *Journal of Computing and Information Science in Engineering*, vol. 5: pp. 247-56.
- [Srinivasan R. S., 1994] Srinivasan R S (1994) "A theoretical framework for functional form tolerances in design for manufacturing " Ph.D Thesis. University of Texas
- [Srinivasan R. S. *et al*, 1996] Srinivasan R S, Wood K L, McAdams D A (1996), "Functional tolerancing: A design for manufacturing methodology," *Research in Engineering Design*, vol. 8: pp. 99-115.

- [Teissandier D. *et al*, 1999a] Teissandier D, Couetard Y, Gerard A (1999a), "A computer aided tolerancing model: proportioned assembly clearance volume," *Computer-Aided Design*, vol. 31: pp. 805-17.
- [Teissandier D. *et al*, 1998] Teissandier D, Couétard Y, Gérard A (1998), "Three-dimensional functional tolerancing with proportioned assemblies clearance volume," In: ElMaraghy H. A., Ed., *Geometric Design Tolerancing: Theories, Standards and Applications*, pp. 171-82, presented at: 5th CIRP Seminar on Computer-Aided Tolerancing, Toronto, Canada.
- [Teissandier D. *et al*, 1999b] Teissandier D, Delos V, Couétard Y (1999b), "Operations on polytopes: application to tolerance analysis," In: Houten F. v. and Kals H., Eds, *Global Consistency of Tolerances*, pp. 425-34, presented at: 6th CIRP International Seminar on Computer-Aided Tolerancing, University of Twente, Enschede, The Netherlands.
- [Tichadou S. *et al*, 2007] Tichadou S, Kamali nejad M, Vignat F et al (2007), "3-D manufacturing dispersions: two experimental applications," presented at: 10th CIRP International Conference on Computer Aided Tolerancing, Erlangen, Germany.
- [Tichadou S. *et al*, 2005] Tichadou S, Legoff O, Hascoet J Y (2005), "3D geometrical manufacturing simulation - Compared approaches between integrated CAD/CAM systems and small displacement torsor models," *Advances in Integrated Design and Manufacturing in Mechanical Engineering* 201-14.
- [Turner J. U. *et al*, 1987] Turner J U, Wozny M J (1987), "Tolerances in computer-aided geometric design," *The Visual Computer*, vol. 3: pp. 214-26.
- [Varghese P. *et al*, 1996a] Varghese P, N Braswell R, Wang B et al (1996a), "Statistical tolerance analysis using FRPDF and numerical convolution," *Computer-Aided Design*, vol. 28: pp. 723-32.
- [Varghese P. *et al*, 1996b] Varghese P, Zhang C, Wang H-P (1996b), "Geometric tolerance analysis with vectorial tolerancing," *Engineering Design and Automation* 127-39.
- [Vignat F., 2005] Vignat F (2005) "Contribution à l'élaboration d'un modèle 3D de simulation de fabrication pour l'analyse et la synthèse des tolérances, le modèle MMP " Ph.D Thesis. Institut National Polytechnique de Grenoble Mechanical Engineering.
- [Vignat F. *et al*, 2003] Vignat F, Villeneuve F (2003), "3D Transfer of Tolerances Using a SDT Approach: Application to Turning Process," *Journal of Computing and Information Science in Engineering*, vol. 3: pp. 45-53.
- [Vignat F. *et al*, 2005] Vignat F, Villeneuve F (2005), "Simulation of the manufacturing process(2): Analysis of its consequences on a functional tolerance " presented at: 9th CIRP International Seminar on Computer-Aided Tolerancing, Arizona.
- [Vignat F. *et al*, 2007a] Vignat F, Villeneuve F (2007a), "Simulation of the Manufacturing Process, Generation of a Model of the Manufactured Parts," In: *Digital Enterprise Technology*, Cunha P. F. and Maropoulos P. G. Eds: Springer US, pp. 545-52.

- [Vignat F. *et al*, 2007b] Vignat F, Villeneuve F (2007b), "Simulation of the Manufacturing Process, Generation of a Model of the Manufactured Parts," In: Cunha P. and Maropoulos P., Eds, *Digital Enterprise Technology: Perspectives and Future Challenges* pp. 545-52, presented at: 3rd International Conference on Digital Enterprise Technology, Bath.
- [Vignat F. *et al*, 2008] Vignat F, Villeneuve F, Kamalinejad M (2008), "From the nominal model to a Model of Manufactured Parts in a CAD context," pp., presented at: CIRP Design Conference Netherlands.
- [Vignat F. *et al*, 2009] Vignat F, Villeneuve F, Kamalinejad M (2009), "Analysis of the deviations of a casting and machining process using a Model of Manufactured Parts," presented at: 42nd CIRP Conference on Manufacturing Systems Grenoble, France
- [Villeneuve F. *et al*, 2001] Villeneuve F, Legoff O, Landon Y (2001), "Tolerancing for manufacturing: a three-dimensional model," *International Journal of Production Research*, vol. 39: pp. 1625-48.
- [Villeneuve F. *et al*, 2005a] Villeneuve F, Vignat F (2005a), "Manufacturing process simulation for tolerance analysis and synthesis," In: *5th International Conference on Integrated Design and Manufacturing in Mechanical Engineering, Advances in Integrated Design and Manufacturing in Mechanical Engineering*, Bramley A. and Brissaud D. *et al* Eds. Bath, ENGLAND: Springer, pp. 189-200.
- [Villeneuve F. *et al*, 2005b] Villeneuve F, Vignat F (2005b), "Manufacturing process simulation for tolerance analysis and synthesis," *Advances in Integrated Design and Manufacturing in Mechanical Engineering* 189-200.
- [Villeneuve F. *et al*, 2007] Villeneuve F, Vignat F (2007), "Simulation of the manufacturing process in a tolerancing point of view: Generic resolution of the positioning problem," In: Davidson J. K., Ed., *Models for Computer Aided Tolerancing in Design and Manufacturing* pp. 179-89, presented at: 9th CIRP International Seminar on Computer-Aided Tolerancing, Arizona.
- [Wade O. R., 1983] Wade O R (1983), "Tolerance Control " In: *Tool and Manufacturing Engineers Handbook*, vol. 1: Machining. Dearborn, MI: Society of Manufacturing Engineers (SME), pp. 1-60.
- [Ward K., 1992] Ward K (1992) "Integrating Geometric Form Variations into Tolerance Analysis of 3D Assemblies " Ph.D Thesis. Brigham Young University Mechanical Engineering.
- [Weill R., 1997] Weill R (1997), "Dimensioning and tolerancing for function," In: *Advanced Tolerancing Techniques*, Zhang H. C. Ed.: Wiley, pp. 329-54.
- [Whitney D. E. *et al*, 1994] Whitney D E, Gilbert O L, Jastrzebski M (1994), "Representation of Geometric Variations Using Matrix Transforms for Statistical Tolerance Analysis in Assemblies," *Research in Engineering Design-Theory Applications and Concurrent Engineering*, vol. 6: pp. 191-210.
- [Whybrew K. *et al*, 1990] Whybrew K, Britton G, Robinson D *et al* (1990), "A graph-theoretic approach to tolerance charting," *The International Journal of Advanced Manufacturing Technology*, vol. 5: pp. 175-83.

- [Wirtz A., 1991] Wirtz A (1991), "Vectorial tolerancing: a basic element for quality control," pp. 115-27, presented at: Computer-Aided Tolerancing: Proceedings of CIRP Seminars Penn State, USA.
- [Wirtz A. *et al*, 1993] Wirtz A, Gachter C, Wipf D (1993), "From unambiguously defined geometry to the perfect quality control loop," *Annals of the CIRP*, vol. 42: pp. 615-18.
- [Yu K. M. *et al*, 1994] Yu K M, Tan S T, Yuen M F (1994), "A Review of Automatic Dimensioning and Tolerancing Schemes," *Engineering with Computers*, vol. 10: pp. 63-80.
- [Zhang C. *et al*, 1993] Zhang C, Wang H P (1993), "Tolerance Analysis and Synthesis for Cam Mechanisms," *International Journal of Production Research*, vol. 31: pp. 1229-45.
- [Zhang G., 1996] Zhang G (1996), "Simultaneous tolerancing for design and manufacturing," *International Journal of Production Research*, vol. 34: pp. 3361-82.
- [Zhang G. *et al*, 1993] Zhang G, Porchet M (1993), "Some new developments in tolerance design in CAD.," pp. 175-85, presented at: ASME 19th Design Automation Conference.
- [Zhang M. *et al*, 2007] Zhang M, Djurdjanovic D, Ni J (2007), "Diagnosibility and sensitivity analysis for multi-station machining processes," *International Journal of Machine Tools and Manufacture*, vol. 47: pp. 646-57.
- [Zhong W. *et al*, 2002] Zhong W, Huang Y, Hu S J (2002), "Modeling variation propagation in machining systems with different configurations," presented at: ASME 2002 International Mechanical Engineering Congress and Exposition (IMECE2002) Louisiana, USA
- [Zhong W. *et al*, 2000] Zhong W, Maier-Sperdelozzi V, Bratzel A et al (2000), "Performance analysis of machining systems with different configurations," presented at: Japan-USA Symposium on Flexible Automation, Ann Arbor, Michigan, USA.
- [Zhou S. Y. *et al*, 2003] Zhou S Y, Huang Q, Shi J J (2003), "State space modeling of dimensional variation propagation in multistage machining process using differential motion vectors," *Ieee Transactions on Robotics and Automation*, vol. 19: pp. 296-309.
- [Zirmi S. *et al*, 2007] Zirmi S, Paris H, Belaidi I (2007), "Analysis of modular fixtures design," *Mecanique & Industries*, vol. 8: pp. 1-6.





## 10 ANNEX

The Kuhn-Tucker equations for a general problem (GP) can be stated as:

$$\begin{aligned}
 & \underset{x}{\text{minimize}} && f(x) \\
 & \text{subject to} && \\
 & G_i(x) = 0, && i = 1, \dots, m_e \\
 & G_i(x) \leq 0, && i = m_e + 1, \dots, m
 \end{aligned} \tag{10-1}$$

$$\begin{aligned}
 \nabla f(x^*) + \sum_{i=1}^m \lambda_i^* \cdot \nabla G_i(x^*) &= 0 \\
 \lambda_i^* \cdot G_i(x^*) &= 0 && i = 1, \dots, m \\
 \lambda_i^* &\geq 0 && i = m_e + 1, \dots, m
 \end{aligned} \tag{10-2}$$

SQP methods represent the state of the art in nonlinear programming methods [Schittkowski K., 1985], for example, has implemented and tested a version that outperforms every other tested method in terms of efficiency, accuracy, and percentage of successful solutions, over a large number of test problems.

Based on the work of and Powel [Powell M., 1978a, , 1979], the SQP allows Newton's method for constrained optimization just as is done for unconstrained optimization. At each major iteration, an approximation is made of the Hessian of the Lagrangian function using a quasi-Newton updating method. This is then used to generate a QP sub problem whose solution is used to form a search direction for a line search procedure.

Given the problem description in Eq. 5-9 the principal idea is the formulation of a QP sub problem based on a quadratic approximation of the Lagrangian function.

$$L(x, \lambda) = f(x) + \sum_{i=1}^m \lambda_i \cdot g_i(x) \tag{10-3}$$

Eq. 5-9 is simplified by assuming that bound constraints have been expressed as inequality constraints. This leads to obtain the QP sub problem by linearizing the nonlinear constraints.

## 10.1 QUADRATIC PROGRAMMING (QP) SUB PROBLEM

$$\begin{aligned}
 & \underset{d \in \mathcal{R}^n}{\text{minimize}} \quad \frac{1}{2}d^T H_k d + \nabla f(x_k)^T d \\
 & \nabla g_i(x_k)^T d + g_i(x_k) = 0 \quad i = 1, \dots, m_e \\
 & \nabla g_i(x_k)^T d + g_i(x_k) \leq 0 \quad i = m_e + 1, \dots, m
 \end{aligned} \tag{10-4}$$

This sub problem can be solved using any QP algorithm. The solution is used to form a new iterate:

$$x_{k+1} = x_k + \alpha_k d_k \tag{10-5}$$

### 10.1.1 SQP Implementation

The SQP implementation consists of three main stages, which are discussed in the following subsections:

- Updating the Hessian Matrix
- Quadratic Programming Solution
- Line Search and Merit Function

#### 10.1.1.1 Updating the Hessian Matrix

At each major iteration a positive definite quasi-Newton approximation of the Hessian of the Lagrangian function  $H$ , is calculated using the Broyden [Broyden C. G., 1970], Fletcher [Fletcher R., 1970], Goldfarb [Goldfarb D., 1970], and Shanno [Shanno D. F., 1970] (BFGS) method, where  $\lambda_i (i = 1, \dots, m)$  is an estimate of the Lagrange multipliers.

$$H_{k+1} = H_k + \frac{q_k q_k^T}{q_k^T s_k} - \frac{H_k^T H_k}{s_k^T H_k s_k} \tag{10-6}$$

where

$$\begin{aligned}
 s_k &= x_{k+1} - x_k \\
 q_k &= \nabla f(x_{k+1}) + \sum_{i=1}^n \lambda_i \cdot \nabla g_i(x_{k+1}) - \left( \nabla f(x_k) + \sum_{i=1}^n \lambda_i \cdot \nabla g_i(x_k) \right)
 \end{aligned}$$

### 10.1.1.2 Quadratic Programming Solution

At each major iteration of the SQP method, a QP problem of the following form is solved, where refers to the  $i^{\text{th}}$  row of the  $m$ -by- $n$  matrix.

$$\begin{aligned} \underset{d \in \mathcal{R}^n}{\text{minimize}} \quad & q(d) = \frac{1}{2}d^T H d + c^T d \\ & A_i d = b_i \quad i = 1, \dots, m_e \\ & A_i d \leq b_i \quad i = m_e + 1, \dots, m \end{aligned} \quad (10-7)$$

The solution procedure involves two phases. The first phase involves the calculation of a feasible point (if one exists). The second phase involves the generation of an iterative sequence of feasible points that converge to the solution. In this method an active set,  $\bar{A}_k$  is maintained that is an estimate of the active constraints (i.e., those that are on the constraint boundaries) at the solution point. Virtually all QP algorithms are active set methods. This point is emphasized because there are many different methods that are very similar in structure but that are described in widely different terms.

#### Line Search and Merit Function

The solution to the QP sub problem produces a vector  $d_k$ , which is used to form a new iteration:

$$x_{k+1} = x_k + \alpha d_k \quad (10-8)$$

The step length parameter  $\alpha_k$  is determined in order to produce a sufficient decrease in a merit function. The merit function used by Powell [Powell M., 1978b] of the following form is used in this implementation.

$$\Psi(x) = f(x) + \sum_{i=1}^{m_e} r_i \cdot g_i(x) + \sum_{i=m_e+1}^m r_i \cdot \max\{0, g_i(x)\} \quad (10-9)$$

Powell recommends setting the penalty parameter:

$$r_i = (r_{k+1})_i = \max_i \left\{ \lambda_i, \frac{1}{2}((r_k)_i + \lambda_i) \right\}, \quad i = 1, \dots, m \quad (10-10)$$



## List of Figures

Figure 2–1: Product life cycle .....	7
Figure 2–2: Product Development .....	9
Figure 2–3: The scope of tolerances in engineering [Srinivasan R. S., 1994] .....	9
Figure 2–4: Ubiquitous role of tolerances in a product life cycle[Hong Y. S. et al, 2002] ...	11
Figure 2–5: Tolerance activities in product life cycle.....	12
Figure 2–6: Main function of the tolerance analysis tool [Salomons O. W. et al, 1996a].....	14
Figure 2–7: Concept of tolerance analysis and synthesis [Shan A. et al, 1999] .....	15
Figure 2–8: Tolerance analysis affects performance and cost.[Chase K. W. et al, 1997a]....	19
Figure 2–9: Vector loop model of a clutch assembly[Chase K. W. et al, 1991].....	20
Figure 2–10: Adding virtual joints and coordinate frames to FE pairs (example of two planes of the same part) to model spatial relationships.[Lafond P. et al, 1999] .....	24
Figure 2–11: Deviation of a plane.....	25
Figure 2–12: Deviation Domain example from [Samper S. et al, 2006] .....	26
Figure 2–13: The association of a PACV with a complex surface[Teissandier D. et al, 1999a] .....	26
Figure 2–14: Cylinder tolerance zone for matrix representation [Desrochers A. et al, 1997]27	
Figure 2–15: Vectorial description [Wirtz A., 1991] .....	28
Figure 2–16: Cylinder surface and surface deviation representation.....	31
Figure 2–17: Error propagation [Huang Q. et al, 2003].....	33
Figure 2–18: Illustration of feature representation [Zhou S. Y. et al, 2003].....	34
Figure 2–19: Composition of overall feature deviation[Zhou S. Y. et al, 2003] .....	34
Figure 2–20: Steps of the derivation of variation propagation model.....	35
Figure 2–21: Concept of state vector [Loose J. P. et al, 2007] .....	37
Figure 2–22: Dimensional errors flow in a multi-station manufacturing process [Zhang M. et al, 2007] .....	37

Figure 2–23: System Performance Analysis Approach[Zhong W. et al, 2000].....	38
Figure 2–24: Point-based workpiece model[Zhong W. et al, 2002] .....	39
Figure 2–25: Model of machining station .....	39
Figure 2–26: Serial machining system [Zhong W. et al, 2000] .....	39
Figure 2–27: Typical tolerance zones (a) 1D, (b) 2D and(c) 3D tolerance zones. (d) The projecting relation of tolerance zones[Lin E. E. et al, 2001].....	40
Figure 2–28: 2D tolerance stack-up analysis [Lin E. E. et al, 2001] .....	42
Figure 2–29: A simple work piece represented by point could [Huang S. H. et al, 2004] ....	43
Figure 2–30: Illustration of errors synthesis [Huang S. H. et al, 2004] .....	45
Figure 2–31: Existing literature about Tolerance analysis in machining.....	48
Figure 3–1: Different possible operation on a lathe.....	51
Figure 3–2: Most frequent fixtures in turning operation.....	51
Figure 3–3: Milling operations.....	52
Figure 3–4: Traditional and modular fixture used in milling operation.....	52
Figure 3–5: Errors in a machining operation [Loose J. P. et al, 2007] .....	54
Figure 3–6: Deviation of a plane and cylinder .....	56
Figure 3–7: Positioning deviation .....	58
Figure 3–8: Contact zone boundary and verification points .....	60
Figure 3–9: Plane-Plane elementary connection.....	61
Figure 3–10: Cylinder-Cylinder elementary connection.....	62
Figure 3–11: 2D example, functional tolerance .....	64
Figure 3–12: 2D example MWP/Fixture assembly illustration .....	64
Figure 3–13: Machining errors.....	66
Figure 3–14: Tolerance (error) stack-up model .....	67
Figure 3–15: Stack- up of formulation.....	68
Figure 3–16: The MMP.....	69
Figure 4–1: Virtual gauge, case-2 with internal mobility .....	72

Figure 4–2: Virtual gauge with DOF .....	74
Figure 4–3: “Bolt” example, Gauge/MMP assembly.....	75
Figure 4–4: GapGP measurement in the case of planar TZ, case of “Bolt” example .....	76
Figure 4–5: GapGP measurement in the case of cylindrical TZ .....	77
Figure 4–6: GapGP measurement in the case of a cylindrical tolerance zone with maximum material condition .....	78
Figure 5–1: solution for worst case identification.....	83
Figure 5–2: “Bolt” example, Virtual gauge and verification points .....	85
Figure 5–3: Positioning lay out 3-2-1c.....	90
Figure 5–4: Positioning lay out 3-2-1r .....	90
Figure 5–5: Positioning lay out 4-1-1 .....	91
Figure 5–6: Co-relation between deviations parameters (rx, ry) .....	92
Figure 5–7: Planar variation zone .....	93
Figure 6–1: Manufacturing simulation, the MMP (nominal part in blue and actual part in red) .....	99
Figure 6–2: Virtual gauge, MMP and DisGP .....	100
Figure 6–3: MWP/Fixture assembly with a floating link, “Bolt” example.....	107
Figure 6–4: Proposed algorithm for finding the best position of virtual gauge .....	111
Figure 7–1: Monte Carlo simulation .....	114
Figure 7–2: Defect generation for the case of a cylindrical variation zone (dependent parameters) .....	115
Figure 7–3: random generation of defects-Case two .....	116
Figure 7–4: Planar variation zone .....	117
Figure 7–5: MWP/Fixture assembly with a floating link.....	118
Figure 7–6: Distribution of link parameters in the allowed domain .....	119
Figure 7–7: Definition of “Double inclined plane” example .....	119
Figure 7–8 : Optimization by SQP, First section, with GapGP expression .....	123
Figure 7–9 : Optimization by GA, First section, with GapGP expression.....	123



Figure 7–10: Mc results for first-section.....	124
Figure 7–11: Performance of SQP with different initial guess points, with GapGP expression .....	125
Figure 7–12: A part with two machined surfaces .....	127
Figure 7–13: Optimization by SQP, Second section, with GapGP expression.....	128
Figure 7–14: Optimization by GA, Second section, with GapGP expression .....	128
Figure 7–15: MC simulation results, Second section.....	130
Figure 7–16: “Bolt” example: functional tolerance .....	132
Figure 7–17: “Bolt” example, MWP/Fixture secondary link adjustment .....	133
Figure 7–18: Optimization with SQP, with GapGP expression.....	135
Figure 7–19: Optimization with GA, with GapGP expression .....	135
Figure 7–20: MC simulation for “bolt” example .....	136
Figure 7–21: “Bolt”, Clearance for MWP/Fixture secondary link.....	140
Figure 8–1: The developed solution techniques for tolerance analysis by using the MMP.	141

## List of tables

Table 1-1: Literature relevant to computerized tolerance chart analysis/synthesis [Huang S. H. et al, 2004] .....	2
Table 3-1: MMP parameters notation .....	58
Table 3-2: Elementary connections and related link torsor with their LLCS .....	63
Table 3-3: MWP/Fixture Assembly (NPC and positioning functions) based on the example in Figure 3–11 .....	65
Table 5-1: "Bolt" example, Gauge/MMP assembly.....	87
Table 5-2: Different type of tolerance that can be handled by proposed solution technique.	88
Table 5-3: Elementary connection, local coordinate system (LLCS) and blocking DOF .....	89
Table 6-1: MWP/Fixture Assembly based on the example in Figure 6–1 .....	106
Table 6-2: Assembly procedure for "Bolt" example in Figure 6–3 .....	108
Table 7-1: Fixture/MWP assembly for the "Double inclined plane" .....	121
Table 7-2: Interval approach results for "Double inclined plane" example with DisGP and GapGP expression .....	122
Table 7-3: "Double inclined plane" example, range of defect parameters, Coefficient matrices and functional elements torsor with intervals .....	123
Table 7-4: $GapGP_{min}$ and $DisGP_{min}$ obtained for first section .....	126
Table 7-5: final points obtained for first section .....	129
Table 7-6: Second section-Deviation range for "Double inclined plane" manufacturing process .....	129
Table 7-7: $GapGP_{min}$ and $DisGP_{max}$ obtained for second section.....	130
Table 7-8: Final points obtained for second section .....	131
Table 7-9: Proposed process plan for the "Bolt" .....	133
Table 7-10: Deviation range for "bolt" manufacturing process .....	136
Table 7-11: "Bolt" example-Coefficient matrices and functional elements torsor with intervals.....	137

Table 7-12: Interval approach results for “Bolt” example with DisGP and GapGP expression ..... 138

Table 7-13: Worst GapGP<sub>min</sub> and DisGP<sub>min</sub> obtained for “Bolt” example ..... 139